# Novel Technologies and Measurement of Microvascular Blood Flow in Muscle

By

**Andrew D. H. Clark,**

**B Med Sci, MB BS**

**Submitted in fulfilment of the requirements for the degree of Doctor of Philosophy**

**Discipline of Biochemistry, School of Medicine, University of Tasmania**

**(October, 2004)**

## DECLARATION

**This thesis contains material which has not been accepted for the award of any other degree or diploma, except where due acknowledgement is given. To the best of my knowledge and belief, this thesis contains no material previously published or written by another person, except where due reference is made in the text.**

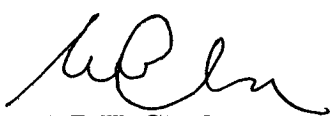

**A.D.H. Clark**

## AUTHORITY OF ACCESS

**This thesis may be made available for loan and limited copying in accordance with the Copyright Act 1968.**

**A.D.H. Clark**

## PREFACE AND ACKNOWLEDGEMENTS

My involvement in microvascular muscle research began in 1997 while undertaking an elective during the fourth year of my medical degree in the Biochemistry Department at the University of Tasmania. I would like to thank the members of the Muscle Research Group, particularly my father, Professor Michael Clark who together with Dr Steve Rattigan, later to become my PhD supervisor, helped me adapt laser Doppler flowmetry for the measurement of microvascular blood flow in muscle, particularly in the blood perfused rat hindlimb. It was the energy, professionalism and guidance of this whole team that was instrumental in encouraging me to maintain an ongoing interest in research in this field.

I undertook two visits to Dr Gene Barrett's group at the University of Virginia, Charlottesville, where I was able to further explore laser Doppler flowmetry with more sophisticated equipment, including a scanning Laser Doppler instrument (courtesy of Ms Colleen Green, and Dr George Rodheaver, Department of Plastic Surgery, University of Virginia). I would like to thank Dr Barrett for his efforts in organising my visits and for his knowledge and guidance while acting as my co-supervisor while I was in the USA. I am indebted to Dr Michelle Vincent, Dr Matthew Coggins, Dr Dana Dawson and Dr Jonathan Lindner at UVA for their help, expertise and friendship during these visits, particularly in sharing their expertise in the technique of Contrast Enhanced Ultrasound .

In 2003 and having completed my medical training and internship, I wanted to return to research and took an opportunity to work with Professor Coen Stehouwer and his team at the Vrije University, in Amsterdam. During that stay my role was to apply the experience I had gained in laser Doppler flowmetry with rats to assess changes in human muscle while these subjects underwent a hyperinsulinaemic euglycaemic clamp. This work was carried out with Dr Renate de Jonge under Professor Stehouwer's supervison and I would like to thank them both for allowing me to contribute to this work.

**In summary, I would like to thank Dr Steve Rattigan for his excellent and patient supervision, and my father for his encouragement and enthusiasm. I would also like to thank my colleagues at the University of Tasmania, Dr Jo Youd and Dr Michelle Wallis for their help and contributions at various stages.**

**Sections of this work were supported by grants from the NHMRC, National Heart Foundation of Australia, American Diabetes Association and NIH (USA).**
**I was supported in part by an Australian Postgraduate Award and the NIH grant for the tenure of this candidature.**
**The bulk of the data contained in this thesis have been published and/or presented at scientific meetings and because the papers are multi-author some of the data have appeared in previous theses and been duly recognised. The publications and presentations are listed below.**

**Publications:**

Clark MG, Newman JMB & **Clark ADH**. Microvascular regulation of muscle metabolism. In: *Nutrition in the ICU: Curr. Opin. Nutr. Metab. Care,* 1: 205-210, 1998.

Clark MG, Rattigan S, Clerk LH, Vincent MA, **Clark ADH**, Youd JM & Newman JMB. Nutritive and non-nutritive blood flow: rest and exercise. *Acta Physiol. Scand.* 168: 519-530, 2000.

**Clark ADH**, Youd JM, Rattigan S, Barrett EJ & Clark MG. Heterogeneity of laser Doppler flowmetry signal in perfused rat muscle indicative of nutritive and non-nutritive flow. *American Journal of Physiology; Heart and Circulation.* 280(3): H1324-33, 2001.

**Clark ADH**, Barrett EJ, Rattigan S & Clark MG. Insulin stimulates laser Doppler signal by rat muscle in vivo consistent with nutritive flow recruitment. *Clinical Science* (London) 100(3): 283-90, 2001.

Clark MG, **Clark ADH** & Rattigan S. Failure of laser Doppler signal to correlate with total flow in muscle: Is this a question of vessel geometry? *MicroVasc Res* 60(3): 294-301, 2000.

Clark MG, Barrett EJ, Richards SM, **Clark ADH** & Rattigan S. Microvascular involvement in insulin resistance of skeletal muscle. Proceedings of the 7th World Congress for Microcirculation. pp. 31-37, Monduzzi Editore S.p.A. –Medimond Inc: Bologna, 2001.

Vincent MA, Dawson D, **Clark AD**, Lindner JR, Rattigan S, Clark MG, Barrett EJ. Skeletal muscle microvascular recruitment by physiological hyperinsulinemia precedes increases in total blood flow. Diabetes. 51(1):42-8, 2002.

Dawson D, Vincent MA, Barrett EJ, Kaul S, **Clark A**, Leong-Poi H, Lindner JR. Vascular recruitment in skeletal muscle during exercise and hyperinsulinemia assessed by contrast ultrasound. Am J Physiol Endocrinol Metab. 282(3):E714-20, 2002.

Wallis MG, Wheatley CM, Rattigan S, Barrett EJ, **Clark ADH** & Clark MG. Insulin-mediated hemodynamic changes are impaired in muscle of Zucker obese rats. Diabetes 51:3492-3498, 2002.

de Jongh RT, **Clark ADH**, Ijzerman RG, Serne EH, de Vries G & Stehouwer CDA. Physiological hyperinsulinaemia increases intramuscular microvascular reactive hyperaemia and vasomotion in healthy volunteers. Diabetologia, 47: 978-986, 2004.

**Conference Abstracts and Presentations:**

Youd JM, Rattigan S, **Clark ADH** & Clark MG. Blood flow and glucose uptake by muscle. Proceedings of the Australian Society for Biochemistry and Molecular Biology, 30: Sym 32-06, 1998.

Clark MG, Rattigan S, Youd JM & **Clark ADH**. Update on the role of endothelial dysfunction in glucose disposal: the need for a microvascular perspective. Wellcome Trust Frontiers Meeting, Cambridge UK, May 1999.

**Clark ADH**, Barrett EJ & Clark MG. Insulin mediates capillary recruitment in rat skeletal muscle in vivo: studies using laser Doppler flowmetry. American Diabetes Association, San Diego USA, June 1999.

Vincent MA, Dawson D, **Clark ADH**, Leong-Poi H, Clark MG, Rattigan S & Lindner JR. Physiologic Hyperinsulinaemia mimics the capillary recruitment induced by exercise in skeletal muscle in vivo. The American Diabetes Association, San Antonio USA, June 2000.

Lindner JR, Dawson D & **Clark ADH**. Capillary Recruitment in Response to Insulin is Comparable to That Seen During Exercise. American Heart Association Conference November 2000.

**Clark ADH**. "Lasers, Bubbles and Enzymes - Measuring nutritive blood flow in skeletal muscle" RACS Tasmanian Branch Annual Meeting Cradle Mountain, Tasmania June 2001.

# TABLE OF CONTENTS

ABBREVIATIONS

| | |
|---|---|
| A-V | arteriovenous (difference) |
| BP | blood pressure |
| bpm | beats per minute |
| BSA | bovine serum albumin |
| CEU | contrast enhanced ultrasound |
| Δ | change in |
| 2DG | 2-deoxyglucose |
| EDL | extensor digitorum longus (muscle) |
| eNOS | endothelial nitric oxide synthase |
| FBF | femoral arterial blood flow |
| g | gram |
| GIR | whole body glucose infusion rate |
| h | hour |
| HPLC | high performance liquid chromatography |
| HR | heart rate |
| 5-HT | 5-hydroxytryptamine (serotonin) |
| IMGU | insulin-mediated glucose uptake |
| Ins | insulin |
| i.p. | intraperitoneal |
| i.v. | intravenous |
| KH | Krebs Henseleit (buffer) |
| l | litre |
| LDF | laser Doppler flowmetry |
| L-NAME | Nω-nitro-L-arginine-methyl ester |
| MAP | mean arterial pressure |
| ml | millilitre |
| min | minute |
| 1-MU | 1-methyl urate |

| | |
|---|---|
| 1-MX | 1-methyl xanthine |
| NE | norepinephrine (noradrenaline) |
| NO | nitric oxide |
| NOS | nitric oxide synthase |
| PCA | perchloric acid |
| PET | positron emission tomography |
| PI3-kinase | phosphatidyl inositol-3 kinase |
| PKB/Akt | protein kinsae B |
| Plan | plantaris (muscle) |
| Ra | rate of glucose appearance |
| Rd | rate of disappearance of glucose |
| RG | red gastrocnemius (muscle) |
| R'g | glucose uptake as measured by 2-deoxyglucose uptake |
| RU | resistance units |
| s | second |
| SE | standard error |
| Sol | soleus (muscle) |
| Tib | tibialis (muscle) |
| TNFα | tumor necrosis factor α |
| VENIRKO | vascular endothelial cell insulin receptor knock-out (mouse) |
| $VO_2$ | oxygen consumpyion |
| VR | vascular resistance |
| WG | white gastrocnemius (muscle) |

## ABSTRACT

In the field of microvascular blood flow, particularly to the skeletal muscle, there has been a considerable history of reference to the incongruity of total limb blood flow and actual myocyte perfusion. Embedded in such an idea is the concept that flow to skeletal muscle should be composed of two physiologically distinct circulations – one that perfuses the myoctes (and therefore may be called "nutritive") and another which must act as a form of physiological shunt or "non-nutritive". The "nutritive and non-nutritive flow" hypothesis was renewed by the muscle research group of the Biochemistry Department at the University of Tasmania to explain perfusion dependent metabolic effects of vasoconstrictors on skeletal muscle.

This thesis focuses on the assessment of microvascular perfusion, compared to total flow, in skeletal muscle and in particular in relation to reports of direct and indirect effects of insulin to increase microvascular perfusion of this tissue *in vivo*. Initially laser Doppler Fluxmetry technology (LDF) was applied to estimate muscle perfusion. For the purposes of verification and comparison two other techniques under development by our group, contrast enhanced ultrasound (CEU) and 1-methyl xanthine metabolism, were also used.

In the first section of this thesis the variable of total flow is eliminated by using a constant flow (pump perfused) rat hindlimb. During the application of vasoconstrictors that caused either predominantly nutritive or non-nutritive flow LDF estimation of perfusion was found to be highly variable in spite of the constant total flow. LDF comprises a non vectorial voltage measurement generated by particle movement through a volume of tissue illuminated by the laser light.

LDF measurement using a large probe was highly correlated with the metabolic changes induced by changes in nutritive and non-nutritive flow. However, LDF measurement using a smaller implantable probe which measures particle movement in a smaller volume of muscle tissue, showed that there is considerable heterogeneity of response.

To better understand the factors that influence changes in the LDF measurement LDF measurements were made of flow controlled through fabricated glass capillary arrays of various architectures.

The third study addressed changes induced by insulin *in vivo*, in anaethetised rats during a hyperinsulinaemic euglycaemic clamp. Using a large surface LDF probe the LDF signal from the muscle increased during the administration of insulin. In contrast the LDF signal did not increase during epinephrine administration even though the epinephrine caused a comparable increase in femoral artery blood flow as seen with insulin. Furthermore the time course of LDF change in the presence of insulin was more closely aligned with changes in glucose uptake than it was with changes in femoral blood flow.

In the final series of experiments using LDF, changes due to insulin in human muscle was assessed. The results suggested that physiological hyperinsulinaemia stimulated not only total blood flow and skin microvascular perfusion, but also augmented human skeletal muscle microvascular recruitment and vasomotion as detected directly by laser Doppler measurement.
In the second technique, CEU, microbubbles (an albumin membrane encapsulating an inert gas in the form of a 4 micron diameter sphere) act as contrast when tissue is visualised using ultrasonography. Analysis of the rate and extent of contrast (microbubble) appearance during imaging of the target tissue allows us to calculate indicators of the microvascular velocity and microvascular volume.

The third technique based on capillary endothelial metabolism of the exogenous substrate 1-methylxanthine, was developed at the University of Tasmania. 1-Methylxanthine is a reporter substrate, which as it passes through the nutritive capillary route of the muscle is metabolized to 1-methyl urate; metabolism is proportional to available capillary surface area.

To consolidate the LDF findings, the two additional techniques for assessing changes in capillary recruitment were used. Once again, the hyperinsulinaemic euglycaemic clamp was used but on this occasion a physiologic dose of insulin was infused. Microvascular recruitment (measured by 1-MX metabolism as well as by CEU) increased during insulin

administration. Furthermore, at certain time points microvascular recruitment occurred without changes to femoral artery flow. From these studies it was evident that insulin increases tissue perfusion by recruiting microvascular beds, and at physiological concentrations this precedes increases in total muscle blood flow by 60–90 min. Since there was no change in the mean red cell velocity, it seem likely that insulin had increased capillary recruitment by redistributing blood flow from other vessels possibly non-nutritive.

In the final study capillary recruitment was again measured by the metabolism of infused 1-methyl xanthine and used to assess responses to insulin in normal colony rats as well as lean and obese Zucker rats (an animal model for type 2 diabetes). It was concluded that muscle insulin resistance of obese Zucker rats is accompanied by impaired hemodynamic responses to insulin including markedly impaired capillary recruitment and femoral blood flow when compared to lean Zuckers or colony control rats.

Taken together, the findings embodied by this thesis show that the three techniques of LDF, CEU and 1-MX metabolism, each detect a vascular effect of insulin *in vivo*, characterized by capillary recruitment. This was detectable at physiologic insulin and occurred in both muscle of rats and humans. In addition, LDF added a further aspect of insulin action of an insulin-mediated increase in vasomotion at low frequency, very likely suggesting increased neural activity.

# CHAPTER 1
# General Introduction

## 1.1 The haemodynamic actions of insulin

### *1.1.1 Early studies*

The clinical use of insulin began in the 1930's but was not limited to the treatment of diabetes. Early literature shows that massive doses (40-280 units) of insulin were employed in the treatment of schizophrenia. Thus in 1939 (1) we find the first report of increased blood flow in the forearm, hand and leg of seven schizophrenic patients as a result of insulin administration. In the same report systolic and diastolic blood pressure were also elevated and there was a slight decrease in oxygen consumption across the forearm. Other researchers had noted earlier that lower doses (40-80 units) induced hypoglycaemia and the attendant expected symptoms of elevated pulse rate, blood pressure and perspiration (59). However, the hypoglycaemic stress endured by patients to whom the large doses of insulin were administred was profound and considered at the time to be the main cause of the accompanying haemodynamic changes, even when experiments of this kind were repeated at lower doses of insulin.

French and Kilpatrick in 1955(63) investigated the role of adrenaline in the hypoglycaemic response to 150 mU insulin/kg. Blood flow changes were detected at 40min after injection of insulin but comparison of responses between hypertensive patients, patients after splanchnicectomy or sympathectomy led these workers to conclude that adrenaline was not responsible for the majority of the clinical features of the acute hypoglycaemia, including the increased hand blood flow. Ginsberg and Paton in 1956 (66) specifically examined the effects of bilateral adrenalectomy on insulin action. They found that 30 min after insulin (100 mU/kg) there was a 100% rise in blood flow to the forearm. In adrenalectomised patients forearm blood flow remained elevated even though hypoglycaemia and the immediate reactions to the hypoglycaemia had

passed. Allwood et al (3) applied similar doses of insulin (100mU/kg) to study the forearm circulatory changes specifically during the insulin-induced hypoglycaemia. Both cutaneous and muscle blood flow increased; skin to approximately twice the resting value and muscle, slightly less, to 175% of the resting value. Interestingly, skin blood flow decreased initially and this was attributed to either the adrenaline release or an increased sympathetic vasoconstrictor activity. However, neither the increase in skin blood flow that followed, nor the increase in muscle blood flow was concluded to be fully the result of such changes. These workers also showed that adrenaline (10μg i.v.) markedly increased muscle blood flow and decreased skin blood flow.

Administration of highly supraphysiological ("pharmacological") doses of insulin revealed other effects that were less visible at the lower doses. For example, Pereda et al (132) found that, in lightly anaesthetized dogs treated with a neuromuscular blocking agent, insulin (2-3units/kg i.v.) gave an early transient pressor response 2-9 min after injection. This response occurred in the presence of hyperglycaemia and in the absence of hypoglycaemia. Furthermore, the response could be produced when insulin was given in the carotid artery in doses that caused no effect when injected in a systemic vein. The authors concluded that insulin was having a direct effect on the brain.

One early study in rats where blood flow was measured following insulin (1 unit/100g) or glucose (100mg/110g) administration reported an increase in hepatic blood flow and attributed this to vasodilatation resulting from the hypoglycemia (55). A similar increase in liver blood flow due to glucose, however, could not be explained. The gastrocnemius muscle showed no increase in blood flow due to the single injection of 1 unit of insulin per 100g.

From this older literature, it is apparent that pharmacologic doses of insulin mostly produced marked increases in limb and skin blood flow that were not the result of the accompanying hypoglycaemia, adrenaline or elevated sympathetic outflow.

### *1.1.2 Contemporary views*

Contemporary literature contains certain parallels to the older literature, but contemporary techniques for measuring limb blood flow, particularly with thermal dilution catheters, and labelled microspheres, are more refined. Thus there are a number of *in vivo* studies ((43;62;65;80;102;146), but not all (50;51;78;79;198), that have reported an effect of insulin to increase plasma or blood flow to skeletal muscle in humans (43;62;65;146) and in animals (80;102).

Interest in this area was hightened in the 1990s by Baron and his colleagues when they reported insulin's ability to increase total blood flow to skeletal muscle, and suggested that this may in fact enhance insulin action by augmenting the delivery of insulin and glucose to muscle cells (96). The observations were made in human subjects during a hyperinsulinaemic euglycaemic clamp (i.e. glucose is infused concomitantly with the insulin to maintain blood sugar levels at baseline) to minimise the possible counter-regulatory effects of responding to glucose levels altered by the insulin. Some research groups repeated these findings in both humans (e.g.(5;52)) and animals (102;143); however, there was considerable variation between studies in the magnitude of the response, and in fact some groups have failed to observe changes in flow with insulin (e.g.(61;198)) . Changes in flow after insulin administration were detected not only by thermodilution, but by dye dilution, plethysmography, and by positron emission tomography (PET) combined with $[^{15}O]H_2O$ in human subjects and by ultrasound in animals (see (36) for refs.). Infusion of insulin systemically versus local intra-arterial infusion also does not seem to explain the difference, as vasodilation has been reported in both situations. One group did report greater increases in flow when the local intra-arterial infusions in the forearm were combined with an infusion of a physiological concentration of glucose. Even so, the magnitude of vasodilation was similar in forearm and calf during systemic insulin infusion. (see (36) for refs.)

While the hyperinsulinaemic, euglycaemic clamp is a commonly used technique which has many advantages for scientific research, it is unphysiological because high insulin

levels are not normally sustained for long periods following a meal. It is therefore important to note that in less artificial experiments, an increase in skeletal muscle blood flow was demonstrated following an intravenous glucose (101;183) oral glucose load (14) and a carbohydrate meal (154).

In the fullest perspective, the role of the increase in total blood flow mediated by insulin must be seen as controversial. For example, one research group has claimed that insulin-mediated changes in total blood flow relate poorly to muscle glucose uptake under a number of circumstances (197), including insulin dose and time course. In addition there have been studies where total flow changes persist when glucose uptake is inhibited (152). Also, most vasodilators that augment total blood flow to the limbs do not enhance insulin action nor do they overcome insulin resistance (97;115;117). Thus, on balance, a role for increased total blood flow in insulin-stimulated glucose uptake is not compelling.

The issue that the insulin-mediated vasodilatory effect is the result of increased SNS activity also is still not fully resolved. This has been addressed by Spraul, Ravussin and Baron (163) who examined the relationship between vasodilation, muscle sympathetic nerve activity (MSNA) and insulin action during sequential euglycemic clamps at low and high insulin doses. These authors found that there was no correlation between incremental MSNA and leg blood flow, whole body glucose uptake or leg glucose uptake. But insulin was found to stimulate MSNA more rapidly than vasodilation, characteristically occurring only after 45 min in insulin sensitive subjects.

Overall, there remains considerable interest in the possibility that insulin-mediated changes in muscle blood flow are somehow linked to improving access for insulin and perhaps glucose (96), more particularly, that a defect in this process might be responsible for part of the insulin resistance in muscle of Type II diabetics. Research from Bergman and his colleagues has played a key role in the general concept that mechanisms proximal to insulin-stimulated cellular glucose uptake, and possibly related to altered vascular function, could contribute to insulin resistance (196). They sought to explain a fundamental characteristic of insulin action: the paradox of the differential time course of

insulin action between cells versus intact tissues *in vivo*. Thus, the *in vivo* sluggishness was proposed to be due to insulin transport across the capillary endothelium of skeletal muscle and to test this they examined the temporal relationship between insulin concentrations in plasma versus interstitial fluid (lymph) during euglycaemic clamps in dogs. In all situations the insulin concentration in the interstitium was only 50-70% of that in the plasma, even under steady state conditions (17). These findings implied that the plasma insulin signal is both retarded and attenuated at the site of insulin action: the skeletal muscle cell. Interestingly, the 3:2 concentration gradient was not eliminated even at the highest insulin concentrations leaving the group to conclude that a transendothelial insulin gradient is present which is not receptor-mediated and is nonsaturable. More importantly, Bergman et al. proposed that the transport step is rate-limiting for insulin action since the rate of glucose uptake by skeletal muscle cells is exactly proportional to the interstitial and not the plasma insulin concentration (196). Subsequent measurement of interstitial levels of insulin by microdialysis have confirmed the findings from Bergman's group (82) by showing that interstitial levels of insulin are indeed lower than arterial levels.

A number of research groups seized on the idea that impaired vascular function might contribute to insulin resistance and set out to explore the mechanistic basis of insulin-induced vasodilation. For example, Scherrer's group showed insulin-induced vasodilation was opposed by the cortisol analog, dexamethasone (153). Dexamethasone also induced a comparable insulin resistance with or without the fatty acid oxidation inhibitor, acipimox, even though acipimox had normalised muscle blood flow (174). It thus seemed likely that products of fatty acid oxidation specifically impaired insulin-mediated vasodilatory effects. However, Intralipid infusion in humans blunted GIR and total glucose uptake but not the increase in limb blood flow, although Intralipid alone acutely increased limb blood flow (182). More extensive exposure to Intralipid (8h) did block the insulin-mediated increase in leg blood flow and the indices of NO production, along with an inhibition of whole-body glucose uptake (168). This was one of a number of reports that linked NO production to insulin-mediated vasodilation. For example, L-NMMA was found to block insulin-stimulated muscle blood flow during a 2h clamp, but did not affect

insulin-induced stimulation of whole body glucose uptake (152). This finding differed somewhat from that of Baron's group who found that L-NMMA blocked approx. 21% of the insulin-mediated glucose uptake by the leg (15). Baron et al also showed that the NO-dependent vasodilator, methacholine increased leg blood flow in the human and increased leg glucose uptake (15). This remains the only vasodilator that has been reported to augment insulin-mediated muscle glucose uptake in association with increased limb blood flow (150).

### 1.2 Evidence for two vascular flow routes in muscle

A number of studies done at the University of Tasmania (discipline of Biochemistry) over the last fifteen years using the perfused rat hindlimb support earlier proposals by others that there are two flow routes in muscle. One appears to be in intimate contact with the myocytes and able to exchange nutrients and hormones freely and thus regarded as nutritive. Another with essentially no contact with myocytes and regarded as non-nutritive [the history and background of this concept together with references can be found elsewhere (32),(33)]. Some of the non-nutritive route may supply muscle associated connective tissue (septa and tendon) (122) and there is indirect evidence that the non-nutritive route for the myocytes is in fact nutritive for associated adipocytes (39). In addition, there are indications that the non-nutritive vessels carry a flow reserve which can redistribute to the nutritive route during periods of high metabolic demand, such as during exercise (35) or following a meal to allow insulin-mediated glucose uptake into muscle. The balance between these two circuits is controlled by vasomodulators and neural input. In the constant flow pump-perfused hindlimb, our group has classified vasoconstrictors according to whether they increase or decrease metabolism (type A and type B respectively) (32). Examples of type A vasoconstrictors include low dose norepinephrine, angiotensin II, vaspressin and low frequency SNS activation and all type A vasoconstrictors increase oxygen consumption. Serotonin, α-methyl serotonin, high dose NE and high frequency SNS activation are all type B vasoconstrictors and these decrease oxygen consumption and metabolism generally (32).

Changes in flow redistribution due to the vasoconstrictors are suggested from vascular casts and changes to the pattern of red cell washout (121). In addition, aerobic contraction of the calf muscle group of the constant-flow perfused rat hindlimb when stimulated by an electrode placed on the sciatic nerve, is increased or decreased by infusion of type A or B vasoconstrictors, respectively (53;141). Furthermore, there is evidence that oxygen uptake by resting muscle is a function of oxygen delivery (90), thus offering an explanation why the vasomodulator-mediated redistribution of flow within muscle has such profound effects on oxygen uptake. It now appears likely that a large proportion of the muscle undergoes a physiological hypoxia during type B vasoconstrictor activity. But, as indicated above, the constant vasomotion activity may allow the sharing of this over the entire muscle with time. Thus, only the phosphocreatine/creatine ratio (not ATP/ADP) is compromised by a low ratio of nutritive/non-nutritive flow. For example during serotonin-mediated vasoconstriction, and this is reversed when the nutritive/non-nutritive ratio is increased upon serotonin withdrawl (181). Our group has proposed that the presence of the non-nutritive route in muscle may explain two phenomena which are developed further in sections below. These are a), the ability of many systemic vasodilators (e.g. bradykinin, nitroprusside or adenosine) to markedly increase limb blood flow without affecting insulin-mediated glucose uptake (115;124) or ameliorating insulin resistance (117); and b), the ability of insulin to increase capillary recruitment without either an increase in limb blood flow or a slowing in mean cell velocity in the capillaries (180). The notion of a non-nutritive route or functional shunt to explain the differences in clearance of intramuscular injected or infused markers due to exercise or vasodilators is not new and was invoked in the past by other researchers [see (35) and references therein].

## 1.3 The need to measure microvascular flow - possibilities including a flow through metabolised substrate and imaging of tissue perfusion

The need to be able to assess changes in muscle microvascular flow became apparent to a number of laboratories in the 1990s, but methods were largely indirect. For example, Bonadonna et al., (20) utilised a pulse injection into the brachial artery of 1-[$^3$H]-L-

glucose, an extracellular marker that fills both blood vessels and the interstitial space. Data from the washout curve allowed an estimate of the amount of tissue drained by the deep forearm vein to be estimated. The workers showed there was no change in the amount of muscle tissue drained comparing saline and a physiological dose of insulin (400 pM). But there was an increase in the extracellular volume in response to supraphysiological levels of insulin (5600 pM) suggestive that capillary recruitment had occurred. Yet other researchers have used intravital microscopy to directly assess capillary flow in the spinotrapezius muscle (143). These studies showed that a subcutaneous injection of insulin to anaesthetised rats dilated precapillary arterioles but did not alter vasomotion, whereas following glucose infusion to obtain similar insulin levels, there was an increased vasomotion, and a small constriction. Such changes were interpreted as evidence that insulin may have both a vasoconstrictor action and a larger vasodilatory action that must act in a coordinated manner to achieve a more optimal perfusion of the microvasculature. (143).

Our laboratory, cognizant of the controversy concerning the role of total blood flow in insulin action to control muscle glucose uptake and aware that contemporary methods were inadequate to assess microvascular perfusion, set out to develop new, more direct methods.

The initial intent was to design a method where metabolism of an introduced exogenous substrate would be a reflection of the extent of exposure of the substrate to an enzyme located in the nutritive capillaries. A number of criteria needed to be met. First, that the substrate was not vasoactive itself and therefore unable to influence the distribution of flow (i.e. the nutritive/ non-nutritive ratio). Second, that the substrate was metabolised to only one product by the capillary enzyme and that both the substrate and product were each recoverable from plasma and assayable. Third, that changes in metabolism of this substrate matched the change in nutritive/ non-nutritive flow that could be manipulated by the type A and B vasoconstrictors described above. A number of candidate substrates were tested, including those for phosphatases, 5'nucleotidases, proteases (angiotensin

converting enzyme), and xanthine oxidase. The substrate that fulfilled each of these criteria was 1-methylxanthine (1-MX), and this was targeted for xanthine oxidase.

Immunohistochemical evidence had shown that xanthine oxidase is concentrated in the muscle capillaries and is much less expressed in larger vessels and muscle itself (70;83). In the perfused rat hindlimb at constant flow there was a stoichiometric conversion of 1-MX to 1-methyl urate and both substrate and product were recovered without further metabolism. In addition, the changes in 1-MX metabolism correlated positively with changes in the proportion of nutritive flow in pump-perfused muscle under a number of conditions (137;199;199). More importantly, when applied to anaesthetised *ad lib* fed rats *in vivo* insulin (at doses which increased insulin levels 4-fold) increased 1-MX metabolism (138) in association with increased glucose uptake of hindlimb muscle. The changes in 1-MX metabolism were considered indicative of capillary recruitment that was nutritive to the muscle cell. Although at this relatively high dose, the insulin-mediated increase in capillary recruitment was accompanied by an increase in femoral artery blood flow, epinephrine infusions which produced similar increases in femoral artery blood flow did not affect capillary recruitment (measured by 1-MX metabolism), indicating that the two processes, capillary recruitment and total flow, could be dissociated. This finding suggested that a vasodilator, such as epinephrine, could increase total leg blood flow *in vivo* without increasing capillary recruitment or glucose uptake and could thus explain the human data where a number of vasodilators similarly increase flow but differentially affect glucose uptake. As alluded to above, the total flow increase in these circumstances is likely to be carried by the non-nutritive route.

There are now a number of experimental situations where our group has deliberately attempted to test the association between capillary recruitment and glucose uptake as regulated by insulin. In the first of these, a vasoconstrictor ($\alpha$-methyl serotonin), that decreases nutritive flow in perfused muscle (120), was found to inhibit insulin stimulated hindlimb 1-MX extraction *in vivo* and to impair insulin-mediated glucose uptake in the same hindlimb muscles (139). The serotonin agonist thus induced a state of insulin resistance with hypertension by preventing capillary recruitment and

presumably causing predominantly non-nutritive flow. Another approach involved TNFα, which is elevated in various insulin resistant states. When this was administered acutely it completely blocked the haemodynamic actions of insulin, including the increase in 1-MX metabolism and approximately 50% of the insulin-mediated glucose uptake (200). A third intervention involved the effect of acutely elevated free fatty acids through the infusion of Intralipid and heparin. Insulin-mediated capillary recruitment was markedly impaired in conjunction with impaired muscle glucose uptake (38). Taken together, insulin-stimulated glucose uptake by the hindleg *in vivo* was found to correlate tightly with 1-MX metabolism, an indicator of capillary recruitment, but showed no significant correlation with total limb flow (139) that was measured in these same studies. Thus, it would seem likely that this vascular action of insulin enhances perfusion of muscle, independently of changes in total flow, particularly in a time perspective. We have speculated that if this proves to be so, then insulin-mediated redistribution of blood flow from the non-nutritive route is likely (36).

A reasonable criticism that might be leveled at the 1-MX method is that it is an indirect method and cannot indicate relative flow distribution. Thus 1-MX reports only on the change in available capillary area for nutrient exchange. Our second technique is based on ultrasound imaging of the perfused microvasculature and not only has the potential to confirm the findings with 1-MX but to extend the information to relative flow distribution. Contrast-enhanced ultrasound (CEU) imaging as we, along with our collaborators at the University of Virginia, have now adapted for skeletal muscle microvasculature is based on that described by Wei et al. (191) for cardiac muscle in which microbubbles of albumin provide the contrast medium. Using a modified medical ultrasound / echocardiography machine the ultrasound probe is positioned over the target tissue (in this case skeletal muscle) and emits sonic energy and simultaneously transduces reflected energy to form a transverse sectional image through the muscle. The tissue to be measured receives the microbubbles via the vascular route at a steady state concentration, usually by way of systemic infusion. Under normal ultrasound imaging conditions the microbubbles resonate and become highly visible to the transducer therefore acting as a "contrast". The acoustic signal that is generated from the

microbubbles exposed to ultrasound is proportional to the concentration of microbubbles within the volume of tissue being imaged. The bubbles can consist of many different materials but the essential components are a hydrophobic – hydrophillic bilayer that encapsulates an inert gas. Furthermore the bubbles themselves must have no metabolic or vascular effect on the organism. These microbubbles can be destroyed (i.e. burst) by a pulse of high energy ultrasound thereby clearing the volume of tissue being imaged of any intact (and therefore contrast capable) microbubbles. Undestroyed bubbles from the neighbouring tissue then flow into the field of the ultrasound image to be reimaged after a set period of time. During an imaging sequence, the interval between the destructive high energy pulses (which is also used for imaging) is progressively prolonged to allow more replenishment of the microbubbles into the microcirculation. Once the images are collected a background subtraction (representing large vessels which fill rapidly) is made to isolate effects on capillaries and allow calculation of the "microvascular volume". The time rate of appearance of the microbubbles allows an estimate of the microvascular average filling velocity.

## 1.4 A place for Laser Doppler Flowmetry in assessing microvascular flow in muscle?

Another technique that could be applied to measuring microvascular perfusion in muscle is laser Doppler flowmetry (LDF). This has been used for a number of years to study skin blood perfusion and several research groups have documented impaired skin microvascular reactivity in diabetic subjects (23;77;158). In such studies microvascular function was assessed by measuring vasodilation in the forearm skin in response to iontophoresis of acetylcholine (77;158) although hyperemic response to local heating (23) was also used. Most significantly, Serne et al (157) have shown that iontophoresed insulin directly vasodilates skin microvasculature.

### *1.4.1 What does LDF measure?*

The interpretation of Doppler frequency shifted light backscattered from tissue to measure particle velocity was described (46) only four years after the first working Laser was demonstrated (111). However, the concept of laser Doppler flowmetry (LDF) as a means of measuring tissue perfusion is attributed to Stern (169) in 1975. In that work, spectral analysis of the photocurrent produced by backscattered Helium – Neon red Laser light from a human fingertip showed a clear difference between normal flow and after occlusion of the brachial artery. In the following years the instrument was redesigned and refined, most significantly by firstly allowing the laser light to be transmitted and received via fibre optic cables to allow more ease of positioning a probe head over the tissues. Additionally an empirically based processor was added in order to give a real time index of LDF value.

It may be argued that the term "flowmeter" or "flowmetry" is a misnomer as the technology is not usually able to estimate "flow" per se (i.e. volume per unit time). However, this terminology has been in widespread use and persists today although attempts have been made to refer to the technology as laser Doppler fluxmetry instead. laser Doppler flowmetry is purported to give a "real time measurement of microvascular blood cell perfusion through tissue" [Oxford Optronix, Oxford, UK literature 1998].

The theoretical basis of LDF is the utilisation of the well known Doppler frequency shift phenomenon that occurs when any type of regular wave pattern is reflected from an object in motion relative to the observer. A laser Doppler flowmeter consists of a probe attached to the main laser generating and detecting unit. The probe cable has one or more fibre optic cables that transmit the laser light to the tissue which then reflects and refracts throughout the tissue illuminating a volume of it. Via a separate, or the same, fibre optic cable, Laser light is transmitted from this volume back to the unit for sensing and processing. Laser light has the advantage over other types of light because it is monochromatic and relatively noise-free making interpretation of Doppler shifts possible even though the particle speeds are extremely small compared to the speed of the laser

light. When the laser light enters the target tissue (which must be translucent) the light is repeatedly reflected, refracted and absorbed. This multiple scattering process produces a volume of isotropic illumination in front of the probe head within the target tissue. This volume is not fixed for each unit/probe setup and depends upon the intensity of the laser light, the optical qualities of the target tissue, and the angle of incidence of the laser from the probe (tilting the angle of incident light increases the amount of light deflected before it enters the tissue). All moving solid objects capable of reflecting red light traversing the volume of illumination will be struck by beams of scattered laser light, and on each occasion the light reflects from a moving object it will be Doppler shifted. Thus the volume of illumination will contain a proportion of Doppler shifted laser light and the rest will be unshifted. Most of the light from the volume of illumination will diffuse into the tissues or be emitted away from the tissues. But the efferent optical fibres will carry some of the light "back scattered" from the volume of illumination back to the photodetectors in the laser Doppler flowmeter unit. The photodetectors convert the constituent light frequencies into electrical frequencies which are then immediately combined to generate new frequencies. This can involve either the sum of the two component frequencies or the difference between the component frequencies. The former frequencies have magnitudes of the order of $10^{15}$ HZ and are too high to be contained by electrical circuitry and are promptly dissipated. The remaining frequencies are identical to the Doppler evoked frequency differences and appear as a standard magnitude distribution (power spectrum) of frequencies lying within the range of 0 to 20 khz. (Oxford Optronix, UK, literature supplied with instrument, 1998). It is this product of power spectral area and mean frequency that is given the name "flux" which, within certain limitations (but suitable for physiologic purposes) is linearly related to the perfusion of a tissue by erythrocytes. The flux signal represents perfusion and is related to the mean particle (in biological tissue this can exclusively refer to erythrocytes) velocity and to the concentration of erythrocytes.

Having considered the theory behind the generation of the LDF signal it is now worth considering what it is that is actually measured by the instrument and some of the limitations in the use of the instrument. Although the LDF signal is linearly related

(within certain circumstances) to erythrocyte concentration and mean erythrocyte speed, it is not possible to calibrate this signal in terms of real units of flow. The missing parameter is that of sampling volume, which as alluded to earlier cannot be accurately predicted and is different each time the probe is directed at a different area of each tissue and at each different tissue. A thorough definition of "perfusion" is still lacking. For the purposes of helping to define what the LDF measures Leahy et al. (99) proposed the following definition: "Perfusion is the product of local speed and concentration of blood cells". The general sense of meaning of "perfusion" in physiological parlance is as an indication to the degree to which the tissues are nourished by the microcirculation and it is quite possible to imagine two separate examples of where the mathematical definition of perfusion are identical, but conceptually the degree of nourishment is quite different.

What can cause an increase in LDF signal "flux" or "perfusion" even though the total inflow to the organ is constant? One possibility is that flow has been diverted from outside the measurement field (ie outside the volume of illumination) into it. Alternatively, particularly in the case of vasoactive substances (e.g. vasoconstrictors such as norpinephrine or serotonin and vasodilators such as insulin) redistribution of blood flow between vessels of different architecture, may also explain a change in LDF signal. This will be a particular focal point of this thesis.

It is important to note that use of LDF probes to measure muscle microvascular blood flow has generally been restricted to resting muscle. This is not because the method per se would be invalid but because it cannot be assured that muscle movement and particularly muscle fibre contraction does not dislodge the placement of the probe.

### *1.4.2 Biological zero*

Any solid particle traversing the sampling volume of the LDF probe contributes to the flux signal, in most instances where living vertebrate tissue is the target the predominant signal generation will be due to the movement of erythrocytes (and to a much lesser extent other blood cells such as leukocytes and platelets). But an unpredictable portion of

the signal generation will be due to the movement of any number of other structures that are not necessarily blood borne such as vascular smooth muscle, skeletal muscle, cell membranes, organelles and vesicles. In addition to this, a volume of stationary blood is also capable of generating an LDF signal, probably through the process of Brownian motion. (108). When the LDF probe is targeted at a truly inanimate object the flux will register as zero with no baseline drift. But when the LDF probe is positioned over targets of organic tissue *in vivo* or *in vitro* and the blood flow is dropped to zero (e.g. by pressure cuff or artery clamp) the flux value does not drop all the way to zero. This value represents the amount of the flux signal which is not due to blood cell perfusion and is called the biological zero. This is subtracted from all LDF measurements previously taken from that exact spot. Otherwise, percentage changes in the flux will not reflect true changes. Historically, the biological zero has been found to be quite variable and often quite large when compared to the signals gained from basal flow. Chaplin and Hill (26) found the biological zero in murine tumours to vary from 4 to 77% and (108) reported an average biological zero of 73% of the basal in rabbit tenuissimus muscle.

As discussed earlier, LDF measures "microvascular perfusion", a product of local speed and concentration of erythrocytes (99). But this exists only within certain limits and LDF signal does not always correlate with total flow to the organ being monitored. For example, Kuznetsova et al. (93) measured LDF signal recorded from the biceps femoris muscle of anaethetised and ganglion blocked rats. Total muscle blood flow as assessed by radioactive microspheres was unchanged with the administration of angiotensin II (AII) and phenylephrine whilst LDF signal was increased. In further experiments they found that isoproterenol decreased LDF signal despite a large increase in total blood flow to the limb.

We have seen in previous work from this laboratory and discussed earlier in this Chapter how nourishment and perfusion of the rat hindlimb changes in spite of a constant total arterial inflow (32). Furthermore other *in vivo* studies have indirectly measured changes in capillary recruitment (by the 1-MX method) occurring independently of changes in total flow (138;139). These same vasomodulators also markedly alter muscle metabolism

only when they are being delivered by the vascular route (ie *in vitro* perfusion or *in vivo* but NOT when the muscle is incubated with the vasomodulators, (140)). Therefore a key question must surely be "what changes are occurring in the microvascular flow distribution to cause these metabolic alterations?" The approach of this thesis will be to assess LDF as a means of measuring changes in nutritive flow in muscle. Comparisons will be made to data from the two other methods referred to earlier of 1-MX metabolism and CEU. Attempts will be made to rationalise LDF signal changes from changes in cell speed in the absence of perfusion changes, flow being diverted into and out of the volume of illumination, modified pattern of flow within volume of illumination, and changes in haematocrit.

## 1.5 Aim

The aim of this thesis was to compare LDF with 1-MX metabolism and contrast enhanced ultrasound for the assessment of microvascular flow in skeletal muscle and in particular in relation to reports of direct and indirect effects of insulin to increase microvascular perfusion of this tissue *in vivo*.

# CHAPTER 2

## General Methods

### 2.1 Animal care

Animals were of either of three strains: Hooded Wistar (University of Tasmania), Wistar (University of Virginia) or Zucker (brought into Tasmania from Monash University Animal Breeding Facility, Melbourne). Hooded Wistar rats were raised on a commercial diet (Gibsons, Hobart) containing 21.4% protein, 4.6% lipid, 68% carbohydrate, and 6% crude fiber with added vitamins and minerals together with water *ad libitum*. Rats were housed at a constant temperature of 21 ± 1°C in a 12h/12h light/dark cycle. All procedures adopted and experiments undertaken were approved by the University of Tasmania Animal Ethics Committee, in accordance with the Australian Code of Practice for the Care and Use of Animals for Scientific Purposes (1990). Unless indicated otherwise rats were 'fed', in having had free access to food and water up to the time of experimentation.

### 2.2 Hindlimb perfusion

The surgical and perfusion procedures were essentially as described by others (149) with modifications by Colquhoun *et al.* (42). Briefly, animals were anaesthetised via an intra-peritoneal injection of pentobarbital sodium (60 mg.kg body wt) and the tail and tarsus of the perfused legs tied off firmly. An incision was made along the midline of the abdomen and the epigastric vessels and the iliolumbar vessels all ligated. Following this the testicles were ligated and removed. Ligatures were then placed around the duodenum and the rectum, and the large and small intestines were excised. Since only one hindleg was perfused, flow was prevented from entering the contralateral leg by ligation of the

opposite common iliac artery and vein. Prior to cannulation of the abdominal aorta and vena cava, heparin (1000 I.U.kg body weight$^{-1}$) was injected into the vena cava. A further ligature was placed around the abdomen (at the level of the L3~L4 vertebrae region) to prevent access of the perfusate to the muscles of the back. The perfusion medium used for perfusions was a modified Krebs-Henseleit bicarbonate buffer containing 7.1% (wt/vol.) bovine serum albumin (BSA, fraction V; Boehringer Mannheim, Australia), 8.3 mM glucose, 2.54 mM $CaCl_2$, 118 mM NaCl, 4.7 mM KCl, 1.2 mM $KH_2PO_4$, 1.2 mM $MgSO_4$, and 25 mM $NaHCO_3$. Once made, the perfusion buffer was filtered using a 0.45µm pore filter under pressure to ensure, that it was free of any particulate matter. The buffer was maintained at a pH of 7.4 by saturation with 95% air-5% $CO_2$. This was combined with washed bovine erythrocytes to give a final haematocrit of 38%. Heparin (0.2 ml.L$^{-1}$) and pyruvate (0.1 g.L$^{-1}$) were added to the blood mixture. The fresh bovine erythrocytes were filtered through four layers of pre-washed cheesecloth and washed three times using saline (0.9% NaCl). They were then washed twice more in saline and stored in Krebs-Henseleit bicarbonate buffer gassed with 95% air-5% $CO_2$ at 4°C until use. Erythrocytes were never more than 3 days old when used. As with previous similar studies (141), this perfusion medium resulted in minimal oedema.

Hindlimb perfusions of 205 ± 5g rats (local strain of hooded Wistar) were conducted essentially as described previously (141). Modifications included two heat exchangers, bubble trap and a small magnetically stirred injection port (1.0 ml capacity) immediately prior to the arterial cannula (arterial perfusate temperature was 37°C). In addition the rat was placed on a water-jacketed platform heated to 37°C, so that the hindlimb could be maintained at 37°C. The whole apparatus including the rat was contained within a heat-controlled cabinet at 37°C. The buffer reservoir was kept on ice and continuously stirred, whilst being gassed with 95% air-5% $CO_2$. Perfusate was then pumped at a constant flow rate by a peristaltic pump (Masterflex, Cole-Palmer, USA) to a heat exchanger coil where the temperature was brought to 37°C prior to passing through a silastic lung, also gassed with 95%air-5% $CO_2$. Venous oxygen tension was continuously monitored using a thermostatically controlled (37°C) in-line Clark-type oxygen electrode (0.5 ml capacity). Arterial perfusion pressure was monitored continuously via a pressure transducer located

proximally to the aorta. Recording of $PO_2$ and pressure was performed continually by an IBM compatible PC computer with WINDAQ data acquisition software (DATAQ Instruments). Oxygen content was determined using an in-line oxygen analyser (A-Vox Systems Inc, San Antonio, Texas). Oxygen consumption was calculated as described in the respective chapter.

## 2.3 Hyperinsulinaemic clamp

For *in vivo* studies using rats, the hyperinsulinaemic euglycaemic clamp was used. The following details for the insulin clamps have been sourced from other publications from this laboratory (138;139).

Rats were anaesthetized using Nembutal (50 $mg.kg^{-1}$) and had polyethylene cannulas (PE-50, Intramedic®) surgically implanted into the carotid artery, for arterial sampling and measurement of blood pressure (pressure transducer Transpac IV, Abbott Critical Systems) and into both jugular veins for continuous administration of anaesthetic and other intravenous infusions. A tracheotomy tube was inserted, and the animal was allowed to spontaneously breathe room air throughout the course of the experiment. Small incisions (1.5 cm) were made in the skin overlaying the femoral vessels of both legs, and the femoral artery was separated from the femoral vein and nerve. The epigastric vessels were then ligated, and an ultrasonic flow probe (Transonic Systems, VB series 0.5 mm) was positioned around the femoral artery of the right leg just distal to the inguinal ligament. The space surrounding the artery created by its isolation surrounding the flow probe was filled with lubricating jelly (H-R, Mohawk Medical Supply, Utica, NY) to provide acoustic coupling to the probe. The probe was then connected to the flow meter (Model T106 ultrasonic volume flow meter, Transonic Systems). This was in turn interfaced with an IBM compatible PC computer which acquired the data (at a sampling frequency of 100 Hz) for femoral blood flow and blood pressure using WINDAQ data acquisition software (DATAQ Instruments). The surgical procedure generally lasted approximately 30 min and then the animals were maintained under anaesthesia for the duration of the experiment using a variable infusion of Nembutal (0-0.6 $mg.min^{-1}.kg^{-1}$) via the left jugular cannula. The femoral vein of the left

leg was used for venous sampling, using an insulin syringe with an attached 29G needle (Becton Dickinson). A duplicate venous sample was taken only on completion of the experiment (120min) to prevent alteration of the blood flow from the hindlimb due to sampling, and to minimize the effects of blood loss. The body temperature was maintained using a water-jacketed platform and a heating lamp positioned above the rat.

Following a 1 hour equilibration, various protocols as stipulated in each chapter were undertaken. In general the protocols involved hyperinsulinaemic euglycaemic clamps or appropriate controls and occurred over a 2h period.

## 2.4 Contrast Enhanced Ultrasound

CEU has been used extensively in the past to measure microvascular flow in the myocardium (109;130;190). Estimates of microvascular flow using CEU have been validated using 11-μm radiolabeled microspheres to show that there is a strong correlation between the two techniques ($r = 0.96$, $P < 0.001$) (190). The technique was modified for its use for the rat as follows: a linear-array transducer interfaced with an ultrasound system (HDI-5000; ATL Ultrasound) was positioned over the right leg of the rat and secured for the course of the experiment. The adductor magnus and semimembranosus muscles of the hindlimb were imaged in short-axis with intermittent harmonic imaging at a transmission frequency of 3.3 MHz. The mechanical index ([peak negative acoustic pressure] x [frequency]$^{-1/2}$), a measure of acoustic power, was set at 0.9. The acoustic focus was set at the mid-portion of the muscle group. Gain settings were optimized and held constant for the duration of each experiment. Data were recorded on 1.25-cm videotape using a S-VHS recorder (Panasonic MD830; Matsushita Electric). Albumin microbubbles containing octafluoropropane gas (Optison; Mallinckrodt Medical) were infused intravenously at 120 μl/min for the duration of data acquisition. The acoustic signal that is generated from the microbubbles exposed to ultrasound is proportional to the concentration of microbubbles within the volume of tissue being imaged. This greater acoustic signal is represented as a brighter video intensity which is

later quantified by image analysis of the videotape recording. Essentially, all microbubbles within the ultrasound beam are simultaneously imaged and destroyed in response to a single pulse of high-energy ultrasound (190). As the time between successive pulses is prolonged, the beam becomes progressively replenished with microbubbles (190). Eventually, the beam is fully replenished, and further increases in the time between each pulse do not affect microbubble signals in the tissue (Fig. 2.1). The rate of microbubble reappearance within the ultrasound beam provides an indication of microvascular flow velocity (ß), and the plateau video intensity reached at long pulsing intervals provides a measurement of MV (190).

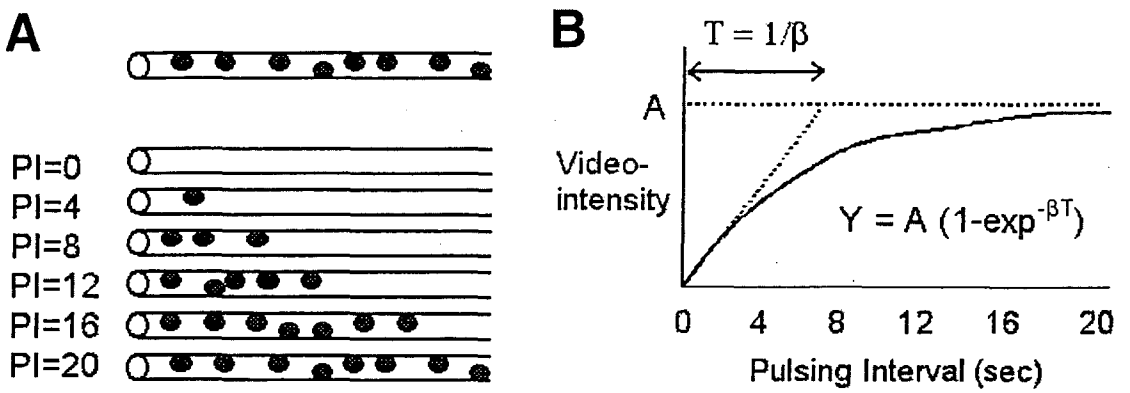


**FIG. 2.1.**

*A*: Schematic depiction of the replenishment of microbubbles in capillaries after a pulse of high-energy ultrasound. As the time between each ultrasound pulse is prolonged, more microbubbles reappear. PI, pulsing interval.

*B*: A typical relation between pulsing interval and acoustic signal, measured as video intensity. As the pulsing interval is prolonged, the number of microbubbles within the capillaries increases, resulting in a higher video intensity. Eventually a plateau is reached where the time interval between each pulsing interval does not cause a further increase in video intensity due to complete replenishment of the vessels in the beam. The asymptote that intercepts the *y*-axis is the maximal video intensity signal and a measurement of MV. The *x*-intercept of the *y*-axis asymptote and the tangent to the upward sloping hyperbolic function is a measure of the rate constant of video intensity rise ($\beta$), an indicator of microvascular flow velocity.

For the current study, images were acquired during continuous imaging and at pulsing intervals from 1 to 20 s. Image analysis was performed off-line. Frames were aligned by cross-correlating several frames at each pulsing interval and were separately averaged and digitally subtracted from averaged frames obtained during continuous imaging (obtained at a pulsing interval of 30 ms), which served as background. Using continuous imaging frames as background allowed for the elimination of the contribution by larger vessels (velocity >100 μm/s) to overall video intensity. The background-subtracted video intensity at each pulsing interval was measured within the area of interest in muscle, and pulsing interval versus video intensity data were fitted to the function [$y = A\ (1 - e^{-ßt})$], where $y$ is video intensity, $t$ is the pulsing interval, $A$ is plateau video intensity (an index of MV), and ß is the rate constant, which provides a measure of microvascular flow velocity (Fig. 2.1, (190)).

## 2.5 Laser Doppler Flowmetry

LDF has a history now dating back almost 30 years in its application to the measurement of blood perfusion in tissue (169). In his work Stern (169) proposed that when coherent light from a device such as a laser emitter impinges on tissue, some of it will be scattered by the moving red blood cells and some by static tissue. If this light which is spectrally broadened due to the Doppler effect is brought to the surface of a sensitive photodetector, optical beating will produce an audio-frequecy photocurrent output. Spectral analysis of the photocurrent produced by the backscattered He-Ne red laser light showed changes consitent with perturbation to flow such as arterial occlusion. For skin Stern (169) noted changes in LDF signal that matched known effects on blood flow due to temperature, posture, respiratory pattern and emotional stimulation. With the introduction of fibreoptics for light delivery and collection, it soon became evident that the distance between delivery and collection fibres determined the volume of tissue under measurement. So, in this thesis a variety of probes were used, including micro-probes that could be impaled into muscle with minimal tissue damage and which because of their small size were able to detect heterogenity of sites. In addition macro-probes were used

which were insensitive to the heterogeneity but rather, detected signal change from the majority site at the surface of the muscle. For all stationary probes there was considerable variation in range of absolute signal, but this was largely attributable to the background scattering and encompassed by the 'biological zero'. In one study a scanning laser probe was used and the LDF signal measured at each point on the surfae of a muscle could be represented as a colour-coded picture of the changes before and after perturbation. Full details on the use of each of these probes, along with a technical description of each apparatus are given in the relevant Chapters.

## 2.6 Analytical methods

A glucose analyser (Model 2300 Stat plus, Yellow Springs Instruments, Yellow Springs, OH) was used to determine whole blood glucose (by the glucose oxidase method) during the experiment. A blood sample of 25 μl was required for each determination. Insulin levels at the beginning and end of the experiment were determined from arterial plasma samples by ELISA assay (Mercodia AB, Sweden). Perchloric acid treated plasma samples were centrifuged for 10 min and the supernatant used to determine 1-MX, allopurinol and oxypurinol concentrations by reverse-phase HPLC as previously described (138).

## 2.7 1-MX metabolism

Since 1-MX (Sigma Aldrich Inc) clearance was very rapid, it was necessary to partially inhibit the activity of xanthine oxidase. To do this, an injection of a specific xanthine oxidase inhibitor, allopurinol (10 $\mu mol.kg^{-1}$) was administered as a bolus dose 5 minutes prior to commencing the 1-MX infusion (0.4 $mg.min^{-1}.kg^{-1}$). This allowed constant arterial concentrations of 1-MX to be maintained throughout the experiment. At the end of the experiment blood was sampled from the femoral vein and carotid artery. From the arteriovenous difference multiplied by the flow, hindleg glucose uptake and 1-MX disappearance were calculated. The latter was used as an indicator of perfused capillary surface area.

## 2.8 Muscle glucose uptake using 2-deoxyglucose

A bolus dose of [$^3$H]2-deoxyglucose (50μCi) was given 45 minutes before the end of the experiment. The removal of 2-deoxyglucose from the blood was determined in plasma samples taken at 5, 10, 15, 30 and 45 minutes following the injection. Muscles were excised at the completion of the experiment and freeze clamped in liquid nitrogen to assess the [$^3$H]2-deoxyglucose-6-phosphate as described previously (200).

The total blood volume withdrawn from the animals before the final arterial and venous samples did not exceed 1.5 ml and was compensated by the volume of fluid infused.

Details on **Data Analysis** and **Statistical Analysis** can be found in each of the relevant individual Chapters.

# CHAPTER 3

## Laser Doppler Flowmetry: measuring nutritive flow in blood perfused rat hindlimb muscle

### 3.1 Introduction

Skeletal muscle microvascular perfusion is not always directly related to the total blood flow of muscle. This has been noted *in vivo* rat muscle using LDF (93). This observation is not new, indeed studies from the 1940s and 1950s (129,186,144,8,9,76,162) have all produced results that point out a discrepancy between total flow and perfusion of the muscle tissue. Although there may be other explanations, such evidence seems to strongly suggest that skeletal muscle does in fact have (at least functionally speaking) two quite separate circulatory systems. To produce a discrepancy between total flow and organ perfusion it was proposed that a functional shunt must exist, acting by denying the opportunity for nutrient exchange to occur between the muscle cells and the constituents of the blood. The two circulations have been referred to as "nutritive" and "non-nutritive" (8;9), and on account of the physiological description of "shunting" in skeletal muscle there was obviously a desire to describe these shunts anatomically. Histological studies (69) had found that there did not exist in muscle a similar arrangement to skin where large diameter (approx 50 μm) arteriovenous anastomoses allowed wholesale shunting of arterial to venous blood. Additionally failure of the hindlimb to pass 12um microspheres through perfused hindlimb (121) muscle essentially disproved the possibility of arteriovenous shunts greater than this size. Grant and Wright (67) first described the anatomical difference of tendon capillaries to those capillaries normally associated with myocytes. It has been theorised that the slightly larger diameter, shorter length and physical isolation of these vessels would conduct flow from the arterial to venous circulation with minimal opportunity for nutrient exchange with the myocytes and therefore possibly be an anatomical explanation of non-nutritive flow. Vessels in the

nutritive pathway were considered to be those in direct contact with the skeletal muscle cells (75).

Research from our laboratory using the constant-flow perfused rat hindlimb has shown that skeletal muscle metabolism including oxygen uptake and lactate release as well as aerobic contractile performance is controlled by vasomodulators that act to alter flow distribution within muscle (32;34). Because of the quite distinctly opposing effects of these vasomodulators they have been classified into two groups, "Type A" and "Type B" vasoconstrictors. Type A vasoconstrictors act to increase metabolism (as indicated by oxygen uptake and lactate release (32) and contractile performance (141)) by redirecting flow from a putative non-nutritive route to nutritive capillaries within muscle (121). Conversely the second group of vasoconstrictors, referred to as Type B, has the opposite effect and acts to decrease oxygen uptake, lactate release (32) and aerobic contractile activity (53). These vasoconstrictors affect metabolism only in a perfusion and not during incubation (140) and their effects are reversed by vasodilators (regardless of the vasodilator mechanism of action) (41;140). Because the changes to metabolism occur in a constant flow perfusion situation they do not exert their effects by altering total flow to muscles but presumably do so by redirecting flow within the hindlimb muscles (121;141). In other words flow is being directed away from the nutritive route (which is most likely to consist of capillaries in intimate and extensive contact with the myocytes) to the non-nutritive route (i.e. functional shunts). Because non-nutritive flow has a converse effect on metabolism it stands to reason that non-nutritive vessels should have the anatomical characteristics to limit the opportunity for nutrient exchange as the blood passes from the arterial to the venous systems. Examples of such anatomical characteristics include: physical isolation from the myocytes (the non nutritive vessels may be located in muscle associated connective tissue), non-nutritive capillaries are shorter, may have larger diameters, or may have endothelial characteristics which impair diffusion. Evidence that vessels associated with connective tissue behave in a pharmacologically different manner from other vessels in muscle can be found in observations made by intravital microscopy in response to hypoxia, beta adrenergic agonists, etc. (104). Grant and Wright (67) anatomically identified vessels in the

connective tissue which they thought may be part of the non nutritive network. More recent studies (122) demonstrated an inverse relationship between perfusion of tendon vessels and muscle metabolism. Indeed, direct evidence for these latter vessels has been obtained by Ley and colleagues (100), who showed them to be major routes for the shunting of leukocytes.

In this Chapter, an investigation was made of the LDF signal responses of macro surface and implantable micro probes positioned on or in hindlimb skeletal muscles, respectively. The responses to changes in total flow and to vasoconstrictors that are known to alter hindlimb metabolism between nutritive and non-nutritive flows were characterised.

## 3.2 Methods

### *3.2.1 Hindlimb Perfusions*

Hindlimb perfusions of 205 ± 5g rats (local strain of hooded Wistar) were conducted essentially as described previously in Chapter 2. In brief, the hindlimb was maintained at 37°C for all blood perfusions. Significant differences from the standard perfusion procedure to help achieve this goal included the use of two heat exchangers (instead of one), and additional bubble traps including a smaller than usual magnetically stirred bubble trap (1.0 ml capacity) downstream from the injection port immediately prior to the arterial cannula specifically to allow bolus injection of vasomodulators. In addition the rat was placed on a water-jacketed platform heated to 37°C, with a thermometer kept in close contact with the dorsum of the hindquarter for monitoring purposes. Initially the flow rate was increased to 15 ml/min for 5 min to clear all red cells of rat origin. Due to the hindlimb being almost fully vasodilated (147), supra-physiological flow rates were required to obtain physiological levels of pressure. Consequently the flow rate of 4.0 ± 0.1 ml/min, equivalent to 0.27±0.01 ml/min/g of muscle, was selected as a compromise. Previous studies using fluorescent microspheres for determining regional flow (137) have suggested that the muscles of the thigh, hip and calf receive flow at approx. 76% of the total hindlimb rate (or 0.20±0.02 ml/min per g). Selected agents known to have

metabolic effects through vasomodulation on the hindlimb were administered either as a bolus injection (NE, angiotensin II, vasopressin, or 5-HT) or in separate experiments as continuous infusions (NE and 5-HT). To hasten complete removal of preceding dose or agent following its administration, flow was momentarily increased to 8ml/min for 2 min. This also improved the reproducibility of subsequent identical doses.

### *3.2.2 LDF*

#### *3.2.2.1 Surface measurements*

A small hole (approx. 4 mm diameter) was made in the skin over the middle of the biceps femoris corresponding to the point "bf" in Figure 3.1. The hindlimb was then clamped by the foot so that the laser Doppler flow probe (Perimed PF 2, operating wavelength of 632 nm) could be positioned over the center of the hole. The probe was placed vertically above and approx. 1 mm from the surface of the muscle, and preliminary experiments showed that such an arrangement produced a LDF signal that was linearly related to changes in perfusion total flow rate, verifying that it was likely that perfusion by blood cells was being detected by the instrument. The probe comprised three fibres each 800 μm diameter with one for illumination and two for detection. Settings on the detector unit were 4 kHz (gain setting 10) with a time constant of 3 s, unless otherwise indicated. The signal (0-5 volts) was continuously recorded on an IBM compatible PC using a DI-190 I/O module and WINDAQ® software. The data are expressed as volts.

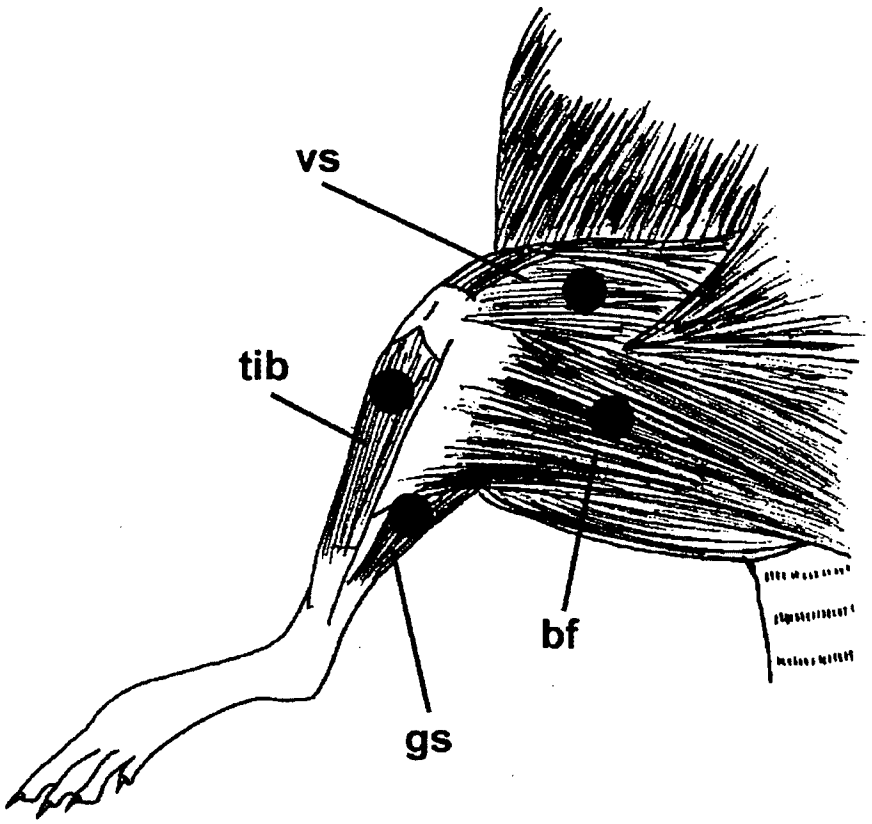


**Figure 3.1. General areas chosen for positioning of LDF probe either on or impaled into muscles of the perfused rat hindlimb.** The macro LDF probe (3 × 800 μm) was always positioned over the biceps femoris at the site designated 'bf' through a hole in the skin. The micro optic fibre probe (0.26mm diameter) was inserted through a small incision in the skin in the approximate positions shown on either the tibialis (tib), vastus (vs), biceps femoris (bf), or gastrocnemius (gs) muscles. The mechanism for insertion of the micro optic fibre probe involved an initial right angle puncture of the muscle surface, insertion for 1 or 2 mm then gentle rotation of the probe so as to be in parallel with the muscle axis, and a further insertion for 3 to 6mm. Apart from the general region indicated, positioning of the micro probes including precise site, initial depth and final penetration was randomly chosen.

*3.2.2.2 Impaled microprobe for within muscle measurement*

A Moor Instruments Lab Server and Lab Satellite fitted with two P10M master probes was used with two P10s TCG 260 μm slave probes each fitted with TCG fixed fibre. The operational wavelength of the laser light source was 780 nm. The fibre consisted of a single core of optic fibre (200 μm diameter) surrounded by protective flexible outer sheath. Following prior skin incision using surgical scissors, the optical fibre was found to be sufficiently robust as to be able to be inserted into the muscle unaided by prior needle puncture. Measurements were made using the P0 setting (MoorLAB V36 embedded software). This setting scales the raw LDF output by a factor of 10-fold and was used to improve the quality of the recorded signal. Subsequently, LDF values were scaled to express the results in perfusion units (PU) by a factor from measurements made on the manufacturer's calibration fluid for each probe. Small incisions were made into the skin covering the mid-region of any two of the tibialis, vastus, gastrocnemius or biceps femoris (Figure 3.1) of the perfused leg and the two probes inserted. The procedure for insertion of each probe involved initial puncturing of the epimysium and muscle body to a depth of approx. 2 mm with the probe at right angles to the muscle surface, followed by rotation of the probe through 90° to be parallel to the longitudonal direction of the muscle fibers. The probe was then inserted a further 3 to 6 mm and taped in place. This procedure avoided wounding and only 4 of the 97 sites were considered corrupted due to bleeding. Apart from the evidence of bleeding it was impossible to entirely rule out tissue damage. Indeed, as pointed out by Oberg (126) using very thin optical fibers (50-200), the trauma can be minimal with little disturbance to blood flow. After completion of the perfusion the final placements were confirmed by surgical examination. In some animals the probes were repositioned in other muscles up to two additional times. This allowed assessment of as many as six different sites per hindlimb. The LDF signal (0-5 volts) was continuously recorded on an IBM compatible PC using a DI-190 I/O module and WINDAQ® software. The data are expressed as perfusion units (PU), to be consistent with the manufacturer's recommendations and to be distinguished from those of the surface probe which differed in size and operating wavelength.

For each perfusion "biological zero" was determined by switching off the perfusion pump for 5 min and waiting until venous perfusate flow ceased, with the LDF probe still in position. Biological zero was not subtracted from any of the data shown.

### *3.2.3 Vasoconstrictor infusions*

To determine linearity of LDF response, perfusion flow rate was varied from 4 through 6 to 8 ml/min and LDF signal recorded. With flow set at 4 ml/min, administration of norepinephrine (NE, 0-0.3 nmol), angiotensin II (0.3 nmol), vasopressin (0.03 nmol), or serotonin (5-HT, 0-3 nmol) was made as a 12.5 or 25 µl bolus (over 2s) into the stirred injection port. In some experiments constant infusions of NE (85 nM) or 5-HT (850nM) were made by infusing into the injection port a concentrated stock solution of each agent at 1.7% of the perfusate flow rate.

### *3.2.4 Perfusion pressure and oxygen uptake*

Perfusion pressure was also continuously recorded using WINDAQ®. Perfusate entering and leaving the hindlimb was passed through an in-line oxygen analyser from A-Vox Systems, Inc, San Antonio, Texas and the signal continously recorded also using WINDAQ®. $VO_2$ was then calculated using the following equation:

$$VO_2\ (\mu mol.h^{-1}.g^{-1}) = \frac{A - V\ O_2\ (ml\ O_2/100ml) \times flow\ rate\ (ml/min) \times 321.43}{Rat\ weight\ (g)}$$

### *3.2.5 Statistical analysis*

Data were analysed using Sigma Stat ™ (Jandel Scientific). Comparison of basal signal strength for nutritive, non-nutritive, and mixed, unpaired analysis (Students' t-test) was used. For comparison of basal signal strength of nutritive, non-nutritive, and mixed sites, unpaired analysis (Students' t-test) was used. For effects of vasoconstrictors and flow on

LDF signal, paired analysis (Students' t-test) was used. Potential correlations were assessed by regression analysis using Sigma Stat ™ (Jandel Scientific).

## 3.3 Results

### *3.3.1 Surface measurements*

The macro LDF probe was designed primarily for measurement of human skin blood flow. It was therefore necessary to consider the suitability of using this instrument to monitor microvascular perfusion in erythrocyte perfused rat hindlimb studies. Others have shown that capillary red cell velocity in resting muscle does not exceed $1 mm.s^{-1}$ for a blood flow of $0.05 ml.min^{-1}.g^{-1}$ (178), thus at a flow rate of $0.27 ml.min^{-1}.g^{-1}$ as used in the present perfusions, cell velocities should still be less than the critical limit of $8 mm.s^{-1}$. This was tested by measuring the LDF signal from the muscle at flow rates between 1 and 10 $ml.min^{-1}$. Within this range of flow rates the signal was found to be linear ($r=0.833$; $P<0.001$, $n=59$). At flow rates above this, the critical limit of red cell velocity of 8 $mm.s^{-1}$ is likely to have been exceeded.

Slight movements of the perfused hindlimb in relation to the probe must not significantly affect the LDF value. This was tested by proving no significant variation in LDF as probe to target distance was varied (whilst directed at the same region of muscle) from 0 to 1.5 mm (not shown).

Positioning of the probe was found to be important and was placed in the same location in the centre of the anterior end of the biceps femoris. Without exception, when measured with the PeriMed macro probe, this site always behaved the same displaying increased LDF signal response to NE and decreased signal response to 5-HT injection. Other sites responded differently. Thus from a total of 28 sites involving 11 in the center of the biceps femoris (all responding as above), 8 on the tibialis anterior and 9 on the tibial tendon of the biceps femoris, 20 responded as above, 3 responded in an opposite manner

(NE inhibitory and 5-HT stimulatory) and 5 appeared as intermediate with no response to either NE or 5-HT.

A time course from a typical experiment is shown in Figure 3.2 where LDF signal on the surface of the biceps femoris muscle vessels was measured as well as perfusion pressure and oxygen uptake for the hindlimb during successive injections (25 μl) of 300 pmol NE and 3 nmol 5-HT. NE (300 pmol), equivalent to a peak concentration of 15-50 nM (estimated from injection and perfusion flow rates), increased LDF signal in association with increased perfusion pressure and a stimulation of oxygen uptake. Values for LDF and oxygen uptake returned to basal approx. 3 min following NE injection. 5-HT (3nmol), equivalent to a peak concentration of 150-500 nM, decreased LDF signal in association with increased perfusion pressure and an inhibition of hindlimb oxygen uptake (Figure 3.3).

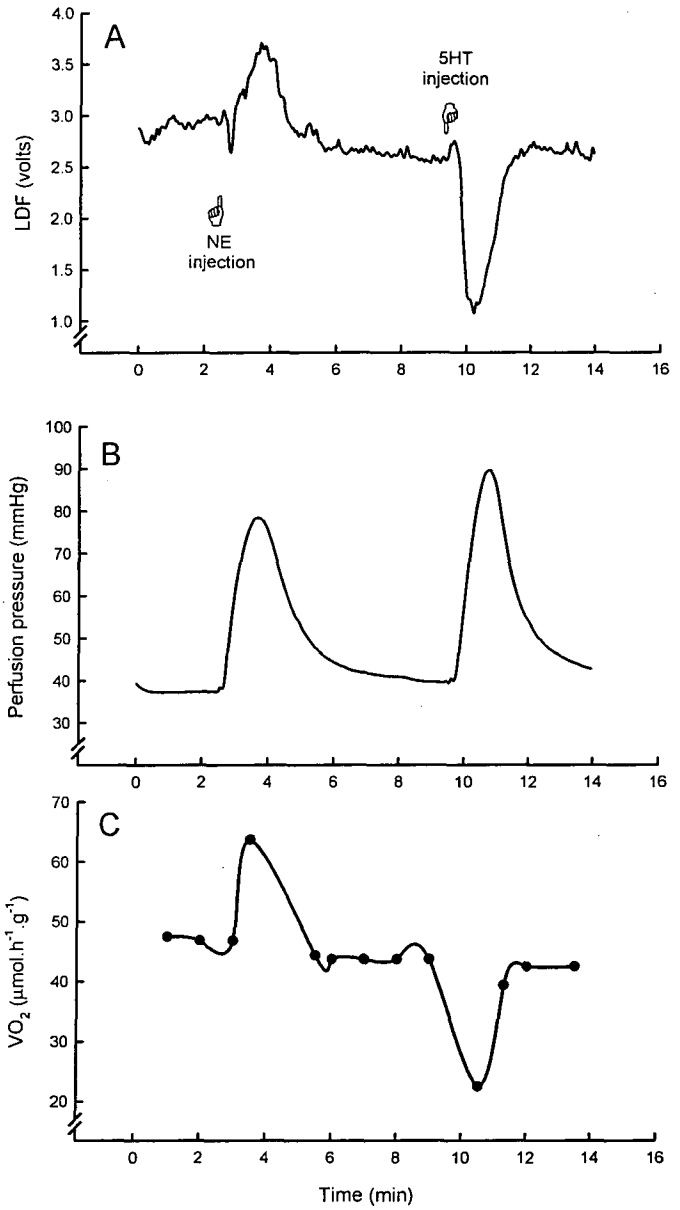


**Figure 3.2 Typical trace of LDF signal from the macro surface probe positioned at the centre of the anterior end of the biceps femoris muscle.** (A), arterial perfusion pressure (B) and oxygen uptake (C) following injection of 300 pmol of NE (Type A vasoconstrictor) and 3 nmol of 5-HT (Type B vasoconstrictor) into the constant-flow perfused rat hindlimb. Biological zero has not been subtracted.

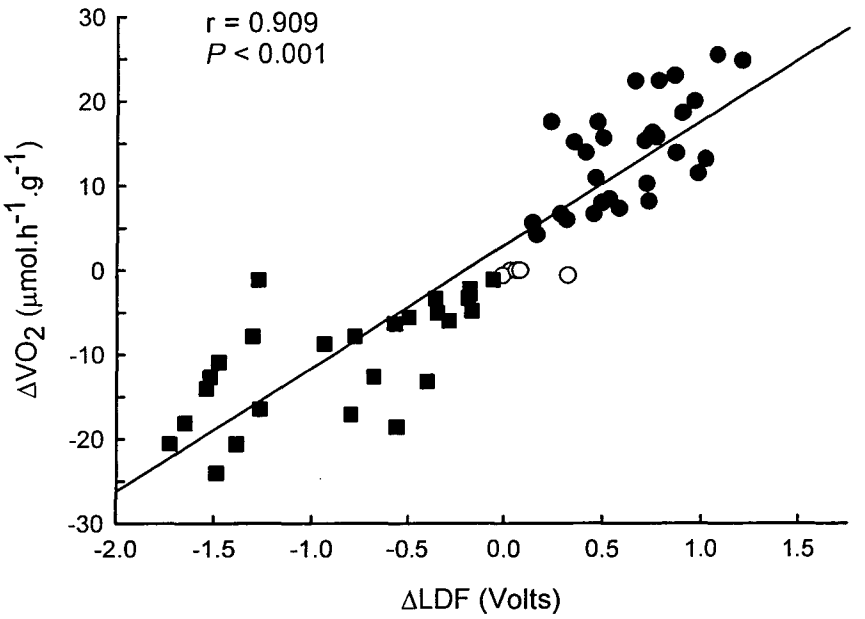


**Figure 3.3 Relationship between peak change in oxygen uptake and LDF signal from the surface macro probe for the constant-flow perfused rat hindlimb.** Values for LDF signal are (●) NE, (○) vehicle, and (■) 5-HT.

### *3.3.2 Impalable probes*

The macro probe has a total diameter, including housing, of 6 mm and could therefore not be impaled into the muscle without serious tissue disruption. As indicated above, provided the probe was positioned over muscle, only NE-positive sites were observed. Thus to investigate signal changes at higher spatial resolution smaller ("micro") impalable probes were used. Figure 3.4 shows the properties of LDF signal from randomly positioned micro probes placed in the tibialis, vastus, biceps femoris, or gastrocnemius muscles. The majority of sites responded positively to norepinephrine bolus (Figure 3.4A) with an increase in LDF signal of greater than 5% of basal, but some clearly responded negatively with a decrease in LDF signal (decreasing by more than 5% of basal). In addition, there was a group that did not respond (i.e. less than ± 5% of basal signal). *Panel B* of Figure 3.4 shows the responses of these same sites to serotonin bolus. Again, three types of response were discernable with the majority responding negatively to serotonin and two other groups where the response was positive (signal increasing) or showing no change. In some sites the negative response to serotonin was so marked that the LDF signal was effectively reduced to biological zero. Invariably, the sites that responded positively to norepinephrine were those that responded negatively to serotonin. These are thus designated as "NE-positive". The other two types of site are designated "NE-negative" or "mixed" depending upon whether the LDF signal decreased in response to norepinephrine and increased in response to serotonin, or showed less than 5% change to either vasoconstrictor, respectively. It is important to note that although norepinephrine and serotonin each cause a pressure rise (vasoconstriction), they have stimulatory or inhibitory effects on whole hindlimb oxygen consumption metabolism, respectively.

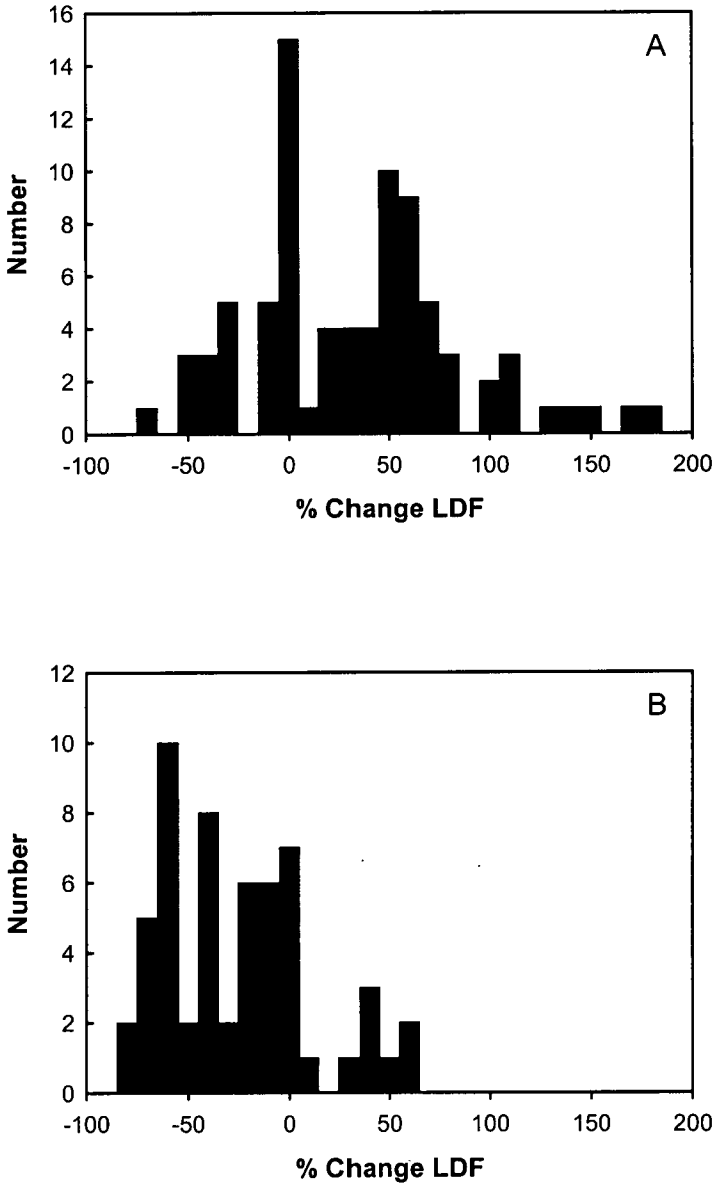


**Figure 3.4 Distribution of LDF signal changes from impaled micro probes.** Values obtained after NE (A) or 5-HT (B) were expressed as a percentage of the basal signal and grouped in intervals of 10% starting from +5% and –5%.

Characteristic traces of NE-positive, NE-negative sites and mixed are shown in Figure 3.5. NE-positive sites showed LDF signal changes in parallel to oxygen uptake, i.e. increases and decreases with NE and 5-HT, respectively. NE-negative sites showed LDF signal changes opposite to oxygen uptake. For the total of 97 sites examined 56.7% were found to be NE-positive, 16.5% NE-negative and 24.7% mixed. Only 2.1% were corrupted due to bleeding. Table 3.1 also shows that basal LDF signal strength was greater at NE-negative sites than either NE-positive or mixed sites and all three sites responded significantly to a doubling of flow rate from 4 to 8 ml/min. Although not shown by the data of Table 3.1 a break down of the data revealed there were differences between the muscle types with basal signal from NE-positive sites in tibialis (24.7 ± 2.2; n=28) similar to gastrocnemius (21.7 ± 4.5; n=12) but greater than either biceps femoris (12.9 ± 2.3; n=6, $P<0.01$) or vastus (12.4 ± 2.8 PU; n=9, $P<0.02$).

Table 3.2 summarizes the response of NE-positive sites to flow and vasoconstrictors, including 5-HT, NE, vasopressin and angiotensin II. Whole hindlimb oxygen uptake as well as perfusion pressure are also shown. Increasing the pump flow rate progressively from 4, though 6 to 8 ml/min increased the LDF signal from 14.2 ± 1.0 to 22.8 ± 1.4 PU. Allowing for a biological zero of approximately 7.4, the increase due to flow represents a 2-fold increase. Whole hindlimb oxygen uptake and perfusion pressure increased by 29.4% and 65.3%, respectively. Three of the vasoconstrictors, NE, vasopressin, and angiotensin II each increased the LDF signal in parallel to their effects on oxygen uptake. 5-HT inhibited both and in many cases the signal strength due to 5-HT was indistinguishable from biological zero for that site.

**Table 3.1 Properties of LDF signal from the randomly positioned muscle micro probes**

| Site Identity | Fraction of Total, % | Basal Signal at 4 ml/min, PU | Range, PU | Signal at 8 ml/min, PU | n |
|---|---|---|---|---|---|
| NE-positive | 56.7 | 20.7 ± 1.8 | 3.4 - 61.9 | 35.8 ± 3.4* | 47 |
| NE-negative | 16.5 | 33.2 ± 5.4# | 10.4 - 87.4 | 53.7 ± 10.5* | 16 |
| Mixed | 24.7 | 22.3 ± 2.7 | 5.0 - 60.1 | 35.7 ± 6.1* | 22 |
| Corrupted | 2.1 | | | | |

Sites were classified as NE-positive, NE-negative or mixed depending on responses to the vasoconstrictors NE and 5-HT as shown in Fig. 3.4. Those deemed as "corrupted" resulted from bleeding at the point of probe insertion. A total of 97 sites were assessed from 35 hindlimb perfusions involving sites on each of the tibialis, vastus, biceps femoris, and gastrocnemius muscles. Response to flow was assessed when flow was increased from 4 to 8 ml/min. Otherwise, flow was maintained constant at 4ml/min. Values are expressed in perfusion units and are means ± SE; *, $P< 0.05$ relative to basal. #, $P< 0.05$ relative to 'NE-positive'. Biological zero has not been subtracted.

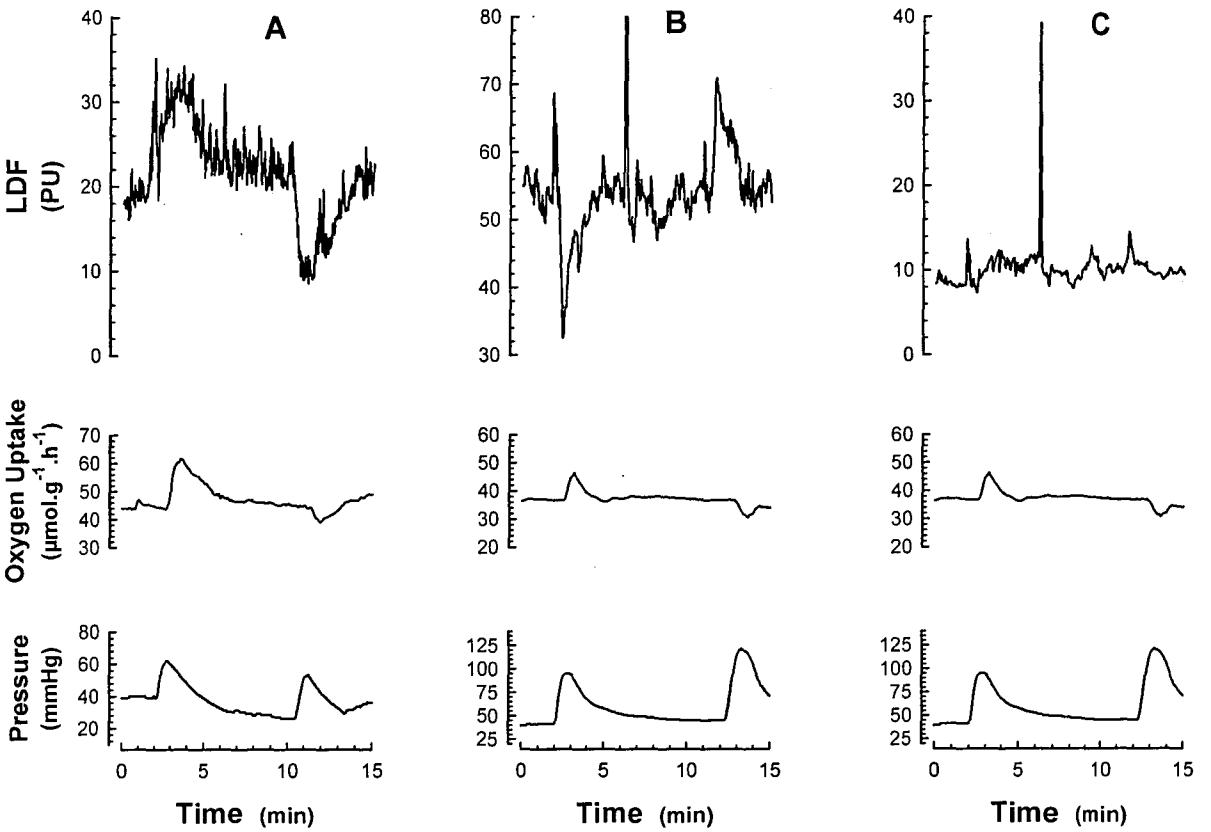


**Figure 3.5 LDF tracings for NE-positive (A), NE-negative (B) and mixed (C) sites from impaled micro probes.** Bolus injections of 3 nmol of NE or 5-HT were made as shown during perfusion of the rat hindlimb at constant total flow and sites classified as described in the text. Perfusion pressures as well as arterial-venous oxygen difference for the whole hindlimb were also recorded. Tracings are representative of the groups whose 'n' values are given in Table 3.1.

**Table 3.2 Characteristics of the NE-positive sites**

| Flow, ml/min | Additions | Peak LDF, PU | Peak $VO_2$, $\mu mol.h^{-1}.g^{-1}$ | Peak pressure, mmHg |
|---|---|---|---|---|
| 4 | none | 14.2 ± 1.0 (8) | 43.5 ± 1.4 (8) | 32.6 ± 1.8 (9) |
| 6 | none | 18.8 ± 1.2 (8)* | 51.6 ± 1.9 (8)* | 43.7 ± 1.7 (9)* |
| 8 | none | 22.8 ± 1.4 (8)* | 54.6 ± 2.4 (8)* | 53.9 ± 1.9 (9)* |
| 4 | none | 15.2 ± 1.2 (9) | 44.1 ± 1.3 (9) | 32.6 ± 2.0 (9) |
| 4 | 5-HT | 6.5 ± 0.7 (9)* | 31.8 ± 1.7 (9)* | 104.8 ± 15.5 (9)* |
| 4 | none | 15.3 ± 1.0 (9) | 44.1 ± 1.5 (9) | 33.7 ± 1.8 (9) |
| 4 | NE | 31.0 ± 5.3 (9)* | 56.4 ± 2.6 (9)* | 55.9 ± 5.1 (9)* |
| 4 | none | 15.5 ± 0.8 (8) | 43.5 ± 1.6 (9) | 35.3 ± 2.2 (8) |
| 4 | AVP | 40.3 ± 10.3 (8)* | 53.7 ± 2.9 (9)* | 69.9 ± 5.3 (8)* |
| 4 | none | 13.9 ± 1.0 (9) | 43.4 ± 2.0 (7) | 34.2 ± 2.3 (8) |
| 4 | AII | 35.5 ± 4.0 (9) | 51.8 ± 2.3 (7)* | 47.9 ± 7.2 (8)* |

Sites identified as NE-positive in initial assessment were further assessed in response to flow change and to bolus injections of serotonin (5-HT, 3 nmol), norepinephrine (NE, 3 nmol), arginine vasopressin (AVP, 30 pmol) or angiotensin II (AII, 300 pmol) Values are mean ± SE with n values shown in parentheses; *, $P<0.05$ relative to 4ml/min "none". LDF values have not been corrected for biological zero.

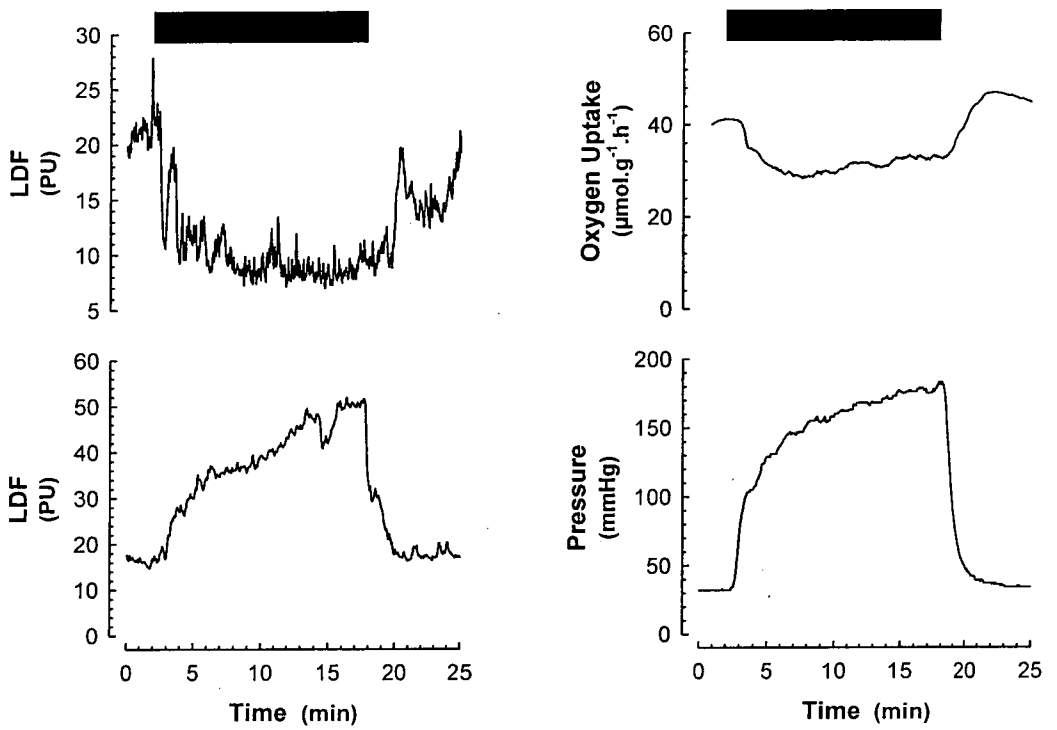


**Figure 3.7 LDF tracing from NE-positive (top, left) and NE-negative (bottom, left) sites using micro impaled probes following the constant infusion of 750 nM serotonin (filled bar).** Hindlimbs were perfused at constant total flow and an infusion of a stock solution of 50 µM 5-HT introduced for the period shown. Representative tracings for perfusion pressure, as well as arterial-venous oxygen difference for the whole hindlimb are also shown.

### 3.4 Discussion

This study represents the second (see also (93)) where there is a major divergence between total flow and LDF measurements in muscle and raises the question as to how this might occur. We believe that two issues have an important bearing; one concerning what LDF probes actually detect and the second, the influence of vessel architecture. For LDF measurements, it is generally thought that movement of the blood cells causes a frequency shift with some of the photons also back-scattered or absorbed by the tissue. Doppler broadened and back-scattered light carry information about the movement and concentration of the cells. LDF probes are thus considered to measure "tissue perfusion". Although this has not been fully defined, Leahy et al. (99) propose that "tissue perfusion" is the product of local speed (non-vectorial) and the concentration of moving cells. However, it is far from clear whether the product derives from equal quantitative input from each or whether one or other has a dominant effect. Equal input would mean that if total (volume) flow remained constant then changes in vessel diameter, distribution of flow from few to many vessels, or the distribution of flow from short to tortuous vessels, should not affect the signal from a LDF probe. To put it another way, the relationship between LDF signal and total flow should always hold. The findings in this present study which clearly show a divergence between total flow and LDF signal have thus necessitated an evaluation of the relationship between vessel architecture and LDF signal. So, in a separate study (Chapter 4) we have constructed models of different vessel architecture from commercially available polymer tubes of a size that even with complex formations fitted comfortably within the field of measurement of a standard LDF probe. We examined the effect of tube architecture on LDF signal using polymer tubes of 250, 100 and 50μm internal diameter. At 3% hematocrit the LDF signal was linear for each of the three tube sizes from 10 to 80μl/h. The signal strength was greatest from the smallest tube and least from the largest tube even though volume flow was the same in each. For a single tube (100μm) that doubled back on itself twice to cross the field of measurement three times, the LDF signal at any flow (10-80μl/hr, hematocrit 3%) was approx. 3-fold greater than that for the same tube crossing the field of measurement once. The effect of progressively switching flow (constant at 120μl/h, hematocrit 9%) from five to one tube

in a manifold of five tubes (100 μm) gave rise to a progressive increase in signal. Overall, the data underscore the predominant role of cell speed (non-vectorial), rather than velocity or cell number in determining LDF signal. If these models can be used as representative of the microvasculature of tissues *in vivo*, then they may help explain a recent report in skeletal muscle where changes in total (volume) flow failed to correlate with LDF signal, *in vivo* (93) as well as the present data in perfused rat hindlimb. In the present experiments which were conducted at constant-flow, norepinephrine (NE) increased the LDF signal at the majority of sites and increased overall hindlimb oxygen uptake. A decrease in vessel diameter due to NE-mediated vasoconstriction of the vessels under the probe could account for the increase the LDF signal. However, while this might explain the effects of NE to increase the LDF signal, it could not account for the effects of serotonin (5-HT), which in the hindlimb also caused vasoconstriction, but at the same LDF sites as where NE was stimulatory, caused a decrease in LDF signal and a decrease in overall hindlimb oxygen uptake. From the tube manifold studies where the LDF signal decreased when flow was switched from one to five identical tubes, it would seem likely that any vasoconstrictor that acts to decrease capillary flow by de-recruiting the number of capillaries perfused without affecting total flow would increase the LDF signal. Thus 5-HT which decreases oxygen uptake and presumably muscle capillary flow might be expected to increase, not decrease, the LDF signal.

One explanation from the perfused tube studies (30) that might account for the effects of NE and 5-HT to increase and decrease the LDF signal, respectively, is that blood flow is redirected to (by NE) or from (by 5-HT) tortuous multiple pass capillaries much as used in the model described above. This would mean that the two networks comprise on the one hand, the long tortuous capillaries that could be considered as nutritive and on the other, relatively short single pass capillaries (possibly "non-nutritive"). Switching the blood flow from one to the other by site-specific vasoconstrictors might then account for the changes in metabolism reported herein. Type A vasoconstrictors such as NE are known to constrict at the region of terminal arterioles. The rise in pressure may be sufficient to overcome the intrinsic resistance of the longer capillaries allowing flow. This would account for the previously observed increase in red cell washout and newly recruited vascular space detected by FITC dextran that accompanied NE-mediated

vasoconstriction (121). In contrast, Type B vasoconstritors such as 5-HT, are thought to vasoconstrict higher in the vascular tree and dilate the arterioles [see (32) and refs therein] lowering the pressure in the vicinity of the capillary networks. Under these conditions flow in the lower resistance short "non-nutritive" capillaries would be favored. Whereas the short "non-nutritive" capillaries are near to the muscle fibers it is also possible that some are contained within the connective tissue that surrounds the bundles of muscle fibers (the epimysium). As such, these would be sufficiently insulated from muscle cells to be functionally non-nutritive. From our previous studies it is clear that some of the non-nutritive connective tissue vessels are located in tendons (8;67;122) therefore outside the present regions of LDF measurement which were located more centrally.

In the present study a distinct heterogeneity of sites was identified from micro LDF probes placed at random in various muscles in the perfused rat hindlimb. The heterogeneity was not detected with the much larger surface probe unless the probe was moved to regions where tendon vessels were apparent. Of the sites examined with the micro probes either of three characters was displayed when the hindlimb was injected with bolus amounts of the vasoconstrictors NE or 5-HT. Some responded with increased LDF signal from NE and decreased LDF signal from 5-HT and were designated as 'NE-positive'. Those responding with decreased LDF signal from NE and increased LDF signal from 5-HT were designated as 'NE-negative' Sites failing to respond to either NE or 5-HT were deemed as 'mixed'. Since the vasoconstrictors, norepinephrine and serotonin have been previously described as increasing or decreasing muscle nutritive flow based on their respective effects to stimulate or decrease muscle metabolism (32), we propose that the NE-positive sites are located in the nutritive vascular route. Similarly, since NE and 5-HT have been previously shown to decrease or increase, respectively, putative non-nutritive flow in tibial tendon vessels of the biceps femoris (122), the NE-negative sites reflect the positioning of the probe in the non-nutritive vascular route. A 'mixed' site could represent a location where nutritive and non-nutritive sites are juxtaposed so a positive response from one is obscured by a negative response of similar magnitude from the other. Indeed, close inspection of 'mixed' traces (e.g. Fig. 3.5C) shows LDF signal fluctuation at the points when NE and 5-HT were injected. It is

unlikely that mixed sites were where there was no blood flow as increasing the flow from 4 to 8 ml/min significantly increased LDF signal at these sites (Table 3.1) and the basal LDF signal was greater than biological zero.

In addition to their differing character with respect to responses to the vasoconstrictors NE and 5-HT two other differences were detected. Firstly, the proportion of sites assessed favored NE-positive over NE-negative by a factor of 56.7% to 16.5%, or approximately 3.5: 1. The ratio may be closer to 2.4: 1 if the assumption that mixed sites comprise equal proportions of NE-positive (nutritive) and NE-negative (non-nutritive) components. Secondly, NE-negative sites, in general, showed a higher basal LDF signal than NE-positive sites (Table 3.1). Together these additional properties suggest that non-nutritive vessels are relatively fewer than nutritive.

Anatomical models of the muscle microvasculature depicted by Lindbom and Arfors and their colleagues (22) as well as those of Myrhage and Eriksson (114) provide a possible explanation for the close co-existence of nutritive and non-nutritive sites within the muscle body. Detailed drawings of the microvasculature of the rabbit tenuissimus muscle (22) show feed arteries that branch to supply transverse arterioles which in turn cross the muscle body (which in this muscle is flat) to firstly supply terminal arterioles and capillaries of the muscle then to end in vessels supplying the connective tissue. Our own recent studies suggest that these vessels nourish attendant adipocytes (39) and thus can only be considered "non-nutritive" for the more metabolically active muscle cells. Furthermore, these connective tissue vessels and their adipocytes are seen in close proximity of the muscle nutritive capillaries (33). Thus two vascular networks operate in parallel and a number of studies using intravital microscopy has shown that relative flow in the two networks can be influenced by various physiologically relevant agents and conditions (22;103-105) that redistribute flow consistent within the two regions representing the nutritive and non-nutritive routes of muscle (35). For the tenuissimus muscle the region containing nutritive capillaries is approximately 3000 μm wide and somewhat less for the non-nutritive (104). Thus a LDF probe of 200 μm dia. could be placed to detect exclusively one or the other route. For muscles other than the tenuissimus that are cylindrical, the same vascular unit is observed (114), but now the transverse arteriole radiates out from the center of the muscle fibril and the connective tissue vessels

are contained in the perimysium. The dimensions are similar but because of the cylindrical nature of the perimysium the probability of positioning a 200 μm probe to measure non-nutritive flow exclusively would be less than for the tenuissimus and the probability of receiving a mixed signal greater. The data obtained in this present study and the conclusions drawn from the perfused polymer tube studies (30) are not inconsistent with this vascular arrangement.

There are relatively few studies deploying intramuscular micro LDF probes (e.g. see (126)) and none has addressed the issue of heterogeneity of response to vasoconstrictors. There are, however, a number of studies where larger LDF probes have been used on the surface of skinned muscle similar to the one reported herein. The larger surface probe records frequency changes from much larger volumes of tissue, in many cases approaching $1 mm^3$ and therefore penetrates considerably below the surface. Of particular interest are studies of muscle blood flow where total and regional flow has been manipulated by pharmacological agents. The findings suggest that the surface LDF probes detect predominantly flow we would characterize as nutritive. In one such study (68), adenosine was infused into anesthetized rabbits. Mean arterial blood pressure decreased, there was an increase in flow heterogeneity, a decrease in local oxygen consumption (vastus medialis) and a decrease in LDF signal in the same region on the contralateral leg. The authors concluded that adenosine had caused a markedly reduced capillary flow with increased tissue oxygenation. The studies herein using the constant-flow perfused rat hindlimb show that vasodilators, such as adenosine, strongly oppose the effect of Type A (cf. Type B) vasoconstrictors such as NE and redirect flow from the nutritive to the non-nutritive route (31).

In a study by Kuznetsova et al. (93), muscle surface LDF signal was recorded from the biceps femoris muscle of anesthetized rats that had been injected with clorisondamine chloride, an autonomic blocking agent that blocks nicotinic ganglionic transmission, as well as the $\beta_1$-blocker, atenolol. Total muscle blood flow was assessed with radioactive microspheres. Infusion of angiotensin II or phenylephrine increased LDF signal without affecting total muscle blood flow. In a separate series of experiments, isoproterenol decreased LDF signal despite a large increase in total blood flow. These findings are consistent with our observations in the constant-flow perfused rat hindlimb where

angiotensin II and phenylephrine are both Type A vasoconstrictors and increase oxygen uptake, by increasing nutritive flow. Furthermore, we have found isoproterenol to be a vasodilator that opposes Type A vasoconstriction and redirects flow from the nutritive to the non-nutritive route. Thus oxygen uptake is inhibited (31).

In skeletal muscle of the rat, LDF signal has been shown to correlate well with other measurements of flow, such as radioactive microspheres or electromagnetic flowmetry, each of which measure volume flow (161). However, as pointed out by Kuznetsova *et al.* (93), the linear correlation may not apply if tissue perfusion, estimated by LDF, changes without any significant change in volume flow to an organ. In fact the principal finding made by these authors was that certain types of vasoconstrictors, as outlined above, were able to cause a dissociation between volume blood flow and LDF signal. Kuznetsova *et al.* (93) were of the view that changes in LDF signal accompanying changes in vascular tone were best explained by changes in red cell velocity. Thus agents such as isoproterenol, that decrease LDF signal in the light of increased total blood flow do so by decreasing red cell velocity, the result of decreased arteriolar-venular pressure gradient. In view of the present studies I would argue that the LDF probe recorded signal from predominantly nutritive region and phenylephrine and angiotensin II increased, while isoproterenol decreased blood delivery to this region. The LDF signal reflected the extent of perfusion of the tortuous nutritive network as predicted from the perfused polymer tube studies (30).

In our perfused hindlimb system, total flow was maintained constant and we have previously shown, using microspheres, that agents such as 5-HT do not alter total flow between muscles of high and low oxidative capacity, or between muscle and non-muscle tissue (137). The fact that 5-HT infusion results in a marked decrease in oxygen uptake, a change in flow pattern (121) and an increase in flow in connective tissue and tendon vessels (122), suggests that 5-HT acts to redirect flow from nutritive capillaries to non-nutritive vessels within the same muscles, which may include tendon vessels. Takemiya and Maeda (173) have reported that at rest blood flow in the tendon of tibialis anterior, gastrocnemius, and soleus exceeds that of the same muscles by a factor of approx. 2-fold. In addition, they showed that norepinephrine, or exercise, decreased tendon vessel flow and that exercise-mediated decrease in tendon vessel flow occurred in conjunction with

increased muscle flow. Together their findings also imply that blood flow can be switched from either of the two routes to match demand.

The proportion by which vasoconstrictors were able to alter muscle metabolism during constant infusion (oxygen uptake was stimulated by 69.5% by NE and inhibited by 29.5% by 5-HT) was similar to the amount that they changed flow indicated by LDF signal at the NE-positive sites ( NE= +51%; 5-HT= –61%). It would therefore seem likely that redistribution of flow between the 'nutritive'(NE-positive) route and nearby connective tissue (such as the perimysium, epimysium or tendon), albeit the 'non-nutritive' (NE-negative) route, could account for the observed changes in metabolism as argued previously (32;35).

In this Chapter nutritive flow is defined in terms of increases in metabolism, specifically oxygen uptake. Other groups have shown that oxygen uptake by the perfused rat hindlimb is dependent on total flow (21). In the present study when flow was increased under basal conditions (no vasoconstrictor) from 4 to 8ml/min, oxygen uptake for the whole hindlimb increased from 45.6 ± 1.9 to 60.9 ± 1.5 ($P$<0.05). Thus the perfused rat hindlimb responds with increased oxygen uptake if nutritive flow is increased by either an increase in total flow or switching flow from the non-nutritive route. However, it is important to note that changes in oxygen uptake should not always be considered as a surrogate indicator of changes in nutritive flow. There may be circumstances, for example when metabolism is increased without change in capillary recruitment (nutritive flow). One such condition would be when uncoupling of respiration occurs. There is evidence that changes in oxygen uptake by the perfused rat hindlimb are not the result of direct metabolic effects of the vasoconstrictors acting on skeletal muscle. Thus, if the vasoconstriction is blocked by the simultaneous infusion of a vasodilator, both the increase in pressure and oxygen uptake are blocked (41). Similarly, 5-HT shows none of the effects seen in perfused hindlimb muscle when added to isolated incubated muscle (140), and the effects in perfusion are blocked by vasodilators (137). Overall, nutritive flow might be defined more generally with regards to microvascular flow that is spatially related to a metabolically active compartment in muscle and facilitates nutrient exchange. In the perfused hindlimb limitation of nutritive flow (for example by serotonin) shunts microvascular flow away from a metabolically active compartment resulting in decreased

oxygen exchange between muscle and perfusate. If oxygen availability becomes limiting in some regions this may secondarily affect fuel metabolism. In addition, blood flow coursing through a muscle bed itself may engender some work on the muscle by mechanisms not yet defined, which alters oxygen consumption. Clearly, oxygen consumption is one particular manifestation of microvascular recruitment that is prominently affected in the perfused hindlimb.

Finally, LDF probe dimensions may be important in determining the nature of the signal received. The surface LDF probe used in this study had a detector surface area of approx. 1 $mm^2$ (two optical fibers of 800 μm dia. each) and when placed on the surface detected signal from a volume of approx. 1$mm^3$ of tissue. When positioned on the center of the anterior end of the biceps femoris the signal appeared to be only of one kind, responding positively to NE and negatively to 5-HT. This contrasts with measurements using a much smaller probe (0.03 $mm^2$) inserted in the muscle, where LDF signals were heterogeneous with some responding as above (i.e. NE-positive), some responding in an opposite manner to the above (i.e. NE-negative), and some failing to respond (mixed). With the smaller probe it was also noted that the NE-positive sites outnumbered the other two by approx. 3:1. Thus it appears likely that the larger probe receives signal from a mixture of sites that convey a character that is predominantly NE-positive. Alternatively, NE-negative sites may not be located near the surface of the muscle, although for various reasons alluded to above this is unlikely.

In summary, micro LDF probes when positioned randomly in the body of a number of hindlimb muscles identify sites that differ in their response to vasoconstrictors. This heterogeneity is not visible to larger probes on the muscle surface. Over half of the sites show properties consistent with a nutritive role for muscle metabolism. Non-nutritive sites are present but at a lower proportion and nearly a quarter of the sites are likely to represent a mixture of both nutritive and non-nutritive. Non-nutritive sites show a higher basal signal. The anatomical nature of these nutritive and non-nutritive vessels are further explored in the next Chapter (Chapter 4), particularly in relation to the effects vessel geometry has on the LDF signal.

# CHAPTER 4

## Defining Nutritive Blood Flow in Skeletal Muscle – A Model Study Using Fabricated Capillaries of Differing Architecture

### 4.1 Introduction

LDF (laser Doppler flowmetry) is purported to measure microvascular perfusion, a product of local speed and concentration of blood cells (99) but there are now a number of reports where a linear correlation between LDF signal and total (volume) flow has been shown to break down (29;93). In one such study (93), LDF signal was recorded from the biceps femoris muscle of anesthetised rats that had been injected with the $\beta_1$-adrenergic blocker, altenolol and clorisondamine chloride, an autonomic blocking agent that blocks nicotinic ganglionic transmission. Total muscle blood flow was assessed with radioactive microspheres. Infusion of angiotensin II or phenylephrine increased LDF signal without affecting total muscle blood flow. In a separate series of experiments, isoproterenol decreased LDF signal despite a large increase in total blood flow (93). Similarly, the findings in the previous chapter (Chapter 3) using micro intramuscular or larger surface LDF probes have shown that vasomodulators can markedly alter signal strength in the constant flow blood perfused rat hindlimb (29). Since these same vasomodulators also markedly alter hindlimb muscle metabolism an obvious question arises as to how these changes in LDF signal occur. One possibility among a number, is that the vasomodulators have acted to modify the pattern of flow. For example, sharing the flow between a greater number of capillaries, or redirecting flow from short relatively straight to more tortuous vessels, or even redirecting flow from smaller to larger vessels etc. In this regard, there is very little information in the literature on vessel architecture and its effects on LDF signal [e.g. (99;123;125-127). The few papers that have appeared have only addressed hematocrit and the correlation between cell velocity and LDF signal (106;107). In the present study we have examined the effect of tube architecture on LDF signal.

The findings suggest that LDF signal, when measured in tissue can be markedly affected by vessel architecture and thus explain situations where a divergence between total flow and LDF signal occur following vasoconstrictor action in muscle.

## 4.2 Methods

### *4.2.1 LDF Measurements*

LDF was conducted using a Perimed PeriFlux PF2 unit operating at 632 nm. The probe (Pf 108) consisted of a bundle (2 mm dia.) of three optic fibers, one illuminating the tissue and two collecting reflected light, each 0.8mm in diameter. The distance from the center of the afferent fiber to the centers of the efferent probes was 0.8 mm and the total area of the detecting fibers was $1mm^2$. Unless indicated otherwise, the signal was collected at 4kHz, gain setting 3 with a time constant of 3.0s. Flow was calibrated using a suspension of red blood cells (3% hematocrit) in gassed perfusion buffer. The cells were pumped at various rates through a single polymer tube 100μm diameter and 10mm in length. This served to establish that the LDF signal was linearly proportional to flow rate. Biological zero ($0.30 \pm 0.02$ volts) was determined at pump setting of zero and was subtracted from all values.

Preliminary data were collected to determine the hematocrit at which the LDF probe failed to see all of the cells. This was judged to have occurred when the LDF signal for a given tube "peaked" as a function of hematocrit. Figure 1 shows that a hematocrit of 3% was suitable for single tube studies of 250μm and smaller. Preliminary data was also necessary to ascertain the cell velocity at which the LDF probe no longer showed a linear relationship between flow and signal. This was found to be approx. 8mm/s (data not shown) and similar to values noted by others (106). Cell speed, or cell velocity if the direction was known, was calculated from flow rate, cell density (hematocrit) and internal dimensions of the tube.

*4.2.2 Red blood cells*

Red blood cells (rat or bovine) were collected and washed six times in BSA-containing and gassed perfusion medium. The perfusion medium was gassed with 95%$O_2$-5%$CO_2$ and contained 118mM NaCl, 4.7mM KCl, 1.2mM $KH_2PO_4$, 1.2mM $MgSO_4$, 25mM $NaHCO_3$, 8.3mM glucose, 2.5mM $CaCl_2$ and 7.1% (w/v) bovine serum albumin (Boehringer Mannheim, fraction V). The cells were counted using a hemocytometer and the hematocrit adjusted using the same buffer. Cell suspensions were kept in tightly capped vials and used freshly on the day of preparation. The hematocrit was set at 3% for larger tube studies; higher hematocrits in tubes of 250 μm obstructed the LDF signal (see Fig. 4.1).

*4.2.3 Artificial capillary systems*

Polymer tubes of 100 and 250μm internal diameter (MicroFil™) were purchased from World Precision Instruments. These were supplied with Luer syringe fittings. The 50μm tube was from Applied Biosystems as routinely used for capillary electrophoresis and was uncoated fused silica.

Single tube studies used a short length (10mm) of each tube fitted into polyethylene tubing, which in turn was fitted onto the needle of a Hamilton 10μl syringe (0.49mm ID). A syringe pump (Harvard Apparatus) was used to deliver constant-flow. The polymer tube was positioned in a V-shaped holder so that its relationship to the LDF probe was always the same. In addition, the probe was secured to a micromanipulator so that fine adjustments in two dimensions (vertical and horizontal) could be made. Polymer tube-polyethylene tubing fittings could be interchanged without disturbance of the probe or its relationship to the tube. Measurements were made at five different flow rates (typically 80, 40, 20, 10 and 5μl/h) and were completed within 4 min before significant settling of red cells had taken place. As a check, periodic samples of blood emerging from the tube were counted using a hemocytometer to ensure that the hematocrit was consistent.

A single tube that doubled back twice so that three segments of the same tube could be viewed by the LDF probe simultaneously, was used to compare LDF signal strength with

the same size tube that crossed the field of measurement only once. The flat array of three tubes side-by-side was constructed to fit into the V-shaped holder described above.

Multiple tube measurements were made using a manifold of five 100μm tubes (40mm in length) glued (Araldite™) into a single 23G syringe needle. The luer syringe fitting on the end of each tube was fitted with buffer-filled tubing (80mm in length) terminating with a three-way tap. Thus, with red blood cells being pumped into the 23G needle at a constant rate, flow could be directed to all five, or to any number less than five tubes by closing the appropriate taps. The tubes emerging from the 23G needle were secured flat under the LDF probe so that all five were completely visible (total width of field for the five = 0.82 mm;), when the probe was 1-1.5mm above the tubes. The tubing and taps were also firmly secured so that manipulation of the taps did not interfere with the LDF signal. Red blood cells were pumped from a 1ml syringe (4.76mm ID) at either 120, 80 or 40μl/h. LDF signals were recorded at 4kHz with gain settings of 3 (single tube) and 10 (multiple tubes) with a time constant of 3s. The hematocrit used was 9%. This allowed a sufficiently strong signal without exceeding the limit of detection of all cells which was approx. 12% hematocrit for a tube of 100μm ID (Fig. 1).

*4.2.4 Statistics*

As appropriate, data were analyzed by linear regression. Other assessments were made using unpaired Students' t-test.

**4.3 Results**

For each of the three tubes 50, 100 and 250 μm diameter, LDF signal was measured at a minimum of four different flow rates ranging from 10 to 120μl/h and at various hematocrits ranging from 0.9 to 45%. Primary plots of LDF signal as a function of hematocrit at each flow rate were constructed to determine the hematocrit at which the signal became limiting. The resultant secondary plot (Fig. 4.1) shows the limiting hematocrit as a function of tube diameter. Thus for the 250μm tube, changes in flow rate for buffers containing hematocrits greater than 3% could not be quantitatively detected. Similarly, the value for the 100μm tube was 12% hematocrit. For the 50μm tube the

upper limit could not be accurately determined. This suggested that at this size of vessel or smaller, any change in flow, providing it did not exceed a cell velocity of 8mm/s, would give rise to a corresponding proportional change in LDF signal, for any dilution of whole blood or hematocrit less than 45%. Flow appeared to be laminar in the larger tubes when pumped with buffer of low hematocrit. At higher hematocrit only the surface layer of cells could be visualized.

Figure 4.2 shows the effect of tube size on LDF signal at various flow rates with a fixed hematocrit of 3%. The signal strength was found to increase as the diameter decreased from 250, through 100 to 50μm, increasing by approximately 50% for a decrease from 250 to 50μm in tube diameter. At the maximum flow rate used (80 μl/h) the cell speed was 0.45, 2.82 and 11.33 mm/s for tubes of 250, 100 and 50μm, respectively. In addition, but not shown, there was an increase in LDF signal strength when similar flow variations were made using a hematocrit of 6% for the 100 and 50μm tubes.
If a single tube was doubled back on itself twice to cross the field of measurement three times (Fig. 4.3, *left panel*) and the signal recorded it was found to be approx. 3-fold greater than that for the same tube crossing the field of measurement once (Fig. 4.3, *right panel*).

To determine the effect of flow redistribution from one to more than one tube, thereby simulating a situation of capillary recruitment, a tube manifold of five identical 100μm tubes was constructed. Taps were fitted to extended tubing from each capillary so that flow in each could be either permitted or blocked. Total flow was kept constant and delivered into the manifold from a 23G hypodermic needle. The five emerging tubes were tightly grouped side by side so that the LDF probe detected change in cell flux in all of the tubes simultaneously (Fig. 4.4, *left hand panel*). Figure 4.4 shows the effect on LDF signal as flow was progressively allowed to enter each of the five tubes. When flow was distributed into all five tubes the signal strength was approx. 30% of that when flow was carried by only one. The change in LDF signal was reversible and identical results were obtained when flow was progressively restricted from five to one tube. Moreover, changing the order in which the taps were opened or closed, did not affect the results,

confirming that all five tubes were equally visible to the detector. The data shown in Fig. 4.4 are from experiments involving a single constant flow rate of 120μl/h which is equivalent to a cell velocity of 4.24mm/s when all of the flow is within one of the 100μm tubes. Similar changes were noted when the lower flow rates of 80 and 40 μl/h were used but a delay developed before the effect of closing or opening the taps became apparent. Higher flow rates approached the limiting velocity for the LDF detector. The study was conducted at only one hematocrit of 9%. This was a compromise, allowing a sufficiently strong signal and low background without exceeding the limit of detection for 100μm tubes of 12% hematocrit.

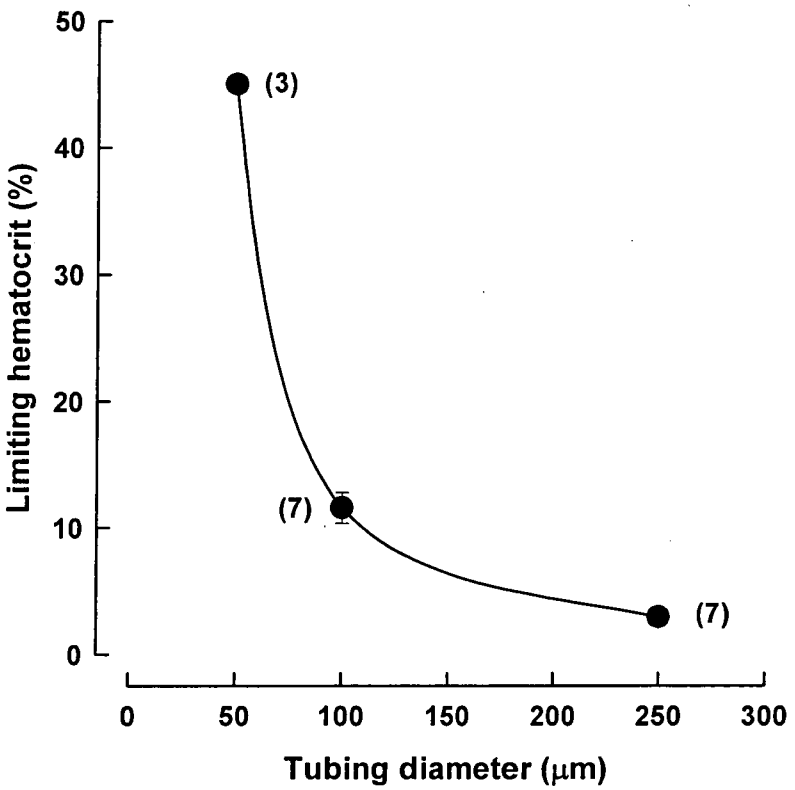


**Figure 4.1 Limiting haematocrit as a function capillary tube diameter.** For each tube, LDF signal was measured for a range of flow rates at various haematocrits ranging from 0.9 to 45%. Primary plots of LDF signal as a function of haematocrit at each flow rate were constructed to determine the haematocrit at which the signal became limiting. The resultant secondary plot is shown. Values are means ± SE, with n-values shown in parentheses.

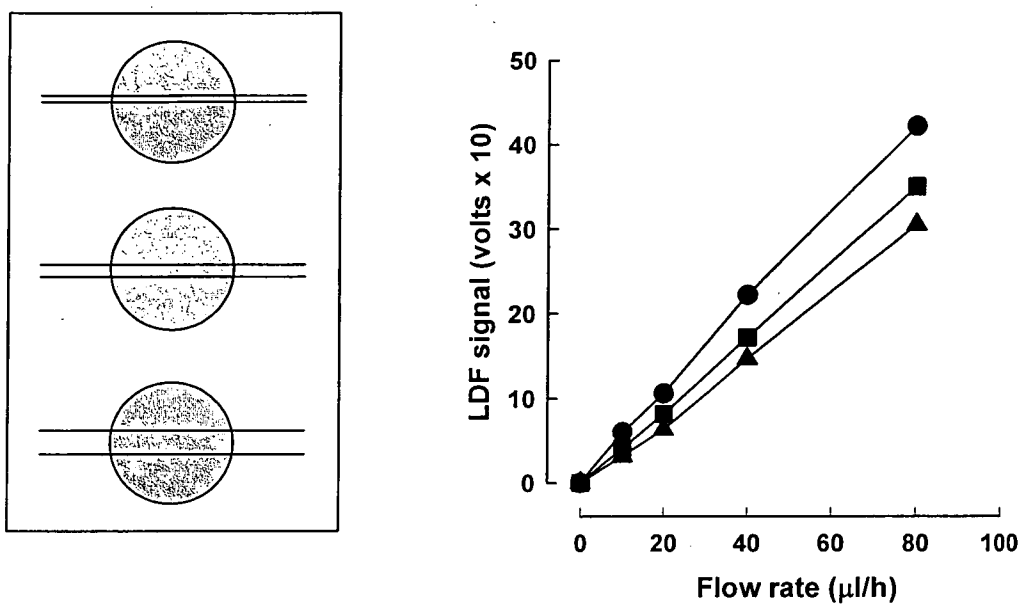


**Figure 4.2 Effect of tube diameter on the relationship between LDF signal and flow rate.** Tube sizes were 50 (•), 100 (■) and 250 µm (▲). The LDF probe was positioned centrally over each tube as shown (*Left panel*). Pump flow rate was varied as indicated with haematocrit set at 3%. Values are means ± SE for n = 5. In all cases the error bars are obscured by the symbol.

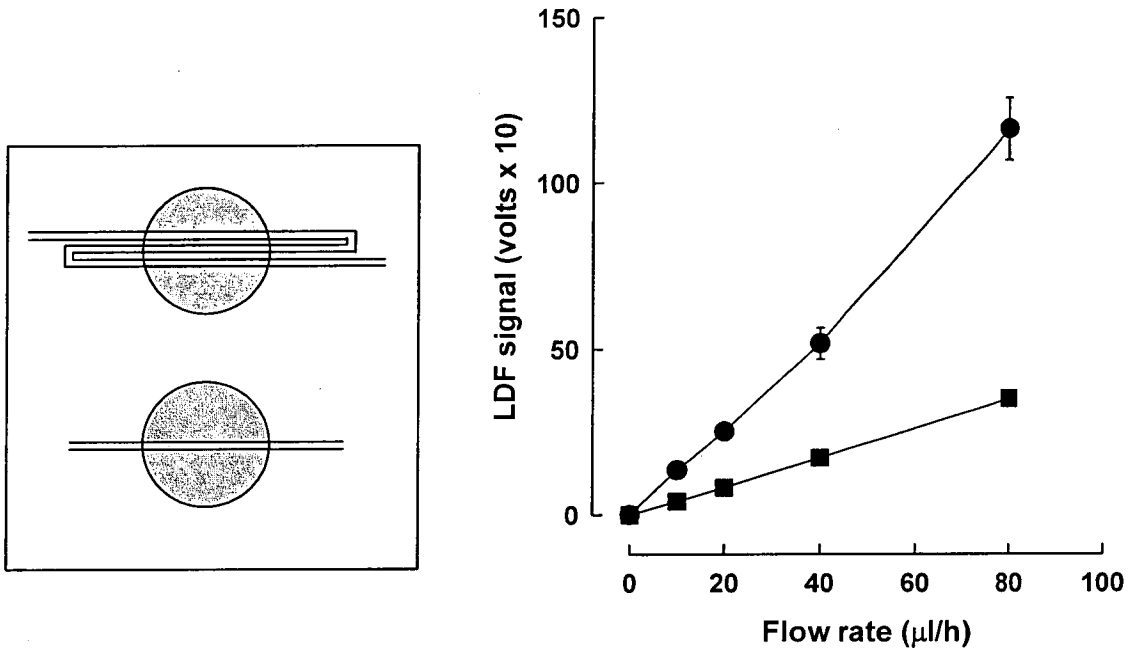


**Figure 4.3 Effect of the tube crossing the field of measurement multiple times on LDF signal.** Two 100 µm tubes were compared (*Left panel*) so that one crossed the field of measurement three times (•) and the other once (■). Flow rate in each was varied as indicated and the haematocrit was 3%. Values are means ± SE for n = 5. Error bars are occasionally obscured by the symbol.

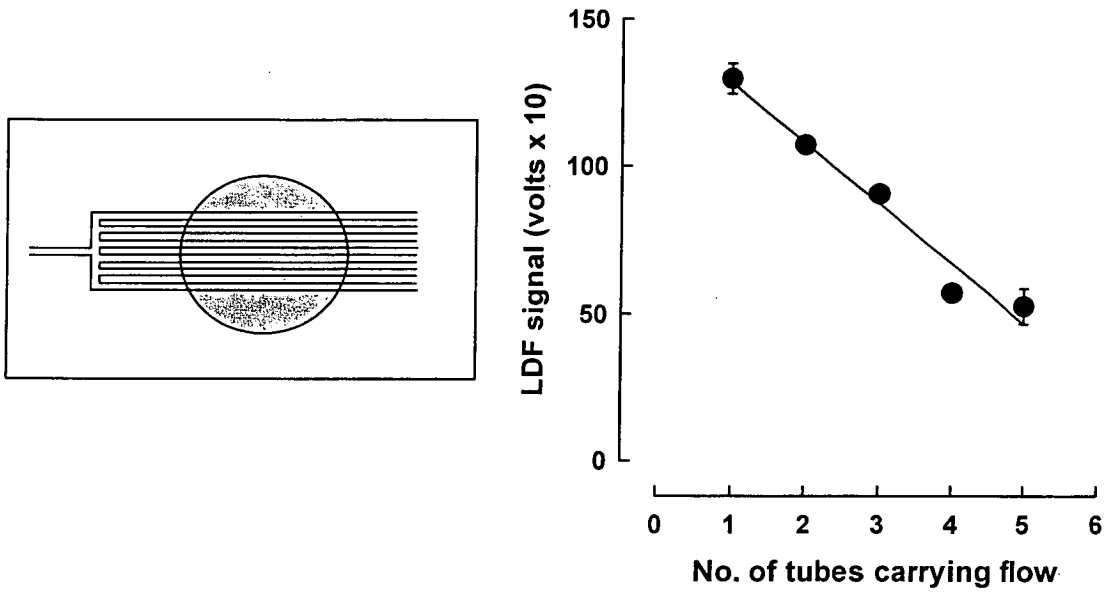


**Figure 4.4 Effect of flow sharing on LDF signal.** A manifold of five identical 100 μm tubes was positioned under the probe as shown (*Left panel*). The haematocrit was 9% and the flow rate constant at 0.12 ml/h. Flow could be controlled to enter only one or any number of the five tubes. Values are means ± SE for n = 6.

## 4.4 Discussion

There is a paucity of information on what LDF probes actually detect when positioned in or on tissues. It is generally thought that movement of the blood cells causes a frequency shift with some of the photons also back-scattered or absorbed by the tissue. The back-scattered and Doppler broadened light carry information about the movement and concentration of the cells. The quantity that is measured in LDF studies is often referred to as "tissue perfusion". Leahy et al. (99) point out that although this quantity has been used extensively, a thorough definition is still lacking. These workers (99) propose that "tissue perfusion" is the product of local speed and concentration of moving blood cells. What is not known is whether the product derives from equal quantitative input from each or whether one or other has a dominant effect. In a practical sense, and without information of this kind, it means that if total (volume) flow remains constant then changes in vessel diameter, distribution of flow from few to many vessels, or distributing flow from short to tortuous vessels, should not affect the signal from a LDF probe. In other words, the relationship between LDF signal and total flow should always hold. With recent reports appearing that show a divergence between total flow and LDF measurements in muscle (93) and Chapter 3, it becomes necessary to explain how this might be so. Our approach has thus been to construct models of different vessel architecture from commercially available polymer tubes of a size that even with complex formations would fit comfortably within the field of measurement of a standard LDF probe. We wished to specifically address three key questions. Firstly, if total flow remains constant and flow is switched from large to smaller vessels, or vice versa, does the LDF signal change? This question is posed because recent studies (93) and those of Chapter 3 have employed vasoconstrictors that may act at a number of terminal arterioles in the field of measurement to cause an overall reduction in average vessel diameter. Secondly, if total flow remains constant and flow is switched from a single pass (crossing the field of measurement only once) to a multiple pass vessel (crossing the field multiple times), does the LDF signal change. There is evidence in the literature that several tissues, including muscle have short thoroughfare vessels as well as long tortuous nutritive vessels and that flow may be switched from one to the other by the action of

vasoconstrictors (32). Thirdly, there has been much recent interest in the possibility that the action of hormones, including insulin, may involve capillary recruitment in muscle (138). If this is so and total flow remains constant, can the LDF signal be expected to change?

In all three of the above situations, we found that LDF signal was markedly affected by the architecture of the vessel in which red blood cells were moving. For the first experimental situation, the LDF signal increased as the vessel diameter decreased. Thus, when flow was switched from the 250μm to the 50μm tube the LDF signal increased by approx. 50%. Since the number of cells moving through the tubes had not changed, the change in LDF signal appears to be attributable to the change in cell velocity. However, the relationship between LDF signal and cell velocity is clearly not linear and the signal did not increase proportionately. The increase in LDF signal was only 50% even though there was a corresponding theoretical 5-fold increase in cell velocity from 0.45 to 2.82 mm/s. The failure to find a direct relationship may result from non-linear motion of the red blood cells at the slower cell velocity in the larger size tube. LDF detectors see cells moving in all directions and are thus non-vectorial in their measurement of motion. This line of reasoning is further developed when the data from the second question are considered (Figure 4.3). In these experiments, LDF signal was measured from a single tube crossing the field of measurement only once left to right with one that doubled back on itself twice and crossed the field a total of three times. For both tubes flow was equal and for the latter flow was left to right, right to left and finally left to right again. Since the LDF signal was approx. 3-fold greater for the multiple pass tube compared to the single pass tube the non-vectorial nature of the LDF signal is emphasised.

In the third series of experiments the notion of capillary recruitment under conditions of constant total flow was explored. A manifold comprising one tube feeding to a maximum of five tubes was used (Figure 4.4). Signal strength was found to be greatest when flow was carried by one tube and least when shared between all five.

Overall, the data underscore the predominant role of cell speed (non-vectorial), rather than velocity or cell number in determining LDF signal. If these models can be used as representative of the microvasculature of tissues *in vivo*, then the findings may help explain recent reports particularly in skeletal muscle where changes in total

(volume) flow failed to correlate with LDF signal, both *in vivo* (93) and in perfused rat hindlimb (Chapter 3). In the hindlimb perfusion experiments which were conducted at constant-flow, norepinephrine (NE) increased the LDF signal at the majority of sites and increased metabolism generally. A decrease in vessel diameter due to NE-mediated vasoconstriction of the vessels under the probe could account for the increase the LDF signal. However, while this might explain the effects of NE to increase the LDF signal, it could not account for the effects of serotonin (5-HT), which in the hindlimb also caused vasoconstriction, but at the same sites as where NE was stimulatory, caused a decrease in LDF signal and a decrease in metabolism.

From the tube manifold studies (Figure 4.4) it would seem likely that any vasoconstrictor that acts to decrease capillary flow by de-recruiting the number of capillaries perfused without affecting total flow would increase the LDF signal. Thus 5-HT which decreases oxygen uptake and presumably muscle capillary flow might be expected to increase, not decrease, the LDF signal.

One explanation from this Chapter that might account for the effects of NE and 5-HT to increase and decrease the LDF signal, respectively, is that blood flow is redirected to (NE) or from (5-HT) tortuous multiple pass capillaries much as depicted by the model for Figure 4.3. This would mean that the two networks comprise on the one hand, the long tortuous capillaries that could be considered as nutritive and on the other, relatively short single pass capillaries (possibly "non-nutritive"). Switching the blood flow from one to the other by site-specific vasoconstrictors might then account for the changes in metabolism that have been reported. Type A vasoconstrictors such as NE are known to constrict at the region of terminal arterioles. The rise in pressure may be sufficient to overcome the intrinsic resistance of the longer capillaries allowing flow. This would account for the previously observed increase in red cell washout and newly recruited vascular space detected by FITC dextran that accompanied NE-mediated vasoconstriction (121). In contrast, Type B vasoconstritors such as 5-HT, are thought to vasoconstrict higher in the vascular tree and dilate the arterioles [see (32) and refs therein] lowering the pressure in the vicinity of the capillary networks. Under these conditions flow in the lower resistance short "non-nutritive" capillaries would be favored. Whereas the short "non-nutritive" capillaries are near to the muscle fibres it is also possible that some are

contained within the connective tissue that surrounds the bundles of muscle fibers (the epimysium). As such, these would be sufficiently insulated from muscle cells to be functionally non-nutritive and may be masked to some degree in terms of LDF signal. In addition, from our previous studies it is clear that some of the non-nutritive connective tissue vessels are located in tendons (8;67;122) therefore outside the present region of LDF measurement which is situated over the center of the muscle.

Finally, this Chapter highlights yet another aspect that must not be ignored when considering data from *in vivo* studies. This concerns the effect of haematocrit to attenuate the LDF signal (e.g. Figure 4.1). Limiting LDF probe signals were identified at 3 and 12% haematocrit for 250 and 100 μm diameter tubes, respectively. Only for the 50 μm tubes was the signal not limited at higher haematocrits. It follows then, that shifts in the relative distribution between larger versus smaller microvessels with characteristically different haematcrits, could affect the observed LDF signal. Similarly, local changes in microvessel haematocrit could also alter the signal characteristics.

In summary, studies presented in this Chapter have indicated the importance of tube architecture in relation to LDF signal strength. Non-vectorial cell speed appears to be a dominant determinant. Any change in vessel architecture that occurs at the site of LDF measurement *in vivo* or in perfused systems must be taken into account when interpreting the data.

# CHAPTER 5

## Changes in Nutritive Blood Flow Patterns Induced by Insulin In Rat Muscle In Vivo: A Study Using LDF

### 5.1 Introduction

Recently, there has been considerable interest in reports that insulin has a hemodynamic vasodilatory effect as part of its action to increase glucose uptake by muscle and that this vascular effect of insulin is impaired in obesity and type 2 diabetes. The reports have generated some controversy where there have been claims and counter claims that glucose and insulin delivery or skeletal muscle perfusion (blood flow) plays an independent role in determining overall rates of insulin stimulated glucose disposal (13;197). All contributors to this controversy have placed considerable emphasis on the putative vasodilatory action of insulin to increase total blood flow. Studies in our laboratory have shown the importance of blood flow distribution in muscle in terms of controlling both metabolism and contractile performance (32). Chapter 3 of this thesis shows how perfusion redistribution associated with significant metabolic changes can occur within muscle even when total limb blood flow is kept constant. Access of nutrients and hormones is a key issue and there exists evidence that blood flow to muscle can be substantial without full access occurring (possibly because a proportion of the flow is carried by a non-nutritive route) (32;36). Thus in this Chapter the relationship between changes in nutritive flow and LDF signal obtained in the constant flow pump-perfused rat hindlimb were then applied to measure changes in LDF signal during the hyperinsulinaemic euglycaemic clamp *in vivo*. Studies were also carried out during epinephrine infusion, as it is known to increase total blood flow to the leg without increasing nutritive (capillary) flow (138).

## 5.2 Methods

### 5.2.1 Perfusion studies

Perfused rat hindlimb studies were conducted as described in detail in Chapter 2, Section 2.1. Total flow rate was maintained at 0.27 $ml.min^{-1}.g^{-1}$ using medium containing red blood cells at 37°C (199). A bolus of norepinephrine was injected to reach approx. 50 nM at the peak which from earlier studies was known to achieve a marked increase in nutritive flow (32). Similarly, a bolus of serotonin was injected to reach 1 μM at the peak and again, was previously known to cause a marked decrease in nutritive flow. Oxygen uptake, a surrogate indicator of nutritive flow in this system when manipulated by vasoconstrictors (32) was determined from the maximum arteriovenous difference and perfusate flow rate (set constant as above) using an in-line oxygen analyser (A-Vox Analyser, A-Vox Systems, Inc, San Antonio, Texas). A small hole (approx. 4 mm dia.) was made in the skin in the middle of the biceps femoris (see Figure 5.1). The hindlimb was then clamped by the foot so that the laser Doppler flow probe (Perimed PF 2, operating wavelength of 632 nm) could be positioned over the centre of the hole, and kept in the same position for the duration of each experiment. For the measurement of red cell flux, the probe was placed vertically above and approx. 1 mm from the surface of the muscle. Settings on the detector unit were 4 kHz (gain setting 10) with a time constant of 3 s, unless otherwise indicated. The signal (0-5 volts) was continuously recorded on an IBM compatible PC using a DI-190 I/O module and WINDAQ® software. The data are expressed as volts × 10.

### 5.2.2 Insulin clamps

For *in vivo* studies, the hyperinsulinaemic euglycaemic clamp was used as described in detail in Chapter 2 and elsewhere (138). In brief, limb blood flow of anaesthetised rats was determined by an ultrasonic flow probe (Transonic®) fitted around the femoral artery. Blood pressure was monitored by a pressure transducer fitted to a carotid cannula. Insulin ($10mU.min^{-1}.kg^{-1}$), epinephrine 0.125 $\mu g.min^{-1}.kg^{-1}$) or saline, as well as glucose

(to maintain blood glucose at 5mM) were infused via a jugular cannula. Insulin was infused at a rate of $10mU.min^{-1}.kg^{-1}$ to raise plasma insulin to the high physiologic concentration. Because the clearance of insulin by the rat is 3-4 fold more rapid than in the human, this infusion raises insulin to levels seen with a 2-3 mU/min/kg clamp in humans and the resulting concentrations mimic those seen in insulin resistant rats models.The protocol was similar to that described previously by Rattigan et al. (138) with 60 min equilibration period before insulin or saline infusion, each of which was continued for an additional 80 min. The leg was carefully skinned and wrapped in clear plastic wrap (Saran Wrap™) to prevent drying.

### 5.2.3 LDF Measurements

#### 5.2.3.1 Scanning LDF

Hindlimb muscle LDF signal was determined using a scanning LDF (Lisca Li PIM 1.0, Laser Doppler Perfusion Imager) at baseline before saline, insulin or epinephrine and at one hour after the commencement of infusion of saline or insulin and 15 min after epinephrine. Positioning of the scanner was made using the knee as a reference (Figure 5.1); this ensured that the area and orientation were identical between animals. Triplicate scans of the hindlimb were made each taking 5min to complete and timed to occur 5 min before, on and 5 min after the times designated above. Each scan was brought on screen and analysed using the manufacturer's operational software to give average perfusion units (volts) of the area analysed. To assess muscle perfusion a square of 225 $mm^2$ in the top left hand corner of each scan and covering mostly muscle (biceps femoris) was analysed (Figure 5.1). Means from triplicate analyses before and after addition of saline (control), insulin, or adrenaline were used for comparison. The scanning probe covered a total area of approx. $900mm^2$ of skinned thigh muscles.

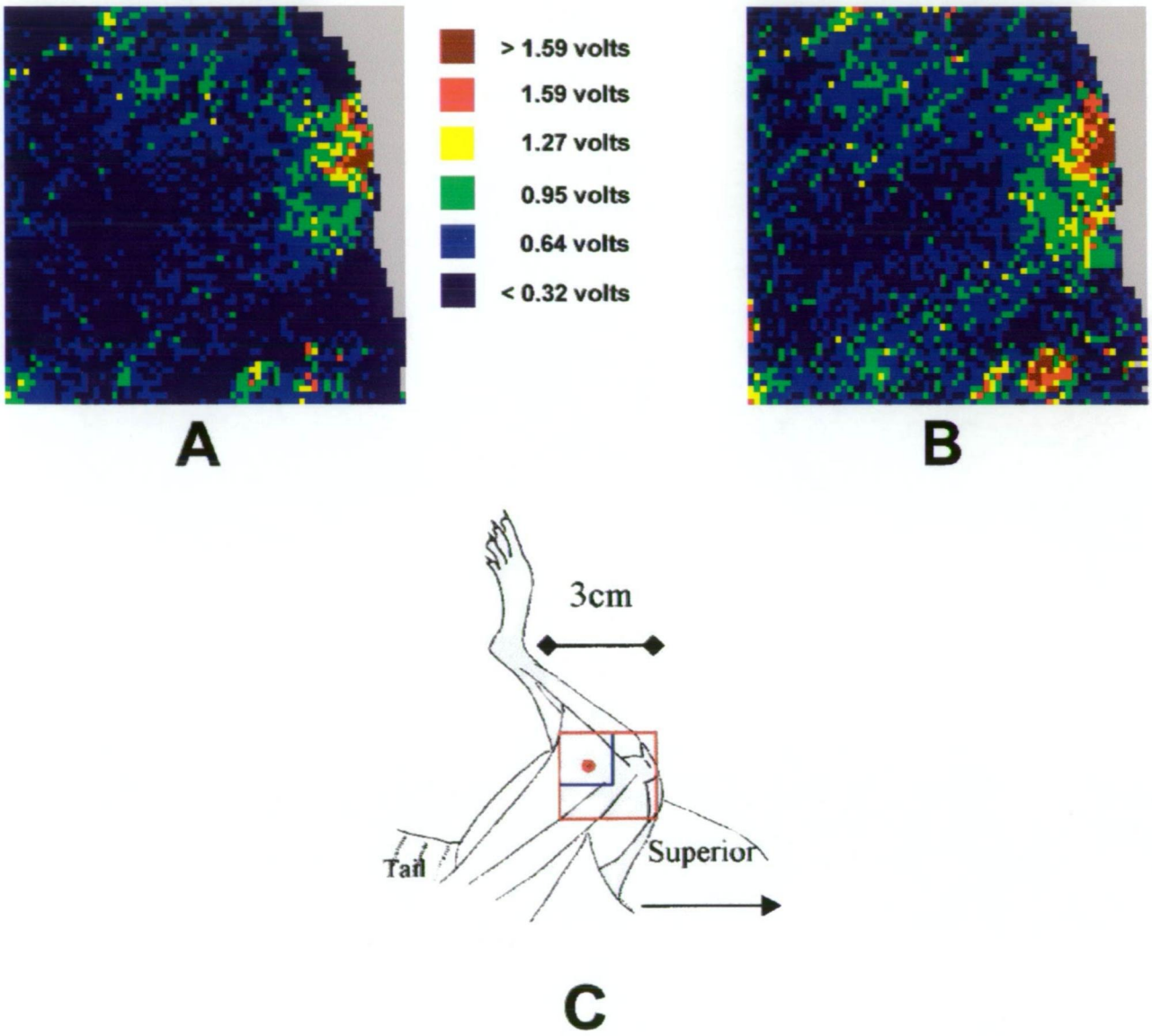


**Figure 5.1 Representative scans of LDF before (A) and after (B) insulin in the same animal.** The area analyzed by the scanning LDF is demonstrated by the red square in (C). The smaller red/blue square in the top left hand corner is predominantly muscle (biceps femoris). The position of the stationary probe is shown as a red dot, in (C). Colour coding to indicate relative perfusion in volts is shown in figure. Each coloured square or pixel represented approx. 0.2 $mm^2$.

### 5.2.3.2 Fixed probe LDF

In a separate series of experiments, using an identical protocol again with 60 min equilibration and a total period of 80 min for insulin or saline infusion, a stationary LDF probe (Perimed Periflux PF 4001with Probe 407) was used and signals were recorded continuously throughout the experiment. The stationary probe was positioned over a 4mm$^2$ area of skinned biceps femoris muscle in an identical position to that used in perfused hindlimb studies above (Section 5.2.1).

Biological zero for both scanning and stationary probes used in the clamps was determined at the end of the experiment after the animal had been administered a lethal dose of anaesthetic and femoral blood flow and heart rate were zero. For the scanning probe this involved conducting a complete scan of the entire area exposed (e.g. Figure 5.1). Values for biological zero were 0.22 ± 0.02 volts (total area), 0.23 ± 0.02 volts (biceps femoris muscle) and 0.21 ± 0.02 volts (connective tissue)(n = 5). For the surface probe changes in LDF signal as a result of insulin were expressed relative to the basal signal of 1.00. Absolute values for the basal signal and biological zero were 112 ± 20 and 16 ± 3 perfusion units, respectively for 14 determinations. No value shown has been corrected for biological zero, unless indicated otherwise.

### 5.2.4 Oxygen uptake studies

In a further series of experiments a group of rats underwent identical clamp conditions for the purpose of assessing insulin induced changes in leg oxygen uptake and muscle-specific uptake of 2-deoxyglucose. For oxygen uptake, blood samples were taken from the carotid artery (100 µl) and femoral vein after equilibration (approximately 1h) and 2h after commencement of insulin infusion. Samples of femoral vein blood (100 µl) were collected using a 29G insulin syringe. Total oxygen content of each blood sample was determined using a galvanic cell oxygen analyser (TasCon oxygen content analyser manufactured by the Physiology Department, University of Tasmania) that was standardised against air and corrected to standard temperature and pressure. The rates of

oxygen uptake were calculated from oxygen extraction and femoral blood flow at each time point and expressed per gram wet weight of perfused muscle, as estimated previously (54). For muscle-specific uptake of 2-deoxyglucose, the method of Kraegen et al (91) was used. In brief, this involved intra-arterial injection of a bolus of 50μCi 2-deoxy-D-[2,6-$^{3}$H]glucose (specific activity 44Ci.mmol$^{-1}$, Amersham Life Science) at 45 min before the end of the clamp. Following injection of the bolus, arterial plasma samples (50 μl) were collected at 5, 10, 15, 30 and 45 min. Soleus, plantaris, gastrocnemius red, gastrocnemius white, extensor digitorum longus, and tibialis muscles were removed at the end of the clamp for analysis of [3H]2-deoxyglucose 6-phosphate content and calculation of 2-deoxyglucose uptake (91).

### 5.2.5 Statistics

Repeated measures two-way analysis of variance was used to determine differences and when significant differences were found paired Student's *t*-test was used to test the hypothesis that there was no difference before and after treatment. For the time courses, one-way repeated measures analysis of variance (ANOVA) was performed and when significant difference was found, multiple comparisons (Dunnet's method) were made vs. the time point just before insulin (0 min). Significant differences were recognized at $P < 0.05$.

## 5.3 Results

### 5.3.1 LDF signal and nutritive flow in the constant flow pump-perfused rat hindlimb

Figure 5.2 shows a positive correlation ($r = 0.93$ and $P < 0.0001$) for change in LDF signal as a function of change in nutritive flow as perturbed by either norepinephrine or serotonin.

### 5.3.2 Glucose and oxygen metabolism during the insulin clamps

In keeping with similar experiments conducted previously (138;139) arterial glucose concentrations were not significantly different between saline and insulin animals either before commencement of infusions or at the end of the experiment (data not shown). Insulin increased glucose infusion rate from zero to a maximum of 128 ± 11 $\mu mol.min^{-1}.kg^{-1}$ at the end of the clamp (80 min). The time course which is shown in Figure 5.3 was similar to previously (138), so that following 1h of insulin, glucose infusion had already reached the maximum.

Muscle-specific uptake of 2-deoxyglucose is shown in Table 5.1. Insulin increased uptake in each of the six muscles with an overall average of 2.7-fold. Oxygen uptake was unaffected by insulin.

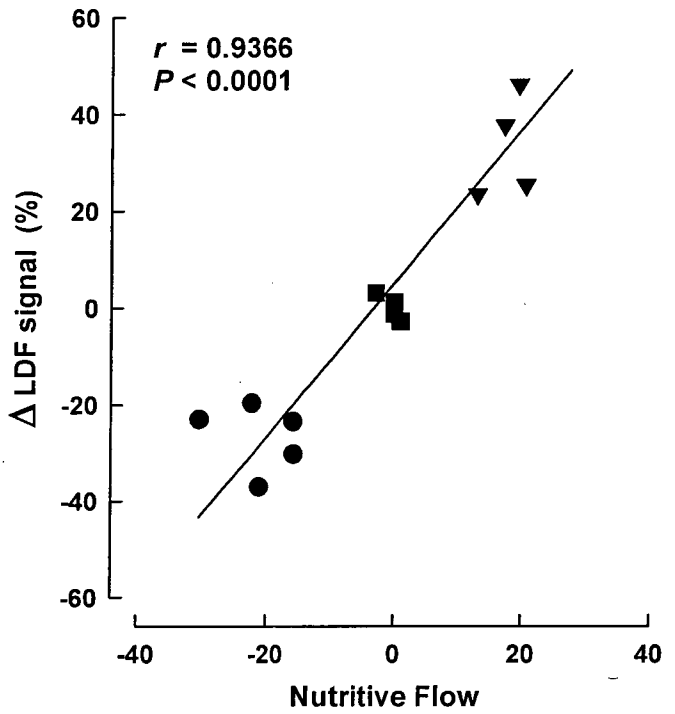


**Figure 5.2 Change in LDF signal as a function of change in nutritive flow in the isolated pump-perfused rat hindlimb.** Single hindlimbs were perfused at constant total flow and bolus amounts of vasoconstrictors injected. Oxygen uptake ($\mu mol.h^{-1}.g^{-1}$) was used as a surrogate indicator of nutritive flow. Values are from individual perfusions were injections were either saline (■),norepinephrine (▼), or serotonin (●).

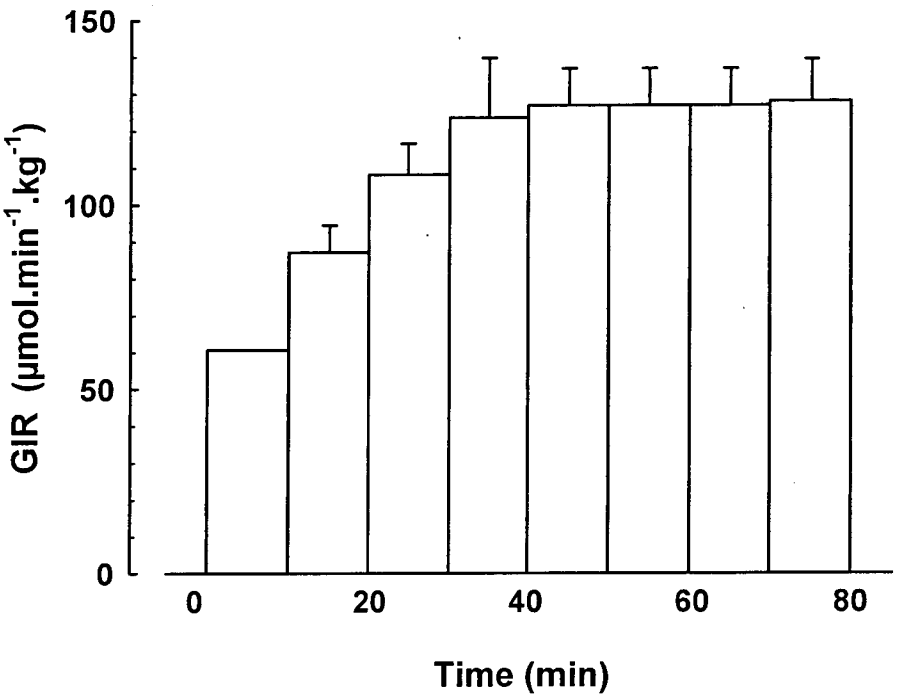


**Figure 5.3 Glucose infusion rates (GIR) required to maintain basal blood glucose at 4.5 ± 0.2 mM during insulin infusion.** Values are means ± SE for 11 animals. The initial (pre-insulin infusion), and steady-state plasma insulin concentrations attained were 390 ± 165 and 1,580 ± 110 pM, respectively (138).

**Table 5.1 Effects of insulin on leg oxygen uptake and 2-deoxyglucose uptake by individual muscles *in vivo***

| | Saline | Insulin |
|---|---|---|
| Glucose infusion rate ($\mu mol.min^{-1}.kg^{-1}$) | | 100.7 ± 3.2 |
| Femoral blood flow ($ml.min^{-1}$) | 0.85 ± 0.05 | 1.2 ± 0.1$^{\#}$ |
| Leg oxygen uptake ($\mu mol.h^{-1}.g^{-1}$) | | |
| Initial (pre-saline or –insulin) | 27.5 ± 3.9 | 24.2 ± 2.2 |
| Final (post-saline or –insulin) | 27.8 ± 3.1 | 22.9 ± 2.3 |
| 2-Deoxyglucose uptake ($\mu mol.h^{-1}.g^{-1}$) | | |
| Soleus | 2.9 ± 0.2 | 9.6 ± 1.5* |
| Plantaris | 2.4 ± 0.1 | 5.0 ± 0.5* |
| Gastrocnemius red | 3.1 ± 0.2 | 11.4 ± 1.2* |
| Gastrocnemius white | 2.0 ± 0.1 | 4.2 ± 0.5* |
| Extensor digitorum longus | 3.4 ± 0.2 | 8.9 ± 1.0* |
| Tibialis | 3.2 ± 0.3 | 8.7 ± 0.9* |

All measurements were made at the completion of the clamp when steady-state had been achieved. Significance of difference: $^{*}P < 0.001$, $^{\#}P < 0.01$ compared with saline (n = 8-10).

### 5.3.3 LDF signal by scanning probe

Figure 5.4 shows that insulin had not increased femoral blood flow at 1h. (cf ref. (138)). However, at this same time point insulin had markedly increased the scanning LDF signal over the biceps femoris [top left hand square within the field of measurement (Figure 5.1)] by 62±8% ($P<0.05$; n=5) (Figure 5.4). Saline infusion controls showed no increase in either femoral blood flow or scanning LDF signal over the biceps femoris at 1h ($P>0.05$; n=4) (Figure 5.4).

Epinephrine is a faster acting agent than insulin and as noted previously (138) increases femoral blood flow. In the present studies epinephrine 0.125 ($\mu g.min^{-1}.kg^{-1}$) increased femoral blood flow by 49±8% ($P<0.05$; n=3) at 15 min. Despite this effect, scanning LDF signal was unchanged (4±8%; $P>0.05$) (Figure 5.4). The rise in LDF signal was greater with insulin than either epinephrine or saline ($P<0.05$; ANOVA).

Figure 5.1 shows representative scans for a saline control (Figure 5.1A) and an insulin clamp (Figure 5.1B) at 1h as well as an illustration to show the area scanned (Figure 5.1C, large square) and the area corresponding to muscle (Figure 5.1C, smaller square). Settings on the scanner were high resolution, threshold voltage 5.30 and 64 x 64 pixels. Since the average area scanned was 900 $mm^2$ each pixel represented approx. 0.2 $mm^2$. Analysis of the total scanned area and of the connective tissue region around the knee failed to reveal an effect of insulin on those scans where a significant increase in muscle signal due to insulin had occurred. Thus values before (Figure 5.1A) and after insulin (Figure 5.1B) were 1.13 ± 0.25 and 1.26 ± 0.22 volts ($P>0.05$; total area) and 2.51 ± 0.35 and 2.69 ± 0.37 volts ($P>0.05$; connective tissue).

### 5.3.4 LDF signal by stationary probe

The stationary probe was positioned over the center of the anterior end of the biceps femoris as in perfused hindlimb studies above and shown in Figure 5.1C (depicted by the red dot). The signal was continuously recorded, and mean values are shown in Figure 5.5

for 0-80 minute period following commencement of insulin infusion. For the stationary LDF probe experiments, insulin at 1h increased femoral blood flow (47%, n=6; $P < 0.05$) and LDF signal 47±12% ($P<0.05$) relative to saline controls (n=5) which did not affect FBF. Epinephrine also increased femoral blood flow (39%) but LDF signal did not change significantly (-0.3%; $P$ = ns; n =5), data not shown. Figure 5.5 shows the time courses for insulin-mediated changes in femoral blood flow (upper panel) and LDF signal (lower panel). The change in LDF signal was significant at 20 min and preceded the increase in femoral blood flow which occurred at 60 min.

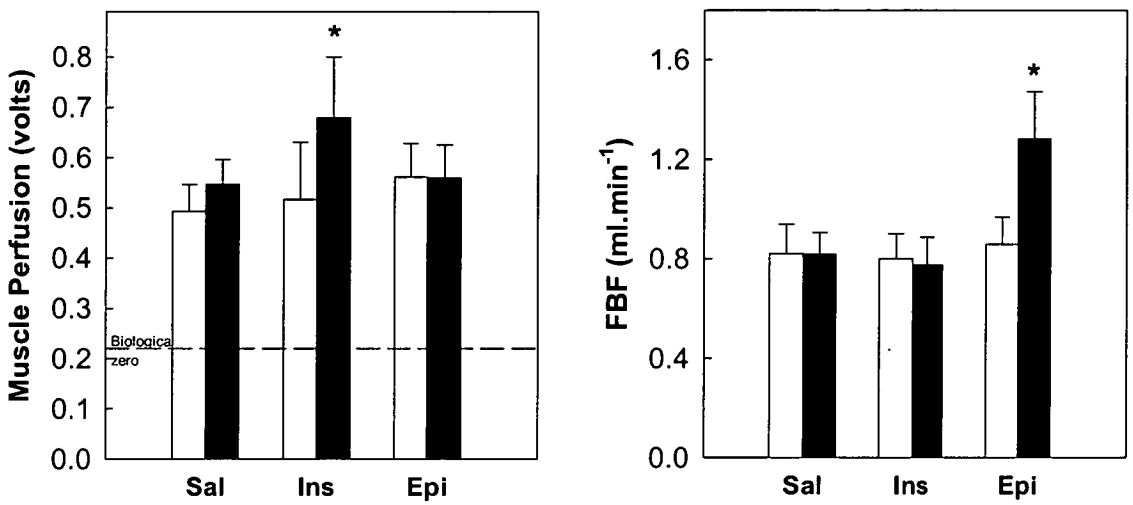


**Figure 5.4 Scanning laser Doppler measurement of lateral surface of thigh muscles (muscle perfusion) and total femoral arterial blood flow (FBF) of anaesthetised rats before treatment (open bars) and following treatment (filled bars) with insulin/glucose (Ins, n = 5), epinephrine (Epi, n = 3) or saline infusions (Sal, n = 4).** Values are means ± SE and were taken at 60 and 15 min after commencement of insulin or epinephrine infusion, respectively . * Significantly ($P < 0.05$) different from pre-treatment values.

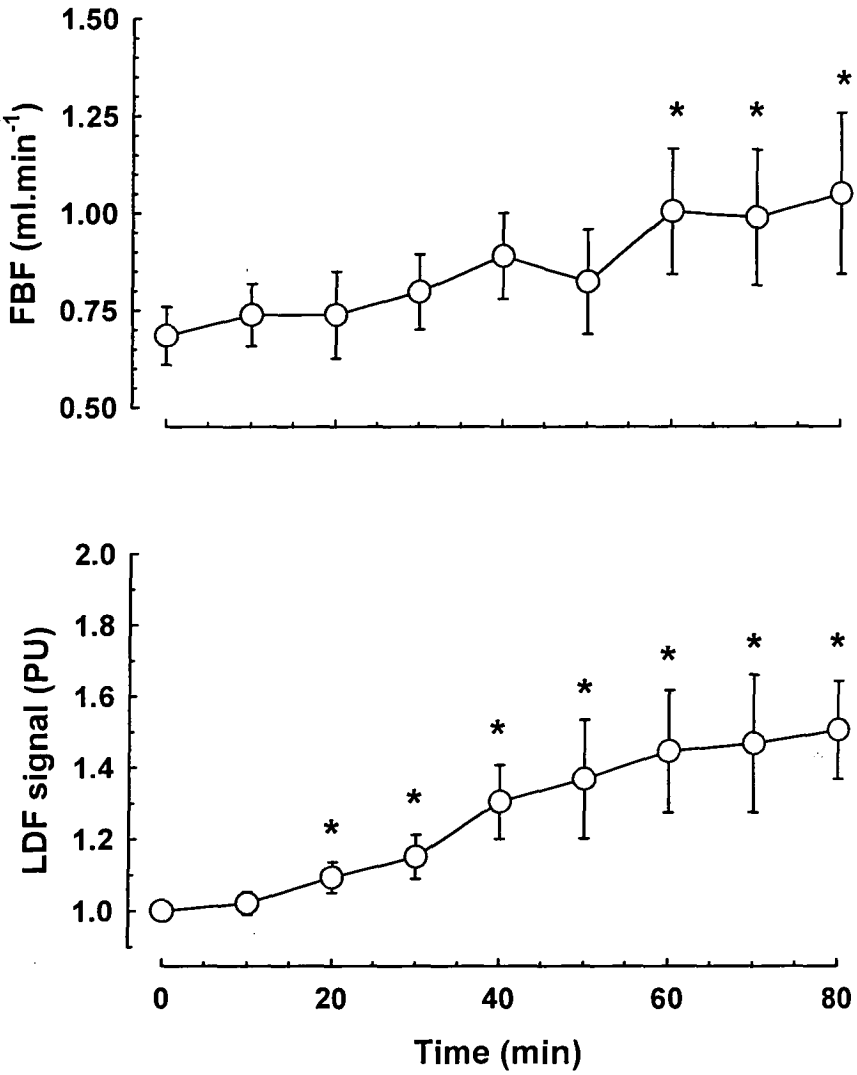


**Figure 5.5 Time course for changes in FBF ( $ml \cdot min^{-1}$, upper panel) and for stationary probe LDF signal in perfusion units (PU, lower panel) during hyperinsulinaemic euglycaemic clamp.** Values are means ± SE for 6 animals. * **Significantly ($p < 0.05$) different from zero time.**

## 5.4 Discussion

The data show that a constant infusion of insulin under euglycaemic conditions has increased the muscle surface LDF signal. This would appear to reflect an increase in nutritive flow in muscle consistent with our previously reported increase in capillary recruitment determined by increased metabolism of the marker substrate 1-MX seen at the same high physiologic dose of insulin (138). The current data show that insulin induces capillary recruitment and enhances glucose uptake, a finding consistent with a metabolic role for capillary perfusion through vessels that facilitate nutrient exchange. The finding that insulin leads to a an increase in muscle capillary flow as measured by LDF and that this occurs over a time course similar to that observed for whole body glucose uptake, is reminiscent of the strong correlation observed between LDF signal from similarly placed probes and oxygen uptake as altered by the two different vasoconstrictors, 5-HT (Type B) and NE (Type A) in the constant-flow pump-perfused rat hindlimb (Fig. 5.2). Oxygen uptake has proved to be a reliable indicator of nutritive flow in perfused hindlimb muscle. However, from several studies where flow has been manipulated by vasoconstrictors, increases in oxygen uptake have always been associated with pressure increase (e. g. see reviews (32;34) and thus the increased pressure may be critical as a positive influence for increased oxygen uptake. In the present series of experiments, and as noted previously (138)), there was very little change in blood pressure (data not shown) and no increase in oxygen uptake during the insulin clamp even though nutritive flow has increased. This finding is consistent with a number of human studies (52), where oxygen uptake by limb tissue (muscle) was also found not to increase. Thus insulin's action to increase muscle capillary flow as detected by the LDF probe in the present study can occur in the absence of an increase in oxygen uptake because there is no increase in pressure. This may be partly due to insulin's proposed NO-dependent vasodilatory action (152), which is discussed in detail later in this thesis. From the model studies (Chapter 4), it would also seem very likely that the increase in LDF signal due to insulin is attributable to the receiving nutritive capillaries being considerably more tortuous, crossing the LDF field of measurement a number of times.

The non-nutritive route that is constricted presumably comprises shorter more direct vessels that reflect a lower LDF signal even when carrying flow.

The increase in capillary flow induced by insulin precedes by at least 30 min changes in total leg flow as detected by the flow probe positioned around the femoral artery. Furthermore, epinephrine which increased total flow had no effect on the LDF signal. An increase in nutritive flow due to insulin without an increase in total flow implies that flow has been redistributed from another route that may not visible to the LDF probe. This may be because of the position or size of the probe. Comparison with the perfused rat hindlimb is helpful in considering these issues. Although almost fully dilated, the isolated perfused hindlimb preparation responds to vasoconstrictors by either increasing or decreasing metabolism, under conditions of constant total flow. Vasoconstrictors that increase metabolism in the constant flow preparation do so by redirecting flow from a "non-nutritive" route located in the closely associated connective tissue of the perimysium and related sheaths. Some of the vessels are visible and relatively free from a background of muscle nutritive capillaries (67) and one study has shown that the vasoconstrictor, NE, that increased overall hindlimb metabolism redirected flow from these vessels to the muscle nutritive route (122). Accordingly, it would seem likely from the present study that insulin has acted similarly to redirect flow from the "non-nutritive" route to the nutritive route. As already discussed above, insulin does not affect blood pressure within this time frame (138), thus recruitment of nutritive flow at the expense of "non-nutritive" flow would appear to involve a combination of vasodilatory and vasoconstrictor activity. There are reports of both vasodilation and vasoconstriction activities of insulin. For example, Renaudin et al. (143) reported that insulin administered *in vivo* to anaesthetised rats caused a marked and durable vasodilation of the terminal arterioles of the spinotrapezius muscle. However, when similar plasma insulin levels (approx. 800 pM) were attained by glucose infusion, partial vasoconstriction of the terminal arterioles occurred (143).

There is some evidence that the surface LDF signal response is heterogeneous for the hindlimb as a whole. Some sites away from the center of the biceps femoris in

perfused rat hindlimb studies were found to respond oppositely to NE and 5-HT (consistent with them being "non-nutritive") or to not respond at all to either agent (possibly mixed) (unpublished observations). In addition, in the present clamp studies with the scanning LDF probe it was apparent that regions away from muscle such as those around the knee, or indeed the total area, including muscle, showed no significant response to insulin suggesting that in some areas flow may have decreased. In one experiment, flow in the connective tissue was actually decreased by insulin.

LDF probe dimensions may be important in determining the nature of the signal received. The stationary LDF probes used in this study when placed on the surface detects signal from a hemisphere with a radius of about 1mm. As shown in Fig. 5.1, when positioned on the center of the anterior end of the biceps femoris the signal appeared to be only of one kind, responding positively to NE and negatively to 5-HT. This contrasts with measurements using a much smaller probe (200 μm) inserted in the muscle, where LDF signals were heterogeneous with some responding as above (i.e. NE positive or "nutritive"), some responding in an opposite manner to the above (i.e. NE negative or "non-nutritive"), and some failing to respond (Chapter 3). Thus it appears likely that the larger probe receives signal from a mixture of sites that convey a character that is predominantly nutritive. Alternatively, "non-nutritive" sites may not be located near the surface of the muscle.

The present findings in the rat *in vivo*, where insulin increased femoral blood flow and increased LDF signal and where epinephrine, despite similar changes in femoral blood flow, did not, is similar to previously reported increase in 1-MX metabolism from this laboratory (138). In that study, 1-MX was infused as a target substrate for capillary endothelial xanthine oxidase. Increased metabolism of this substrate as a result of insulin action was concluded to reflect increased capillary recruitment or nutritive flow. A large part of this conclusion rested on prior knowledge gained from perfused rat hindlimb studies where 1-MX metabolism was shown to closely parallel relative changes in nutritive flow (137;199). Similarly, in the present study we have used prior findings with the perfused rat hindlimb to interpret the nature of the signal changes induced by insulin. Thus an increase in muscle LDF signal due to insulin and independent of changes in total flow support the contention that insulin increases capillary recruitment in human skeletal

muscle (11) and the observation that insulin increased blood volume in human muscle (136).

In conclusion, insulin acts in rats *in vivo* to stimulate LDF signal consistent with capillary recruitment in skeletal muscle. The recruitment may be independent of changes in total blood flow as it precedes temporally the increase in total flow. This dissociation is further seen with infusion of epinephrine which also increased femoral blood flow but does not increase LDF signal. The present findings support previous observations by our group that insulin increases capillary recruitment in rat muscle as measured by 1-MX extraction. In addition, they suggest that recruitment of capillaries may be an important aspect of insulin's effect to increase muscle glucose uptake. The technique of using impaled LDF probes for measuring muscle microvascular flow changes may be applicable to human studies, and this theme is further developed in the next chapter.

# CHAPTER 6

## Changes in Nutritive Blood Flow Patterns and Regulation Induced by Insulin In Human Muscle *In Vivo*: A Study Using Laser Doppler Flowmetry

### 6.1 Introduction

Skeletal muscle is the main peripheral site of insulin-mediated glucose uptake and insulin-mediated vasodilation (10). Defects in this haemodynamic effect of insulin may contribute to diminished insulin-mediated glucose uptake and therefore play an important pathophysiological role in insulin resistance in type 2 diabetes, obesity and hypertension (10).

In the previous Chapter, insulin was shown to increase LDF signal and this was related to changes in skeletal muscle glucose uptake but was independent of changes in total blood flow. In addition, it was shown in Chapter 3 that laser Doppler flow measurements in the constant flow, erythrocyte-perfused rat hindlimb correlate with changes in muscle metabolism, indicative of the ability of this technology to measure erythrocyte movement which is proportional to nutritive flow and separate from total flow.

In humans, hyperinsulinaemia has been demonstrated to induce an increase in the distribution volume of glucose (136) and specifically to increase capillary blood volume as measured with contrast-enhanced ultrasound (40). In human skin, it was recently shown that insulin is capable of inducing functional recruitment of capillaries (157). In addition, insulin has been demonstrated to influence rhythmic fluctuations of the skin microvasculature, so-called vasomotion, by increasing the relative contribution of the frequency interval between 0.01 and 0.02 Hz, in which local endothelial activity is thought to be manifested. This implies that insulin modulates microcirculatory flow through an endothelium-dependent mechanism (157). Although the above-mentioned studies are consistent with an insulin-mediated effect on *intramuscular* microvascular

perfusion, such an effect has never previously been assessed in humans directly with intramuscular laser Doppler measurements.

In humans, the laser Doppler technique has been widely used for measurements of skin blood flow at rest and during provocational manoeuvres (95). In the human skin, reactive hyperaemia after arterial occlusion is commonly applied to assess the vasodilatory capacity of the microcirculation (159;184). The same technique can also be applied to the vasculature of human skeletal muscle. If the probe position remains unchanged, the reproducibility of intramuscular reactive hyperaemia measurements after arterial occlusion has been shown to be excellent (71;95).

The aim of the present study was to apply the experience gained from previous work and shown in the earlier chapters to examine directly, in human muscle, insulin-mediated effects on microvascular reactive hyperaemia after arterial occlusion and on microvascular vasomotion with an implanted laser Doppler probe. It was also aimed to compare changes in LDF signal in muscle with insulin-mediated effects on total blood flow and skin microvascular perfusion.

## 6.2 Methods

The experiments reported in this Chapter were conducted while on a visit to the Vrije Universiteit Hospital, Amsterdam.

### 6.2.1 Subjects

Characteristics of the study population are shown in Table 6.1. All volunteers were healthy as judged by medical history; were non-diabetic [(1997) Report of the Expert Committee on the Diagnosis and Classification of Diabetes Mellitus. Diabetes Care 20: 1183-1197] and normotensive, (<140/<90 mmHg), as determined by a triple office blood pressure measurement. They all were non-smokers and did not use any medication. All participants gave informed consent for participation in the study. The study was undertaken with approval of the local Ethics Committee and performed in accordance with the Declaration of Helsinki.

### 6.2.2 Study design

All individuals underwent the protocol as described in Figure 6.1. All measurements were performed in a quiet, temperature-controlled room (23.4 ± 0.5 °C) and started at 8:00 AM after a 10-hour fast. Baseline measurements were started after the insertion of two polytetrafluoroethylene catheters (Venflon; B-D, Helsingborg, Sweden): one in the right antecubital vein and one in a vein of the opposite arm.

Throughout the study, laser Doppler measurements were performed to study peak reactive hyperaemia and vasomotion in the anterior tibial muscle. The laser Doppler signal which is called "laser Doppler perfusion" (99) is determined by the product of local speed and concentration of moving blood cells(99). The exact volume measured by laser Doppler cannot be determined, nor can the exact haematocrit of the measured blood and consequently, the laser Doppler signal cannot be transformed into a quantitative SI unit (such as volume of blood per unit time per unit mass of tissue), but, alternatively, it is expressed in arbitrary units which can be called perfusion units (PU). Each time the laser Doppler probe is applied to a new volume of tissue the optical properties and microvascular structure of the tissue being monitored will be different. However, so long as these immeasurable variables remain constant, the laser Doppler signal is very useful because any changes that are seen are strongly related to changes that are occurring in local perfusion (99). Thus, only responses in the laser Doppler signal to provocational manoeuvres, such as comparing before and after hyperinsulinaemia, and not the absolute laser Doppler signal, can be compared between individuals (99).

Laser Doppler perfusion in the anterior tibial muscle was measured with a needle probe (model 402; Perimed, Stockholm, Sweden, fibre separation = 0.15mm) sterilized in ethylene oxide. A standard cannula (Venflon 0.9 x 25 mm; B-D) was inserted into the anterior tibial muscle approximately 20 cm proximal to the ankle joint of the non-dominant leg. The needle probe was introduced through the cannula, positioned to protrude 0.5 cm from the tip of the cannula in order to make proper contact with the

muscle tissue, as indicated by a regular and pulsatile laser Doppler signal, and fixated on the skin with a special fixation device (PH 18 Fixation Device; Perimed). The studies were performed with the individuals in the supine position. In order to minimize movement artefacts in the laser Doppler signal, the leg was fixated by resting on a vacuum cushion moulded to hold the limb in a comfortable position.

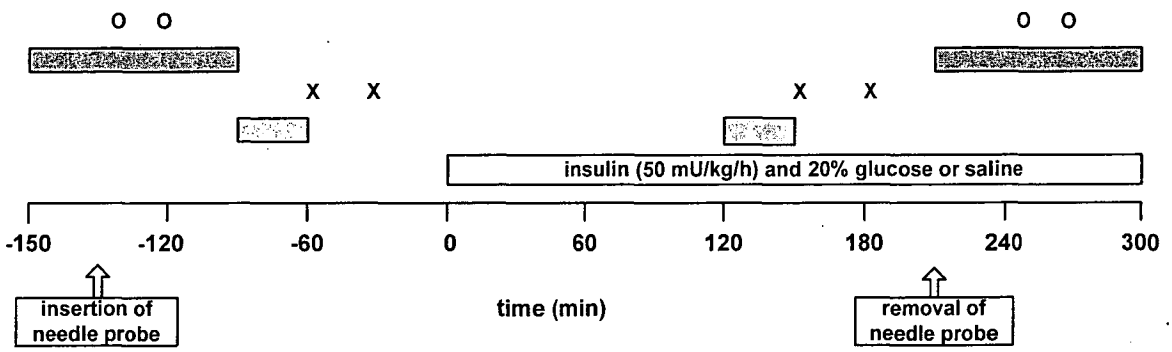


**Figure 6.1 Design of the study protocol.** O = leg blood flow assessed with venous occlusion plethysmography and blood pressure measurements, X = Peak reactive hyperaemia measured with the intramuscular laser Doppler probe, ▭ = Vasomotion assessed with the laser Doppler probe, ▭ = Capillaroscopy and endothelium-(in)dependent vasodilation in skin of the finger

**Table 6.1 Characteristics of the study population**

| | **Mean±SD or N** |
|---|---|
| N (men/women) | 12 (6/6) |
| Age (years) | 27 ± 8 |
| BMI ($kg/m^2$) | 22.6 ± 1.0 |
| WHR | 0.81 ± 0.054 |
| M/I-value ($mg \cdot kg^{-1} \cdot min^{-1}$ per $pmol \cdot l^{-1}$) * 100 | 2.0 ± 0.6 |
| Fasting serum total cholesterol (mmol/l) | 4.2 ± 1.0 |
| Fasting LDL-cholesterol (mmol/l) | 2.3 ± 0.9 |
| Fasting HDL-cholesterol (mmol/l) | 1.4 ± 0.3 |
| Fasting serum triglycerides (mmol/l) | 0.9 ± 0.5 |

M/I-value = glucose infusion rate during the hyperinsulinaemic, euglycaemic clamp, expressed per kg bodyweight, corrected for insulin concentrations in pmol per litre

### 6.2.3 Blood pressure

During the study days, systolic and diastolic blood pressure, and heart rate were determined at the times indicated in Figure 6.1 (Colin Press-Mate BP-8800; Colin, Japan). The average of three consecutive blood pressure and heart rate readings during each period was used for further analyses.

### 6.2.4 Hyperinsulinaemic euglycaemic clamp

Insulin sensitivity was determined with the euglycaemic, hyperinsulinaemic clamp method as described for humans by other researchers (60). The basis of the technique is similar to that used for rats and described in Chapter 2. Briefly, insulin (Velosulin; Novo Nordisk, Bagsvaerd, Denmark) was infused in a primed continuous manner at a rate of 50 mU/kg/hr. Euglycaemia (5 mmol/l) and was maintained by adjusting the rate of a 20% D-glucose infusion based on plasma glucose measurements performed at 5-10 min intervals. Whole body glucose uptake was calculated from the infusion rate during the second hour of the clamp and expressed per kg body weight and per unit of plasma insulin concentration (M/I-value).

To exclude non-specific changes in vascular measurements, a time- and volume-control study was performed. The control study was performed in an identical fashion as the hyperinsulinaemic clamp with the infusion of the same amount of fluids (0.65% saline) and with blood sampling at the same time intervals, but without glucose or insulin infusion.

### 6.2.5 Leg blood flow

Leg blood flow was measured by mercury-in-silastic strain gauge venous occlusion plethysmography (EC6; Hokanson, Bellevue, USA) on the dominant leg with individuals in the supine position with the foot elevated (157). An occlusive cuff was placed proximally around the dominant leg, and the strain gauge was placed around the calf at the largest circumference. Hokanson dedicated software was used (NIVP3; Hokanson) to

automatically balance the plethysmograph, inflate the cuff to 50 mmHg using a E20 Rapid Cuff Inflator and an AG101 Air Source, capture the inflow waveform, and calculate blood flow. Leg blood flow measurements represent the average of 7-9 recordings. The average of two consecutive leg blood flow measurements during each period was used for further analyses. The day-to-day coefficient of variation was 9.6±7.4%, as determined in ten healthy individuals on two separate days.

### 6.2.6 Capillaroscopy and endothelium-(in)dependent vasodilation in skin of the finger

Nailfold capillary studies and iontophoresis studies were performed as described previously (157). Nailfold capillaries in the dorsal skin of the third finger of the non-dominant hand were visualised by a capillary microscope. Two separate visual fields of 1 $mm^2$ were recorded before and after 4 minutes of arterial occlusion with a digital cuff. Perfused capillaries at baseline and directly after release of the cuff were counted for, 15 and 30 seconds, respectively, from a freeze-framed reproduction of the videotape and from the running videotape when it was uncertain whether a perfused capillary was present or not. Perfused capillary density was defined as the number of erythrocyte-perfused capillaries per square millimetre of nailfold skin. Post-occlusive reactive hyperaemia after 4 minutes of arterial occlusion was used to assess functional capillary recruitment. This was calculated by dividing the increase in perfused capillary density during post-occlusive reactive hyperaemia by the baseline perfused capillary density. The day-to-day coefficient of variation of functional capillary recruitment was 15.9 ± 8.0% as determined in ten healthy individuals on two separate days.

Endothelium-(in)dependent vasodilation of finger skin microcirculation was evaluated with laser Doppler measurements in combination with iontophoresis of acetylcholine and sodium nitroprusside, respectively. Acetylcholine (1% Miochol, IOLAB, Bourneville Pharma, The Netherlands) was delivered on the middle phalanx of the third finger of the non-dominant hand using an anodal current, consisting of 7 doses (0.1 milliamps (mA) for 20 s) with a 60-s interval between each dose. Sodium nitroprusside (0.01%, Nipride,

Roche, The Netherlands) was delivered on the same spot of the fourth finger using a cathodal current, consisting of 9 doses (0.2 mA for 20 s) with a 90-s interval between each dose. The day-to-day coefficient of variation of the relative increase from baseline to the final two deliveries was 12.2 ± 9.7% for the iontophoresis of acetylcholine and 16.4 ± 8.1% for sodium nitroprusside, as determined in ten healthy individuals on two separate days. Skin microvascular measurements were performed with a skin temperature above 30 °C and the skin temperature was monitored continuously during the measurements.

### 6.2.7 Reactive hyperaemia in muscle of the lower leg

Intramuscular reactive hyperaemia measurements were started at least 45 minutes after muscle puncture and after stable laser Doppler recordings had been achieved. An occlusive cuff was placed around the distal thigh of the non-dominant leg. After 5 minutes of resting laser Doppler recording, the cuff was rapidly inflated to 200 mmHg (a value much larger than the systolic blood pressure of these healthy volunteers). This pressure was maintained for 3 minutes, which was shown by others (95) to give a maximal hyperaemic response. After release of the cuff, intramuscular reactive hyperaemia was recorded. Baseline perfusion was calculated as the mean value of the 3 minute laser Doppler recording immediately prior to inflation of the cuff. The peak perfusion corresponded with the maximal laser Doppler signal recorded after release of the cuff. The time to peak perfusion was the time between the start of the cuff deflation and the occurrence of the maximal perfusion measurement. Reactive hyperaemia was measured twice with a 20 minute interval between consecutive occlusions. The mean of these two measurements was used in further analyses. For two consecutive measurements in twelve healthy subjects, the coefficient of variation of the relative increase in perfusion and the time needed to reach peak perfusion during reactive hyperaemia were 10.2±4.3% and 16.2±11.4% respectively.

### 6.2.8 Vasomotion in the muscle of the lower leg

The laser Doppler signal waveform was recorded for 30 minutes and vasomotion analyses were performed on a continuous 15 minute sample of this trace which was relatively free of movement artifacts. A bandpass filter with cut-off frequencies at 20 Hz and 20 kHz, and a time-constant of 0.2 s was used. We used Fourier transformation for determination of the contribution of different frequency components to the variability of the laser Doppler signal. The frequency band between 0.01 and 1.6 Hz was studied and divided into a set of intervals. Based upon the work of Stefanovska et al. (164), we chose five frequency intervals: 1) 0.01-0.02 Hz, which is thought to contain local endothelial activity; 2) 0.02-0.06 Hz, which is thought to contain neurogenic activity; 3) 0.06-0.15 Hz, which is associated with the myogenic response of the smooth muscle cells in the vessel wall; 4) 0.15-0.4 Hz, which is the frequency interval of respiratory function; and 5) 0.4-1.6 Hz, which contains the heart beat frequency. For each frequency-interval, the mean energy density was calculated. Data were processed on a personal computer using Perisoft dedicated software (PSW version 3.11, Perimed, Sweden). The day-to-day coefficients of variation of the mean energy density of the frequency intervals 0.01-0.02, 0.02-0.06, 0.06-0.15, 0.15-0.40 Hz and 0.40-1.6 Hz were 23.1 ± 19.0%, 26.8 ± 25.4%, 25.5 ± 22.7%, 27.9 ± 22.5% and 27.5 ± 17.5%, respectively, in twelve healthy subjects.

### 6.2.9 Analytical methods

Plasma insulin concentrations were measured by radioimmunoassay techniques (Medgenix Diagnostics, Fleurus, Belgium). Blood glucose concentrations were determined by the glucose oxidase method with a glucose analyser YSI2300 (Yellow Springs, OH, USA). Serum total cholesterol, HDL cholesterol and triglyceride concentrations were measured by enzymatic techniques (Hitachi 747 model 100, Roche diagnostics, Mannheim, Germany). LDL cholesterol was calculated by the Friedewald formula.

### 6.2.10 Statistical analyses

All variables were tested for normality of distribution. Data are expressed as mean ± SD or median (interquartile range) as appropriate. The paired Student's t-test and the Mann-Whitney (Wilcoxon) paired test were used to study effects of the hyperinsulinaemic clamp and the time-volume control study, and to compare these effects. Pearson's correlation analysis was used to study associations between insulin-mediated effects on total blood flow and intramuscular and skin microvascular perfusion. A two-tailed P-value of $< 0.05$ was considered significant. All analyses were performed on a personal computer using the statistical software package SPSS version 11.0.

## 6.3 Results

### 6.3.1 Metabolic and haemodynamic variables before and during the hyperinsulinaemic clamp.

Table 6.2 shows that during the clamp insulin levels were elevated to 416 ± 82 pmol/l from a baseline of 65 ± 42 pmol/l. In addition, when compared to the control study, hyperinsulinaemia increased total leg blood flow from 0.1 ± 0.6 to 1.0 ± 1.0 ml·min$^{-1}$·100g tissue$^{-1}$ ($P < 0.05$) as assessed by plethysmography (Table 6.2).

### 6.3.2 Capillaroscopy and endothelium-(in)dependent vasodilation in skin of the finger

When compared to the control study, hyperinsulinaemia was found not to have influenced baseline perfused capillary density, but rather to have increased functional capillary recruitment during peak reactive hyperaemia (13.1 ± 10.1 vs. –5.6 ± 11.0%-points, $P < 0.01$) (Table 6.3). Similarly, comparison to the control study showed that hyperinsulinaemia tended to increase acetylcholine-mediated vasodilation (509 ± 534 vs. 114 ± 337%-points), although this was not significant ($P = 0.07$). Hyperinsulinaemia did not significantly change sodium-nitroprusside-mediated vasodilation ($P = 0.2$, Table 6.3).

Similar results were obtained if the absolute increase in perfused capillary density and in laser Doppler perfusion during iontophoresis of acetylcholine and sodium nitroprusside was used instead of the percentage increase (data not shown).

### 6.3.3 Reactive hyperaemia in muscle of the lower leg

Compared to the control study, there was a trend of insulin to increase basal laser Doppler perfusion, but this was not significant ($P = 0.3$) (Table 6.4 and Fig. 6.2). However, hyperinsulinaemia increased both peak laser Doppler perfusion (218.0 ± 166.3 vs.5.3 ± 97.1 PU, $P < 0.01$) and the absolute and relative increase in laser Doppler perfusion after arterial occlusion (210.8 ± 155.9 vs. 7.1 ± 74.3 PU, $P < 0.01$; 422 ± 327

vs. 11 ± 220%-points, $P < 0.01$, respectively). In addition, hyperinsulinaemia decreased the time needed to reach peak laser Doppler perfusion after arterial occlusion by 3.7 ± 3.1 s (in the control experiment time to peak increased by 1.1 ± 3.1 s, $P < 0.01$). Pearson's correlation analysis demonstrated that insulin-mediated changes in absolute and relative increase after arterial occlusion and time needed to reach peak laser Doppler perfusion were not significantly associated with insulin-mediated effects on total leg blood flow (Pearson's correlation coefficient; $r = 0.19$, $P = 0.5$; $r = 0.15$, $P = 0.6$ and $r = -0.16$, $P = 0.5$, respectively).

### 6.3.4 Vasomotion in the muscle of the lower leg.

Table 6.5 shows energy densities of the intramuscular laser Doppler signal within each frequency interval and the calculated total energy density within the interval from 0.01 to 1.6 Hz. As compared to the control study, hyperinsulinaemia increased the intramuscular energy density of the frequency intervals between 0.01 and 0.02 Hz (median (interquartile range); 1.36 (0.49-2.52) vs. 0.44 (-1.02-2.28, $P < 0.01$), and the calculated total energy density (5.88 (1.46-8.38) vs. 0.46 (-1.59-5.32), $P < 0.05$). In order to gain insight into the effect of hyperinsulinaemia on the lower frequencies of the frequency interval between 0.01 and 1.6 Hz, the effect of hyperinsulinaemia on the energy densities of each of the registered frequencies between 0.01 and 0.15 Hz is shown in Figure 6.3. As compared to the control study, hyperinsulinaemia increased the contribution of all frequencies registered between 0.01 and 0.04 Hz in the muscle, but not of those above 0.04 Hz.

**Table 6.2 Metabolic and haemodynamic variables before and during the hyperinsulinaemic clamp (*Insulin*) and time-volume control study (*Control*)**

| | *Insulin* | | *Control* | |
|---|---|---|---|---|
| | Before infusion | During infusion | Before infusion | During infusion |
| Plasma insulin (pmol/l) | 65 ± 42 | 416 ± 82[b] | 45 ± 12 | 35 ± 9[b] |
| Blood glucose (mmol/l) | 4.3 ± 0.2 | 5.0 ±0.1[bd] | 4.3 ± 0.4 | 4.1 ± 0.3[a] |
| Systolic blood pressure (mmHg) | 122 ± 13 | 124 ± 14 | 119 ± 8 | 123 ± 13 |
| Diastolic blood pressure (mmHg) | 66 ± 10 | 65 ± 10 | 64 ± 9 | 67 ± 9 |
| Heart rate (bpm) | 63 ± 10 | 67 ± 10 | 61 ± 9 | 65 ± 10[b] |
| Leg blood flow ($ml \cdot min^{-1} \cdot 100g\ tissue^{-1}$) | 2.6 ± 1.2 | 3.6 ± 0.8[ac] | 2.6 ± 1.0 | 2.7 ± 1.2 |

Values are expressed as mean ± SD; [a] $P < 0.05$ and [b] $P < 0.01$ during vs. before infusion; $P < 0.05$ and [d] $P < 0.01$ change during insulin study versus during control study.

**Table 6.3 Skin microcirculatory measurements before and during the hyperinsulinaemic clamp (*Insulin*) and time-volume control study (*Control*)**

| | *Insulin* | | *Control* | |
|---|---|---|---|---|
| | Before infusion | During infusion | Before infusion | During infusion |
| *Capillary recruitment* | | | | |
| Baseline perfused capillary density (n/mm$^2$) | 33.8 ± 5.5 | 33.8 ± 5.8 | 34.6 ± 5.6 | 36.6 ± 6.6 |
| Peak perfused capillary density (n/mm$^2$) | 49.0 ± 8.0 | 53.3 ± 10.0[ad] | 50.5 ± 9.2 | 50.9 ± 8.0 |
| Perfused capillary increase (n/mm$^2$) | 15.1 ± 5.2 | 19.5 ± 6.7[be] | 15.9 ± 6.4 | 14.9 ± 6.4 |
| Functional capillary recruitment (%) | 46.6 ± 17.5 | 59.7 ± 21.9[be] | 47.6 ± 20.2 | 42.0 ± 22.0 |
| *ACh-mediated vasodilation* | | | | |
| Skin temperature (°C) | 31.1 ± 1.0 | 31.5 ± 0.8 | 30.9 ± 1.4 | 31.7 ± 1.1 |
| Baseline skin laser Doppler perfusion (PU) | 24.0 ± 9.7 | 20.5 ± 7.5 | 28.8 ± 8.5 | 26.4 ± 12.0 |
| Plateau skin laser Doppler perfusion (PU) | 148.7 ± 79.3 | 204.8 ± 78.0[b] | 197.0 ± 125 | 191.8 ± 70.0 |
| ACh-mediated vasodilation (%) | 491 ± 196 | 1000 ± 499[bc] | 593 ± 355 | 707 ± 268 |
| *SNP-mediated vasodilation* | | | | |
| Skin temperature (°C) | 31.4 ± 0.78 | 31.4 ± 1.1 | 31.2 ± 0.8 | 32.2 ± 1.0 |
| Baseline skin laser Doppler perfusion (PU) | 22.0 ± 6.7 | 23.4 ±9.2 | 24.4 ± 12.0 | 25.5 ± 10.2 |
| Plateau skin laser Doppler perfusion (PU) | 166.6 ± 78.0 | 159.1 ± 81.2 | 160.1 ± 66.0 | 193.4 ± 98.8 |
| SNP-mediated vasodilation (%) | 719 ± 433 | 623 ± 352 | 632 ± 278 | 745 ± 446 |

Values are expressed as mean ± SD; n = number of perfused capillaries; ACh = acetylcholine; SNP = sodium nitroprusside; PU = arbitrary perfusion units; [a] $P < 0.05$ and [b] $P < 0.01$ during vs. before infusion; [c] $P = 0.07$, [d] $P < 0.05$ and [e] $P < 0.01$ change during insulin study versus during control study.

**Table 6.4 Reactive hyperaemia measurements in the tibial muscle of the lower leg before and during the hyperinsulinaemic clamp (*Insulin*) and time-volume control study (*Control*)**

| | *Insulin* | | *Control* | |
|---|---|---|---|---|
| | Before infusion | During infusion | Before infusion | During infusion |
| **Baseline laser Doppler perfusion (PU)** | 35.7 ± 19.2 | 42.9 ± 18.1 | 30.0 ± 14.9 | 29.2 ± 14.1 |
| **Peak laser Doppler perfusion (PU)** | 193.7 ± 100.0 | 412 ± 203[ab] | 176.2 ± 69.6 | 181.5 ± 83.5 |
| **Absolute increase (PU)** | 158.0 ± 97.8 | 369 ± 202[ab] | 146.3 ± 68.4 | 153.3 ± 76.1 |
| **Relative increase (%)** | 565 ± 358 | 987 ± 605[ab] | 622 ± 337 | 633 ± 366 |
| **Time to peak (s)** | 12.0 ± 5.7 | 8.4 ± 4.1[ab] | 11.1 ± 4.7 | 12.2 ± 5.7 |

Values are expressed as mean ± SD; PU = arbitrary perfusion units; [a] $P < 0.01$ during vs. before infusion; [b] $P < 0.01$ change during insulin study versus during control study.

**Table 6.5 Energy densities of microvascular laser Doppler perfusion within each of the five frequency intervals and the total energy density in muscle of the lower leg before and during the hyperinsulinaemic clamp *(Insulin)* and time-volume control study *(Control)***

| | *Insulin* | | *Control* | |
|---|---|---|---|---|
| **Frequency domain** | Before infusion | During infusion | Before infusion | During infusion |
| **0.01 – 0.02 Hz** | 2.33 (1.65-3.50) | 5.78 (3.69-8.83)[ad] | 2.01 (1.10-2.80) | 2.15 (1.09-4.43) |
| **0.02 – 0.06 Hz** | 1.14 (0.92-1.86) | 1.36 (0.83-2.83) | 0.92 (0.58-1.43) | 0.95 (0.66-3.01) |
| **0.06 – 0.15 Hz** | 0.83 (0.68-0.97) | 1.14 (0.79-1.43) | 0.58 (0.44-1.04) | 0.51 (0.34-1.81) |
| **0.15 – 0.40 Hz** | 0.57 (0.37-0.70) | 0.84 (0.54-1.48) | 0.42 (0.31-0.78) | 0.39 (0.27-0.95) |
| **0.40 – 1.60 Hz** | 0.46 (0.36-0.77) | 0.75 (0.45-1.10) | 0.40 (0.21-0.59) | 0.37 (0.22-0.64) |
| **Total energy density** | 5.83 (4.19-8.13) | 12.87 (7.54-16.64)[ac] | 4.69 (2.84-6.62) | 4.24 (2.59-10.94) |

Values are expressed as median (interquartile range); [a] $P < 0.01$ during vs. before infusion; [b] $P = 0.07$, [c] $P < 0.05$ and, [d] $P < 0.01$ change during insulin study versus during control study.

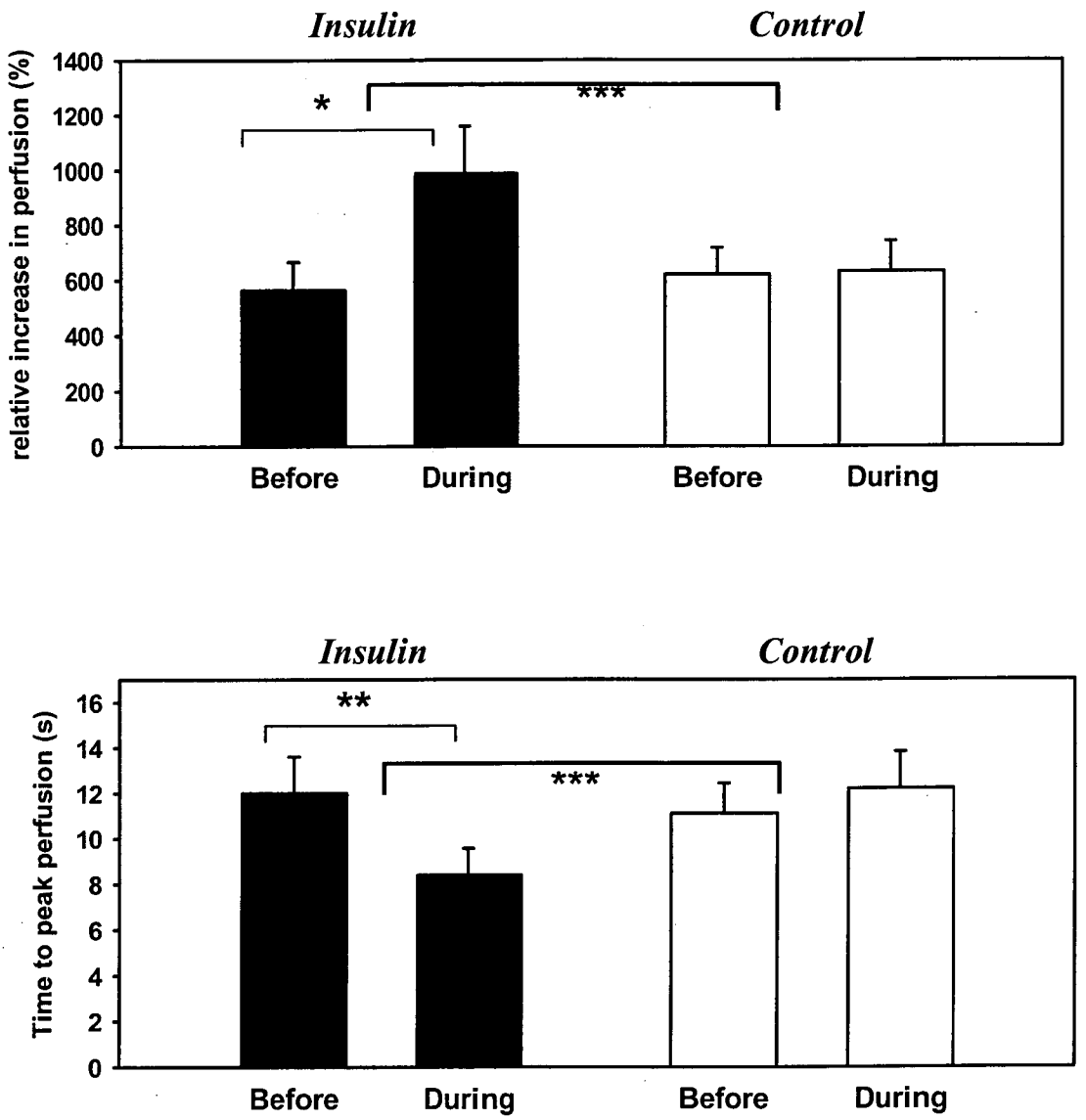


**Figure 6.2 The relative increase in intramuscular perfusion after arterial occlusion (upper panel) and time needed to reach peak intramuscular perfusion after arterial occlusion (lower panel) before and during the hyperinsulinaemic clamp (*Insulin*) and time-volume control study (*Control*).** $^{*}P < 0.05$ and $^{**}P < 0.01$ during vs. before infusion; $^{***}P < 0.01$ change during insulin study versus during control study

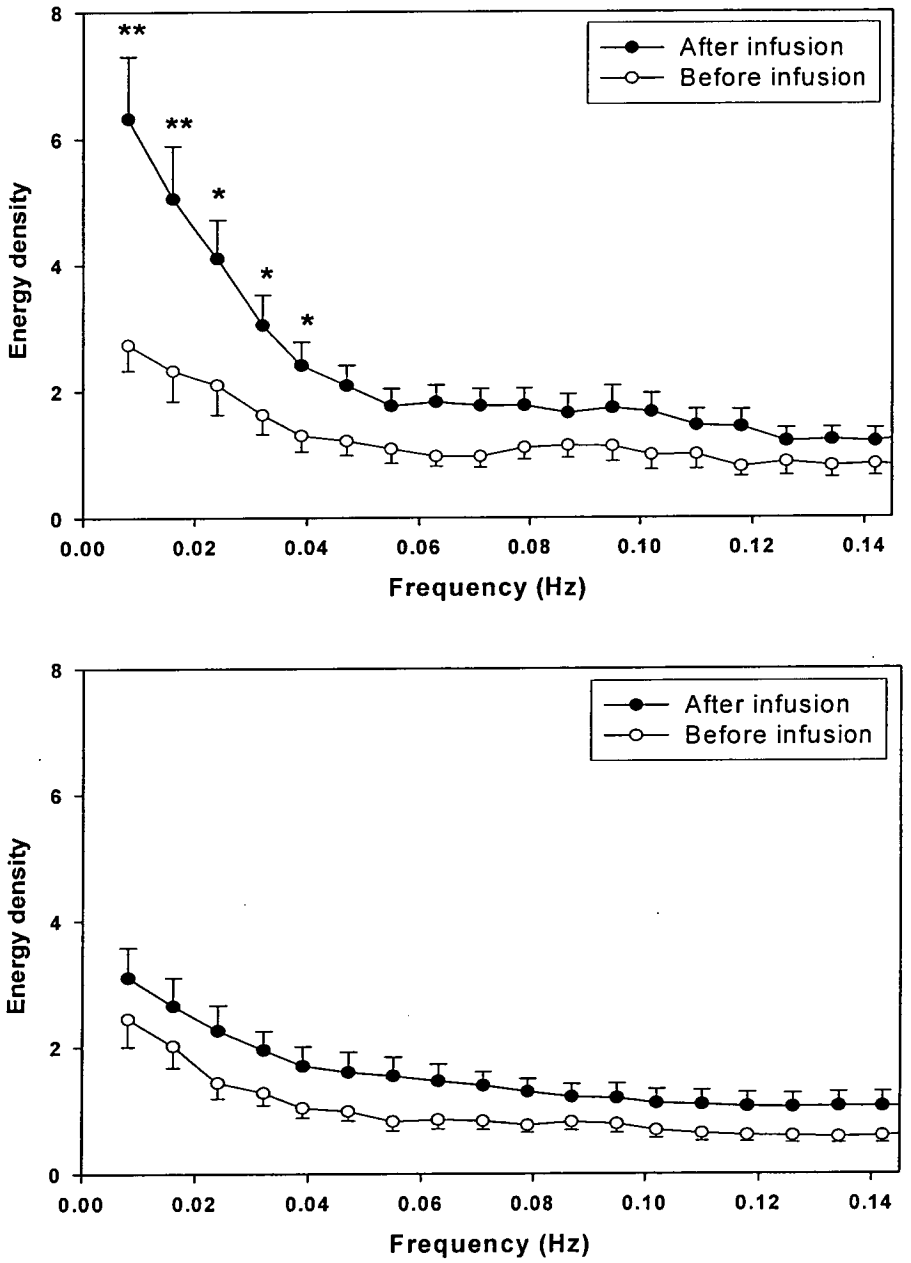


**Figure 6.3 The contribution of frequencies between 0 and 0.15 Hz to the total energy density of microvascular intramuscular vasomotion before and during the hyperinsulinaemic clamp (*Insulin*; upper panel) and time-volume control study (*Control*; lower panel).** $^{*}P < 0.05$ and, $^{**}P < 0.01$ change during insulin study versus during control study

## 6.4 Discussion

The main finding of this Chapter is that insulin affects intramuscular microvascular perfusion as estimated with the laser Doppler technique. We show that hyperinsulinaemia increases two different measures of intramuscular microvascular activity: reactive hyperaemia after arterial occlusion and vasomotion. Hyperinsulinaemia increases the maximal reactive response in intramuscular laser Doppler perfusion following 3 minutes of arterial occlusion and reduces the time needed to reach this maximal response. In addition, hyperinsulinaemia increases intramuscular microvascular vasomotion, in a way indicative of an increase in the contribution of endothelial and neurogenic activity. This confirms previous findings of an insulin-induced increase in total leg blood flow (37;157) and demonstrate insulin-induced increases in skin capillary recruitment after arterial occlusion and endothelium-dependent vasodilation. Taken together, these data show that the vascular effects of insulin are not limited to total blood flow and skin microvascular function during provocational manoeuvres, but extend to microvascular perfusion in human muscle.

The present results are in agreement with previous studies by other researchers that have demonstrated insulin-mediated effects on microvascular perfusion in human muscle using positron emission tomography or contrast-enhanced ultrasound (40;136). However, since each of those methods have not been used to measure muscle perfusion in real time, changes in vasomotion have been undetected.

It is important to note that in the present Chapter hyperinsulinaemia stimulated the response of intramuscular microvascular perfusion when measured during reactive hyperaemia. Hyperinsulinaemia stimulated the response of intramuscular microvascular perfusion during reactive hyperaemia. The stimulatory effect of hyperinsulinaemia might be due to a decreased sensitivity to vasoconstrictor or an increased sensitivity to vasodilatory stimuli. The mechanisms responsible for the increase in vascular perfusion after arterial occlusion are not fully understood. There may be a role for accumulation of metabolic vasodilators, myogenic and/or neurogenic mechanisms (193). It seems unlikely

that hyperinsulinaemia decreases sensitivity to vasoconstrictive effects, because, both in the isolated rat arteriole and in the human forearm, hyperinsulinaemia has been shown to increase vasoconstrictive effects by inducing endothelin-1 activity (25;58). In humans, insulin has been shown to stimulate vasodilatory effects by inducing endothelial nitric oxide (NO) production (165). A role for NO in intramuscular reactive hyperaemia is supported by most (47;57;112), but not all studies (172) using venous occlusion plethysmography. Therefore, in the present study, enhanced endothelial NO production might contribute to insulin-mediated changes in intramuscular reactive hyperaemia. Evidently, this and other possible mechanisms in intramuscular reactive hyperaemia, and insulin-mediated effects thereon, remain to be further investigated.

In this study, as in many previous studies, insulin induced an increase in the total leg blood flow (37;157;183). It cannot be excluded from the present data that insulin-mediated changes in intramuscular reactive hyperaemia are (partly) caused by the increase in the total leg blood flow. However, insulin-mediated changes in intramuscular reactive hyperaemia were not associated with insulin-mediated changes in total leg blood flow. In addition, both in animal and in human studies there is increasing evidence that insulin influences the microvascular blood flow distribution pattern independently of changes in total blood flow (28;40;180). Moreover, iontophorised insulin can directly increase skin microvascular perfusion, indicating a direct local effect (157).

Intramuscular reactive hyperaemia measurements with the laser Doppler have been used and validated in previous studies (71;95;119). Calculation of the relative increase in intramuscular perfusion allows correction for differences in baseline intramuscular perfusion. This is of importance, because previous studies have shown that intramuscular laser Doppler perfusion at rest shows considerable spatial variation at different measurement sites (71;95). The present experiments were performed in conscious, healthy subjects. Although movement of the leg was reduced to a minimum by the use of a vacuum cushion and a probe fixation device on the skin, slight changes in the probe measurement angle and depth could not be avoided. The laser Doppler signal consists of the average perfusion in all arterioles, venules and capillaries of a certain measured

volume of muscle tissue. Slight changes in this measured volume may shift the baseline of the laser Doppler signal. This limitation of the study necessitates cautious interpretation of basal intramuscular perfusion and may partly explain, in addition to the small number of participants, the absence of a significant insulin-mediated effect on basal intramuscular laser Doppler perfusion, which is in contrast with a previous study in anaesthetised rats (29) where relative movement between the probe and the target tissue can be effectively eliminated using clamps. The measurement volume of laser Doppler depends largely on the distance between the transmitting and receiving fibres, the so-called fibre separation (99). A probe with a fibre separation of 0.15 mm, as was used in the current study, probably averages the signal from several different capillary networks. A probe with a larger fibre separation may average perfusion in a larger volume and therefore may be less sensitive to small changes in probe position.

A major advantage of the laser Doppler technique is the possibility to study vasomotion. The origin and control of microvascular vasomotion is still a matter of debate. A central neurogenic regulatory mechanism is suggested by synchronicity on contralateral limbs (151) and by the suppressive effect of central sympathectomy (18). However, local administration of vasoactive substances such as acetylcholine and sodium nitroprusside directly influences vasomotion (94). Furthermore, vasomotion has been shown in isolated small arteries, indicating a local regulatory mechanism (48). In view of these considerations, it can be suggested that vasomotion is regulated by both local vasoactive substances and influences of the central nervous system. The contribution of different regulatory mechanisms flow can be investigated by analysing the contribution of different frequency intervals to the variability of laser Doppler signal (164). In the present study hyperinsulinaemia increased the contribution of the frequencies between 0.01 and 0.04 Hz in muscle. Stefanovska and co-workers have demonstrated that endothelium-dependent vasodilators specifically increase the contribution of frequencies around 0.01 Hz and concluded that the frequency interval between 0.01 and 0.02 Hz represents endothelial activity (94;164). The insulin-induced increase in this frequency interval in the present study in muscle is in accordance with a similar insulin-induced increase in hand skin found in a previous study (157). It is also in agreement with present and

previous findings of an insulin-mediated increase in endothelium-dependent vasodilation in microvasculature (157) and, in general, with insulin-mediated increases in endothelium-dependent vasodilation in resistance vessels [17, 33]. Stefanovska and co-workers have also demonstrated a frequency peak between 0.03 and 0.04 Hz, which is attributed to neurogenic activity, because it has been shown to disappear completely after ganglionic nerve blockade and after sympathectomy (86). Our results demonstrate an insulin-mediated increase in the contribution of the frequencies around 0.03 and 0.04 Hz. Part of the insulin-mediated effects on microvascular vasomotion might thus be explained by insulin-mediated effects on neurogenic activity. Other studies in larger vessels have demonstrated a stimulatory effect of hyperinsulinaemia on sympathetic neural activation (5;148). Taken together, our data suggest an insulin-mediated effect on microvascular vasomotion by increasing both endothelial and neurogenic activity.

In the current study consistency in insulin-mediated increases in microvascular reactive hyperaemia in finger skin and leg muscle were apparent, as were insulin-mediated increases in microvascular endothelial activity in both finger skin and leg muscle. Although different methods were used to measure microvascular reactive hyperaemia and endothelial function in hand skin and muscle, our results suggests a simultaneous effect of insulin on both skin and muscle microvasculature.

Peak reactive hyperaemia in finger skin is used to detect functional recruitment of initially non-perfused capillaries. Capillaries, especially in the skin, are either intermittently or continuously perfused in the resting state (7;155). Only continuously perfused capillaries were counted in the resting state (baseline perfused capillary density), because intermittently perfused capillaries are an important functional reserve that can be recruited after arterial occlusion (7;155). Functional capillary recruitment can serve as a mechanism to satisfy increased metabolic demands such as during insulin infusion (157). This study and previous data suggest that functional capillary recruitment plays a role in insulin sensitivity and blood pressure regulation by modifying availability of insulin and glucose to muscle cells and total peripheral resistance (156-158).

In the present study an insulin-mediated effect on endothelium-independent vasodilation in finger skin microvasculature was not evident, in contrast with a previous study (157), but this was in agreement with previous findings in resistance vessels (167;171). Apparently, other factors not identified in these studies modulate the effect of insulin on endothelium-independent vasodilation in healthy volunteers.

Hand warming to arterialize venous blood samples during the hyperinsulinaemic clamps was not used in this study because this can induce unwanted systemic effects on vascular function (133). Theoretically it can be hypothesized that the lack of arterialisation of venous blood samples may slightly have overestimated insulin sensitivity (60). However, to our knowledge, all previous studies have demonstrated similarity in measurements of insulin sensitivity with and without arterialisation (6;118;133;185). In any case, this issue does not affect our conclusions with regard to insulin's microvascular effects. Finally, we clamped at euglycaemia (i.e. at 5 mmol/l) instead of at isoglycaemia, which resulted in slightly higher glucose levels during insulin than during saline infusion. It is not clear that this difference affected our results, but, because hyperglycaemia impairs microvascular function (2;143), we may, if anything, have somewhat underestimated insulin-mediated effects on microvascular function.

In conclusion, intramuscular laser-Doppler were successfully used to measure effects of insulin on microvascular perfusion in muscle and in skin. The data show that insulin augments the intramuscular microvascular response to reactive hyperaemia after arterial occlusion. In addition, insulin modulates microvascular blood flow oscillations in the muscle indicating an increased contribution of endothelial and neurogenic activity. Concomitant effects of insulin on total blood flow and skin microvascular measurements were evident. Hence, this study demonstrates that insulin stimulates not only total blood flow and skin microvascular perfusion, but also microvascular perfusion in human muscle.

# CHAPTER 7

## Changes in Nutritive Blood Flow Patterns Induced by Insulin In Rat Muscle In Vivo: A Study Using Contrast Enhanced Ultrasound

### 7.1 Introduction

In Chapter 5 it was shown that high-dose (10 mU · $min^{-1}$ · $kg^{-1}$) insulin enhanced the laser Doppler signal in rat muscle obtained using either surface scanning or an implantable laser Doppler probe. Again, epinephrine infusion produced a similar increase in hindlimb blood flow but did not alter laser Doppler signal. These data were consistent with earlier findings from our group that high-dose insulin infusion (10 mU · $min^{-1}$ · $kg^{-1}$) increased rat hindlimb blood flow in vivo and also enhanced the conversion of exogenously infused 1-methylxanthine (1-MX) to 1-methylurate (1-MU) by endothelial xanthine oxidase(138). Because this enzyme is located on the capillary endothelial surface (83) the data indicated that insulin enhances the exposure of 1-MX to xanthine oxidase (138). That was the first report providing experimental evidence for an action of insulin on muscle microvascular recruitment. In addition, epinephrine infusions, which enhanced total hindlimb blood flow to a similar degree as insulin infusions, did not affect microvascular recruitment as measured by 1-MX metabolism (138). This suggested that total flow and microvascular recruitment could be dissociated.

In preliminary studies ultrasound was used during albumin microbubble infusion for the first time to estimate microvascular volume (MV) in rat skeletal muscle in vivo (49). From those studies it appeared that exercise, a known stimulus for microvascular recruitment in muscle, enhanced MV. This technique is well suited to repeated measurement of microvascular perfusion in small animals and humans.

In this Chapter, images of microvascular perfusion (using CEU) in rat hindlimb muscle *in vivo* were measured to ascertain whether physiological hyperinsulinemia exerts a hemodynamic action to increase microvascular perfusion. CEU was also used to examine

whether insulin-induced changes in microvascular recruitment and total limb blood flow are temporally coupled.

## 7.2 Methods

The experiments for this Chapter were conducted while on a visit to the University of Virginia, in Charlottesville, USA.

### 7.2.1 Animals

Male Sprague-Dawley rats weighing 250–350 g were obtained from Hilltop Laboratory Animals (Scottdale, PA). Animals were housed at 22 ± 2°C and during a 12:12 h light: dark cycle. The animals were provided food and water *ad libitum*; however, food was removed the night before the experiment. All experiments were approved by the Animal Care and Use Committee of the University of Virginia.

### 7.2.2 Surgery.

The hyperinsulinemic clamp was used as described in detail previously (Chapter 2). In brief, rats were anaesthetised with an intraperitoneal injection of sodium pentobarbital (55 mg/kg body wt). Polyethylene (PE50; Intramedic) cannulas were inserted into the carotid artery for arterial blood sampling and measurement of arterial blood pressure (Transpac IV pressure transducer; Abbott Critical Systems) and into both jugular veins for intravenous infusions. A tracheotomy tube was placed, and the animals breathed spontaneously throughout the experiment. The femoral vessels in the left leg were exposed by a ~1.5-cm incision through the skin overlaying the vessels. The femoral artery was carefully separated from the femoral vein and saphenous nerve. The epigastric vessels were ligated, and a time transit flow probe that measured blood flow continuously by ultrasound (VB series 0.5 mm; Transonic Systems) was positioned over the femoral

artery. The flow probe was interfaced through a flow meter to an IBM-compatible computer. Femoral blood flow, arterial blood pressure, and heart rate were continually measured using Windaq data acquisition software (Dataq Instruments). The animal was maintained under anaesthesia for the duration of the experiment with aqueous sodium pentobarbital (0.6 mg · $min^{-1}$ · $kg^{-1}$) via the carotid artery. A heat lamp positioned above the rat maintained the rat's body temperature.

### 7.2.3 Experimental protocols

After a 60-min stabilization period following completion of the surgical procedure, rats were divided into two groups. Group 1 animals received either normal saline (10 $\mu$l/min, $n$ = 6) or insulin (3.0 mU · $min^{-1}$ · $kg^{-1}$, $n$ = 9) intravenously while maintaining blood glucose at baseline via a variable-rate infusion of 30% dextrose. MV and flow velocity were assessed with CEU at baseline and after 120 min of infusion. In addition, 1-MX metabolism was determined at the end of the 120-min infusion.

In group 2 animals ($n$ = 5), the time course of insulin's action on microvascular blood volume and velocity were assessed by CEU. Measurements were performed at baseline and at 30 and 90 min after initiating insulin infusion. These time points were selected to reflect times at which plasma insulin concentration increases most markedly after a meal (113;177). No measurements of 1-MX metabolism were made in these animals.

Glucose (30% wt/vol. solution) was infused at a variable rate into all insulin-treated animals to maintain euglycemia, and arterial blood glucose was monitored every 10 min for the first hour and then every 15 min for the rest of the study, using an Accu-Chek blood glucose monitoring system (Roche, Indianapolis, IN).

### 7.2.4 CEU

Details for CEU are given in Chapter 2.

To determine the appropriate microbubble infusion dose for *in vivo* imaging and to ensure linearity in the microbubble concentration versus video intensity relation, experiments were performed to define a microbubble dose-response curve both *in vivo* and *in vitro*. For the *in vitro* experiment, the ultrasound probe was immersed in a beaker of water, and video intensity was measured after injection of incremental numbers of microbubbles during continuous mixing with a stir bar. For the *in vivo* experiment, microbubbles were infused into the jugular vein of the rat, and the ultrasound probe was positioned over the thigh of the rat as described above. Background-subtracted video intensity in resting skeletal muscle was determined during step-wise increases in microbubble concentration. A microbubble infusion rate of 120 μl/min was selected for the *in vivo* study because this dose resulted in video intensity measurements that were well within the linear range of the microbubble concentration and video intensity indicated by both the *in vitro* and *in vivo* dose-range experiments, thus making it possible to accurately detect an increase in MV. For the current study, images were acquired during continuous imaging and at pulsing intervals from 1 to 20 s.

### 7.2.5 1-MX metabolism

To date, the best indicator that we have that 1-MX metabolism reflects microvascular perfusion comes from studies of the effect of electrical stimulation of muscle (49;199). We have shown that 1-MX metabolism increases in response to electrical stimulation (a known stimulus for capillary recruitment) in rat hindlimb both *in vivo* (49) and in a perfused preparation (199). In the perfused rat hindlimb preparation, total blood flow is held constant (199), yet 1-MX conversion to 1-MU is increased, suggesting that microvascular perfusion can be affected independently of total flow.

In group 1 rats, 1-MX (0.4 mg · $min^{-1}$ · $kg^{-1}$) was infused intravenously at a constant rate during the last 60 min of each study. It was shown in previous experiments (138) that 1-MX is rapidly metabolized to 1-MU and that it is necessary to partially inhibit the

xanthine oxidase before infusing 1-MX to slow its whole-body clearance and to allow for measurable concentrations in arterial and venous blood. We have performed allopurinol dose-response curves in the rat *in vivo* (data not shown) and found that 10 μmol/kg partially inhibited the xanthine oxidase and allowed steady-state systemic levels of 1-MX to be obtained.

At the end of each experiment in rats from group 1, blood from the carotid artery and femoral vein was sampled and immediately centrifuged, and 100 μl of plasma was added to 20 μl of 2 M perchloric acid. The plasma was immediately neutralized with 12 μl 2.5 mM $K_2CO_3$ and stored at -20°C until analysis of 1-MX.

Plasma 1-MX, 1-MU, allopurinol, and oxypurinol were analyzed using reverse-phase high-performance liquid chromatography from a modified version of the protocol used by Wynants et al. (194). The metabolites were separated and analyzed using an Ultrasphere ODS column (25 cm, 5-mm particles; Beckman) at 1.0 ml/min. Two buffers were used for the aqueous mobile phase. Buffer A consisted of 4.35 mM acetic acid, and buffer B consisted of 87 mM acetic acid/20% methanol/5% acetonitrile/0.2% tetrahydrofuran, pH 4.0. Buffer A was used during 0–10 min, and at that time buffer B was introduced and buffer A was decreased by using a linear gradient from 10 to 30 min. Buffer B was used from 30 to 40 min. Detection between 0 and 20.5 min was at a wavelength of 250 nm, and between 20.5 and 40 min it was at 272 nm.

### 7.2.6 Statistical analysis

For animals studied in group 1, an unpaired Student's *t* test was used to test differences between saline- and insulin-infused rats for mean arterial blood pressure, heart rate, arterial blood glucose level, vascular resistance, and 1-MX metabolism after 120 min of infusion. A paired Student's *t* test was used to compare the effects of insulin or saline versus baseline on MV, ß, and femoral artery blood flow after 120 min of infusion. For group 2, where each animal served as its own control, repeated-measures analysis of

variance was used to test differences between baseline and 30 and 90 min of insulin infusion on MV, ß, and femoral artery flow. When a significant difference was found, pairwise comparisons by Student-Newman-Keuls test were used to determine at which individual times the differences were significant. For all comparisons, significance was recognized at $P < 0.05$.

## 7.3 Results

### 7.3.1 The effect of insulin on microvascular recruitment and femoral artery flow.

In rats in group 1, arterial blood glucose concentrations remained constant throughout the experiment and were similar in insulin- and saline-treated animals (Table 7.1). To maintain euglycaemia, the insulin group required glucose infusion at an average rate of $11.3 \pm 2.4$ mg $\cdot$ min$^{-1}$ $\cdot$ kg$^{-1}$. Insulin infusion increased the plasma insulin concentration from $52 \pm 13$ to $599 \pm 58$ pmol/l ($P < 0.05$, $n = 4$). Compared with saline, insulin infusion for 120 min did not alter mean arterial pressure or heart rate (Table 7.1). However, hindleg vascular resistance (mean arterial pressure/femoral artery flow) declined significantly ($P < 0.05$) in response to insulin, and femoral artery flow increased ($0.64 \pm 0.05$ to $1.02 \pm 0.10$ ml/min; $P < 0.05$) with insulin but not with saline ($0.79 \pm 0.13$ to $0.68 \pm 0.09$ ml/min) (Figure 7.1 and Table 7.2). Table 7.2 shows that femoral artery flow was significantly higher after 120 min of insulin infusion compared with saline ($P < 0.05$). Compared with baseline, MV markedly increased with insulin ($167.0 \pm 39.8\%$) (Table 7.2) at 120 min. This change was significantly greater ($P < 0.05$) than the $28.2 \pm 13.8\%$ increase seen with saline (Table 7.2). In response to insulin or saline, ß did not significantly change from baseline (Table 7.2).

The effect of insulin and saline on arterial 1-MX concentrations and hindleg 1-MX metabolism is shown in Figure 7.2. At the end of the 120-min experimental period, arterial 1-MX concentration was similar between saline and insulin ($18.3 \pm 3.6$ vs. $16.8 \pm 2.7$ µmol/l). Hindleg 1-MX extraction during saline infusion was $7.1 \pm 0.8$ µmol/l, and

this was not significantly different from the insulin-treated group (7.7 ± 1.2 μmol/l). However, because of differences in total blood flow, 1-MX metabolism was 47% higher ($P < 0.01$) for insulin than saline, consistent with the conclusion that insulin had enhanced the exposure of 1-MX to xanthine oxidase by recruiting capillaries.

### 7.3.2 Time course of insulin's action on microvascular flow.

Figure 7.3A shows the background-subtracted color-coded CEU images (pulsing interval of 20 s) at baseline and after 30 and 90 min of insulin infusion. Progression of the color from red to orange to yellow signifies enhanced video intensity. Insulin produced a higher peak video intensity (MV) at this pulsing interval at both 30 and 90 min of infusion compared with baseline. Figure 7.3B shows the corresponding pulsing interval (1–20 s) versus video intensity data at baseline and after 30 and 90 min of insulin infusion. Again, insulin at 30 min produced a higher plateau video intensity (27 units) than baseline (17 units), indicating increased MV. ß, a measure of red cell velocity, did not change, implying that capillary recruitment had not resulted from the sharing of existent blood flow. The pulsing interval versus video intensity curve obtained at 30 min was similar to that seen at 90 min of insulin infusion.

Table 7.3 shows the effect of insulin on MV, ß, and femoral artery flow at baseline and at 30 and 90 min of infusion in the second group of animals. MV was significantly enhanced by 30 min (12.9 ± 1.8 to 18.9 ± 1.8; $P < 0.001$) of insulin infusion, and this was of similar magnitude to the changes observed at 90 min (20.6 ± 2.2; $P < 0.001$). This occurred at times when there was no discernable change in femoral artery flow. We estimated that we have a >80% power to detect a 20% change in blood flow within 30 min of insulin infusion. ß at these times did not differ from baseline. However, the percent increase in MV appeared to be higher at 120 min in the first group (Table 7.2) than at the shorter times in the second group (Table 7.3). The difference in baseline MV between the two experimental groups is due at least in part to two different batches of microbubbles and modest changes in the gain settings. However, because we measured MV and ß at baseline and during the insulin or saline infusion, each animal served as its own control.

**TABLE 7.1**

**Effect of saline and insulin on systemic and hindleg hemodynamic factors, blood glucose concentrations, and glucose infusion rate required to maintain basal blood glucose at the end of a 120-min infusion period**

| | Saline | Insulin |
|---|---|---|
| Mean arterial pressure (mmHg) | 105 ± 5 | 99 ± 5 |
| Heart rate (beats/min) | 294 ± 21 | 309 ± 22 |
| Hindlimb vascular resistance (mmHg · min · $ml^{-1}$) | 168 ± 20 | 106 ± 12* |
| Arterial blood glucose (mg/dl) | 84 ± 7 | 82 ± 8 |
| Final glucose infusion rate (mg · $min^{-1}$ · $kg^{-1}$) | — | 11.3 ± 2.4 |

Data are means ± SE; $n = 6$ for the saline group and $n = 8$ for the insulin group.

* $P < 0.05$ compared with saline, Student's unpaired $t$ test.

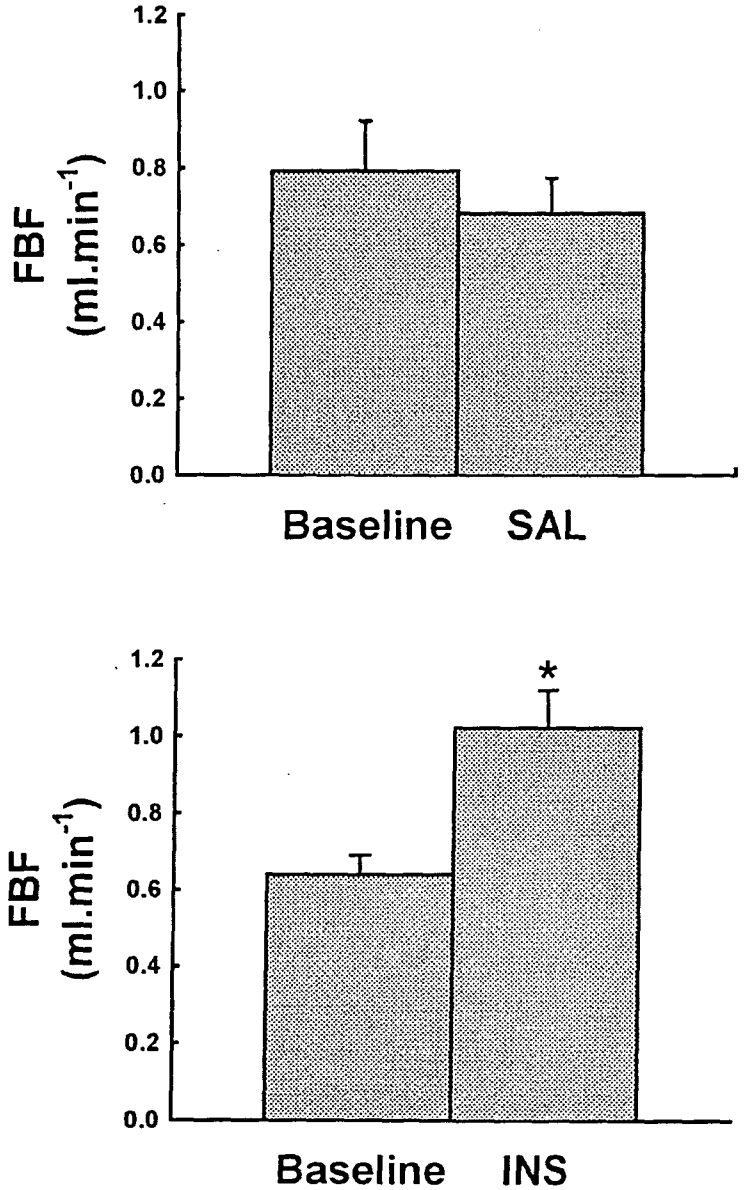


**Figure 7.1 Femoral artery blood flow in response to saline (SAL) or insulin (INS) at the end of the 120-min infusion period.** Values are the means ± SE for six (saline) and nine (insulin) animals. *Significantly different ($P < 0.05$) from baseline.

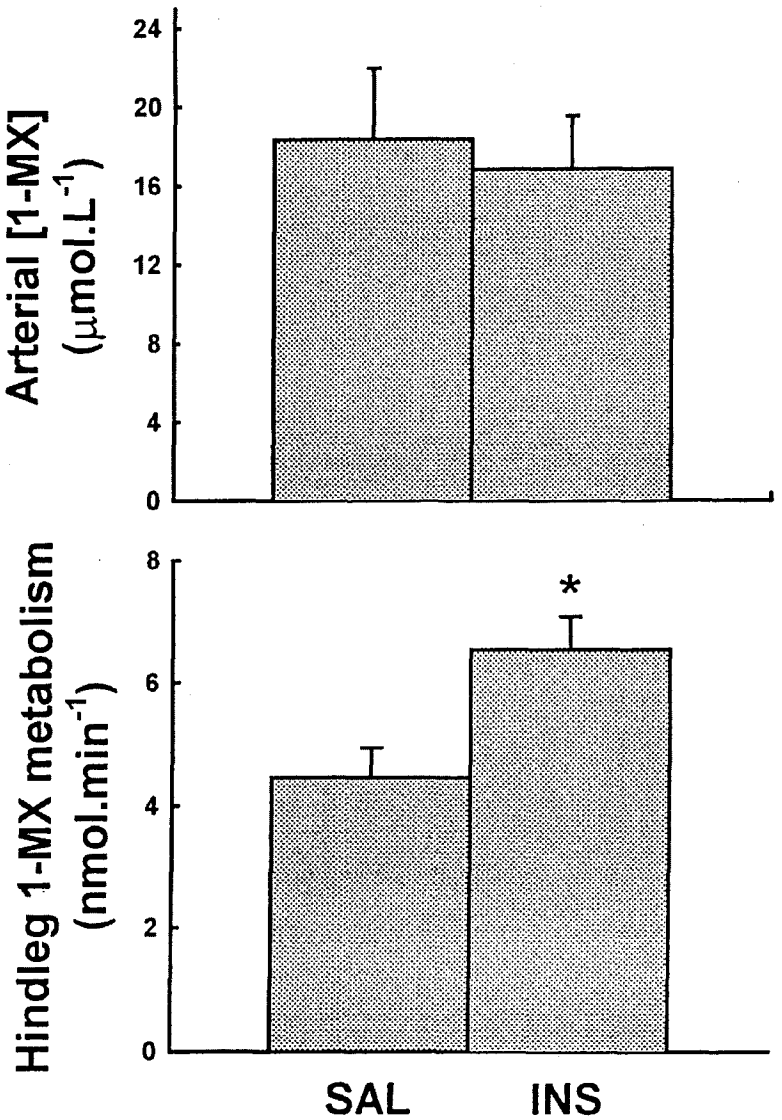


**Figure 7.2 Systemic and hindleg 1-MX values of saline (SAL) and insulin (INS) at the end of the 120-min infusion period.** Values are means ± SE for six and five animals, respectively. *Significantly different ($P < 0.05$) from saline value.

**TABLE 7.2**

**Effect of saline and insulin infusion for 120 min on (FBF) femoral artery blood flow measured by flow probe, MV (microvascular volume), and ß (mean cell velocity) measured by CEU**

| | Baseline | Saline | Baseline | Insulin | *P* (saline vs. insulin at 120 min) |
|---|---|---|---|---|---|
| FBF (ml/min) | 0.79 ± 0.13 | 0.68 ± 0.09 | 0.64 ± 0.05 | 1.02 ± 0.10* | <0.05 |
| ΔFBF (%) | — | -11.8 ± 6.6 | — | 62.7 ± 14.9 | <0.005 |
| MV (video intensity) | 6.1 ± 0.9 | 7.5 ± 0.7 | 6.7 ± 1.7 | 13.4 ± 1.8† | <0.05 |
| ΔMV (%) | — | 28.2 ± 13.8 | — | 167.0 ± 39.8 | <0.05 |
| ß ($s^{-1}$) | 0.10 ± 0.03 | 0.09 ± 0.02 | 0.11 ± 0.02 | 0.14 ± 0.02 | NS |
| Δß (%) | — | 15.0 ± 34.3 | — | 29.5 ± 13.9 | NS |

Data are means ± SE; $n = 6$ for the saline group and $n = 9$ for the insulin group. *P* value compares saline to insulin after 120 min (Student's unpaired *t* test).

* $P < 0.05$ and

† $P < 0.001$ compared with baseline (Student's paired *t* test). FBF, femoral artery blood flow.

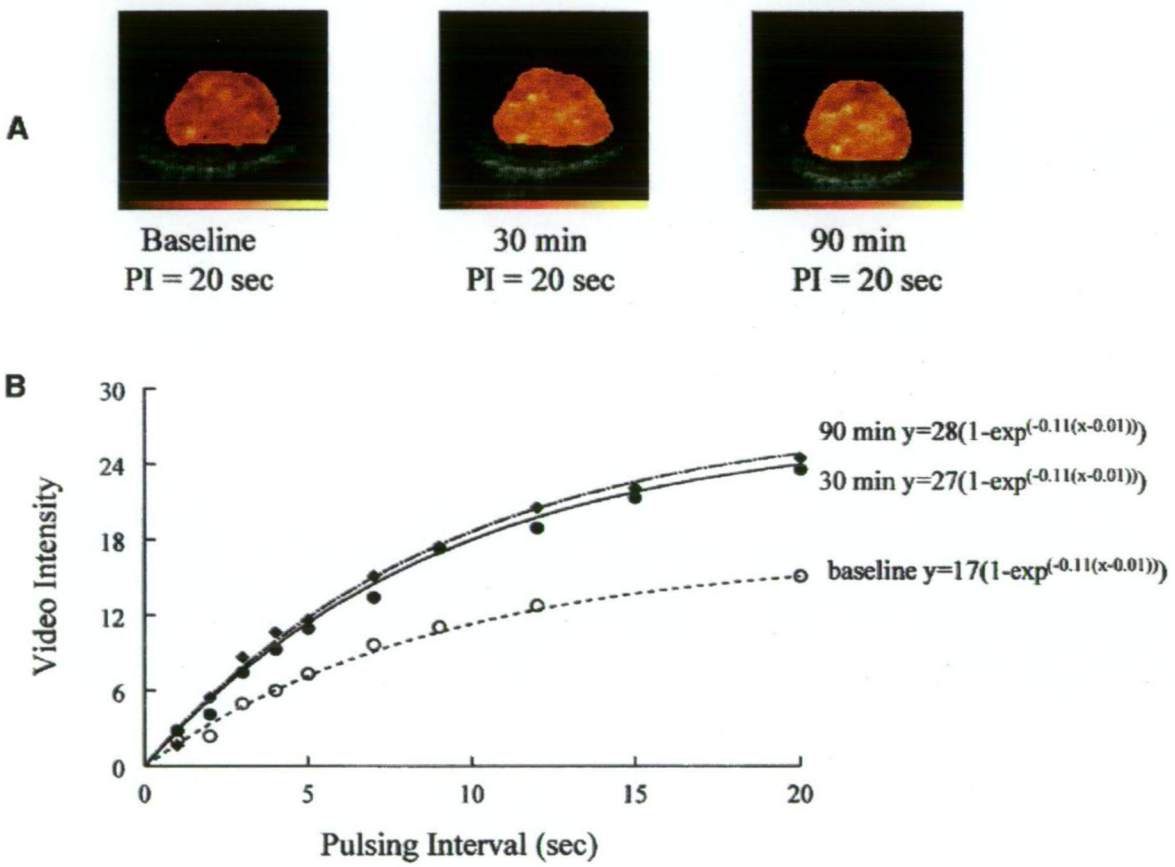


**Figure 7.3 *A*: Examples of background-subtracted colour-coded contrast ultrasound images observed at a pulsing interval of 20s during baseline and after 30 and 90 min of insulin infusion.** Colour changes from red to orange to yellow represent increasing MV. Colour scale (256 levels) for background-subtracted video intensity is at the bottom of each image. *B*: Typical trace of pulsing interval versus video intensity during baseline and after 30 and 90 min of insulin infusion. Data are obtained from adductor brevis and semimembranosus muscles of the rat.

**TABLE 7.3**

**Time course of insulin action on femoral artery blood flow measured by flow probe, MV, and ß measured by CEU**

| | Baseline 0 min | Insulin 30 min | Insulin 90 min |
|---|---|---|---|
| FBF (ml/min) | 0.58 ± 0.08 | 0.55 ± 0.05 | 0.65 ± 0.08 |
| ΔFBF (%) | — | 4.0 ± 3.7 | 13.8 ± 9.4 |
| MV (video intensity) | 12.9 ± 1.8 | 18.9 ± 1.8* | 20.6 ± 2.2* |
| ΔMV (%) | — | 52.8 ± 14.8 | 64.6 ± 9.9 |
| ß ($s^{-1}$) | 0.11 ± 0.03 | 0.10 ± 0.02 | 0.11 ± 0.02 |
| Δß (%) | — | -2.2 ± 10.2 | 8.6 ± 15.2 |

Data are means ± SE; $n = 5$ for each group.

## 7.4 Discussion

At supraphysiological doses, insulin augments total skeletal muscle blood flow in humans (13;197). Some but not all (197) (170) investigators have reported a similar action with insulin at physiological concentrations in humans (170) (14;96) and animal models (135). In addition to dose, the duration of insulin exposure may be important to the enhancement of muscle blood flow, with the effect being greatest after several hours of steady-state hyperinsulinemia (197). The potential importance of these vascular actions of insulin is underscored by the observation that $N^G$-monomethyl-L-arginine methyl ester can block insulin's action on total blood flow and concomitantly inhibit up to 30% of insulin-mediated glucose disposal (12).

In Chapter 5 the microvascular action of insulin in rat muscle *in vivo* was examined using laser Doppler flowmetry (28). The findings suggested that pharmacological concentrations of insulin enhance microvascular recruitment in rat muscle *in vivo*. In the current study, the action of physiological increases in insulin to recruit microvascular vessels was assessed using CEU. It was clear again that insulin increased microvascular blood volume, consistent with microvascular recruitment within muscle. The concordant results observed using two very different approaches suggest that the methods are comparable for assessing microvascular flow, and they provide strong evidence for a physiological action of insulin to regulate microvascular perfusion.

The relative changes in 1-MX metabolism and CEU were not identical; indeed, within the CEU, results seen in groups 1 and 2 were not quantitatively identical. There are a number of things that might contribute to both the 1-MX and CEU measurements and thus influence the quantitative nature of the responses. First, the 1-MX measurement is made across the whole hindlimb (arteriovenous difference x flow), whereas the CEU measurement is made in one area and exclusively in muscle. Therefore, if insulin had no effect to increase flow in nonmuscle tissue (bone and skin), the proportionate rise in MV based on the CEU measurement would be greater than for the 1-MX measurement.

Likewise, it is known that there are significant differences in insulin-induced increases in microsphere perfusion among different types of muscle (i.e., red versus white fibers) (81). Beyond that, it should be recognized that 1-MX metabolism and CEU are fundamentally different techniques for estimating microvascular recruitment. Microbubbles are entirely intravascular and produce a signal that we can measure as video intensity. The background subtraction procedure that we use allows us to remove the contribution from larger vessels, in which flow is rapid; this cannot be done with 1-MX, although it is thought that xanthine oxidase is predominantly a microvascular endothelial marker.

Inasmuch as CEU is a noninvasive method, it permitted repeated measurement of insulin's vascular action in individual animals. We observed that insulin increased MV well before it affected hindlimb total blood flow. Indeed, the changes in steady-state video intensity (MV) at 30 and 90 min during the insulin infusion was not different from those seen at 120 min, by which time total hindlimb flow had begun to rise. This suggests that microvascular recruitment occurred early and remained stable for the duration of the infusion period, and that it occurred independently of changes in total flow. Therefore, insulin-mediated microvascular recruitment and total limb flow follow a different time course. This result is reminiscent of previous findings in Chapter 5 using pharmacological doses of insulin (10 mU · $min^{-1}$ · $kg^{-1}$). In that study, insulin infusion caused an increase in laser Doppler signal in muscle within 20 min that reached a maximum by 50 min. Femoral artery flow measured continuously for the duration of the experiment was not increased until at least the 60 min time point (Chapter 5). Thus, increases in laser Doppler signal preceded by 30–40 min any changes in total muscle blood flow. The marked increase in femoral artery flow seen at 60 min in the laser Doppler study in Chapter 5 was likely caused by the higher dose of insulin (10 mU · $min^{-1}$ · $kg^{-1}$) used for the former study. As noted earlier, epinephrine infusion increases rat hindlimb blood flow without recruiting capillaries, measured by either hindleg 1-MX metabolism (138) or laser Doppler flowmetry (Chapter 5), again providing experimental evidence that changes in microvascular flow can be dissociated from changes in total limb flow. Kuznetsova et al. (93) have also shown dissociation between total muscle flow and microvascular flow, as measured by microspheres and laser Doppler flowmetry, respectively. In those studies,

angiotensin II or phenylephrine infusion into the anaesthetised rat during ganglionic blockade resulted in an increase in laser Doppler signal but no change in total flow. In contrast, isoproterenol markedly enhanced total muscle flow, despite a reduction in laser Doppler signal.

In addition to microvascular blood volume, CEU provides an estimate of ß. The current results showed that ß did not change significantly during the first 90 min of insulin infusion but may have increased at 120 min, a time when hindlimb flow had likewise risen. This is not surprising because the product of ß x MV should provide an index of flow rate at a microvascular level. However, because this product increased without accompanying changes in femoral artery blood flow at 30 and 90 min of insulin infusion, the possibility should be considered that in addition to microvascular recruitment, insulin redistributed flow at the microvascular level within the rat hindleg. Femoral artery blood flow is a measurement of total hindleg flow that feeds muscle, bone, skin, and fat, whereas our measurement of MV and ß is determined within a discrete area of the hindleg that is exclusively in muscle. Thus, it is possible to find a mismatch between total hindleg blood flow and MV x ß within this small area of muscle. For example, we have found in the constant-flow perfused rat hindlimb that microvascular recruitment can increase in muscle without any change in total hindleg flow, and that this is most likely caused by flow redistribution within the hindlimb. Also, as noted previously, muscle blood flow in the rat hindlimb is very heterogeneous, based on the distribution of the different fiber types (80). For instance, in the anaesthetised rat, blood flow (measured by 15-µm microspheres) to the red quadriceps is 9 ml · 100 $g^{-1}$ · $min^{-1}$ but is only 4 ml · 100 $g^{-1}$ · $min^{-1}$ in the white quadricep and the extensor digitorum longus. Thus, based on the distinct differences in total muscle blood flow for each individual muscle of the rat hindlimb, it is highly likely that there could be a mismatch between total hindlimb flow and microvascular flow within a discrete area of muscle.

The albumin microbubbles used as the contrast-enhancing agent averaged 4 µm in diameter, had similar rheology to red blood cells, and were contained entirely within the vascular space (84). As a result, they were an excellent perfusion tracer. Furthermore, over the range of video intensity studied here, there was a linear correlation between the

concentration of microbubbles within the vasculature and video intensity. CEU is particularly useful because it allows background subtraction of the tissue image and thus elimination of signal from large vessels, which fill very rapidly, allowing microvascular flow (which is slower) to be imaged selectively. The CEU method has the additional appeal that it allows imaging of specific regions within muscle and, unlike 1-MX metabolism or measures of total hindlimb flow, is not influenced by contributions from nonmuscle tissue (skin, bone, and adipose tissue). Furthermore, compared with laser Doppler flowmetry, CEU samples a relatively large volume of muscle and does not require surgical exposure of the muscle surface. The laser Doppler method applied to muscle has the potential for producing artifacts, given that it only samples the immediate region around an implanted or surface probe.

Several other investigators have attempted to determine the effect of insulin on muscle microvascular flow. Raitakari et al. (136) used positron emission tomography during inhalation of [$^{15}$O]carbon monoxide. The labeled carbon monoxide binds to erythrocytes, thereby providing a vascular tracer. High-dose insulin concentrations augmented leg blood flow and increased muscle blood volume by 9%. The high dose of insulin used limited any effort to separately assess effects on total flow from those on microvascular recruitment. Moreover, the positron emission tomography method measures blood within both the larger vessels and the microvasculature; thus, changes in MV may not be accurately quantified.

In a subsequent study, Bonadonna et al. (20) used a very different approach and injected a bolus of nonmetabolizable radiolabeled L-glucose into the brachial artery to measure forearm transit time and to estimate extracellular volume. Pharmacological concentrations of insulin enhanced total forearm blood flow, as measured by the dilution of intra-arterially infused indocyanine green dye. The mean transit time of L-glucose lengthened in response to insulin because of an expansion of the extracellular volume by 33%. This measure includes more than the vascular space, and would not report separately on large and small vessels.

More recently, Baron et al. (16) modeled the effects of insulin on microvascular flow by raising and lowering blood flow in the human leg during a steady-state insulin clamp and compared the results to the predicted values of the noncapillary recruitment model of Renkin (145). It was concluded that because glucose uptake was greater than predicted when leg blood flow was increased and smaller than predicted when leg blood flow was decreased, this suggested that the number of perfused capillaries changed considerably under insulin-stimulated conditions, assuming that glucose permeability remained constant. Although it was concluded that insulin-mediated increments in muscle perfusion are accompanied by microvascular recruitment, no direct experimental measure of microvascular recruitment was made.

The relation between insulin's action on total muscle blood flow and its metabolic actions remains embedded in controversy. Yki-Jarvinen and Utriainen (197) have concluded that insulin's effect on total limb flow occurs after its metabolic effects on glucose uptake. It should be noted that this temporal discordance is based on the assumption that insulin's vascular action is restricted to increases in total blood flow. The present study indicated that insulin produces an early hemodynamic action at the microvascular level during a time that insulin is producing a metabolic action. Interestingly, microvascular recruitment (as measured by laser Doppler flowmetry) closely follows changes in glucose infusion rate and not total muscle flow (28). This relation also held for the current study because the glucose infusion rate at 30 min of insulin infusion was 90% of the glucose infusion rate used at 90 min (the plateau for insulin's metabolic action).

Insulin-stimulated total blood flow in many insulin-resistant disease states, such as type 2 diabetes, hypertension, and obesity, is reported to be blunted (11;13;14;96), providing further evidence that the hemodynamic involvement of insulin may be important for its action. However, controversies regarding the vascular actions of physiological doses of insulin persist because some investigators have failed to see an increase in blood flow within healthy humans (116) or an impairment during insulin-resistant states (24;182). None of these studies address separately the actions of insulin on microvascular recruitment and total flow. This is unfortunate because, based on the theoretical models of tissue perfusion developed by Renkin (145), microvascular recruitment might be expected

to be a more potent determinant of tissue glucose exchange than total flow. For instance, we have recently reported that when insulin-mediated microvascular recruitment is prevented with the vasoconstrictor α-methyl-5-HT, an acute insulin-resistant state is induced (139).

In summary, these results indicate that insulin at physiological concentrations recruits flow to the microvasculature in muscle, and at the insulin concentration used here, this effect precedes by at least 60 min any changes in total muscle blood flow. Changes in total muscle blood flow have later onset and do not involve further changes in the microvasculature. Therefore, a full assessment of the role of insulin's vascular actions in healthy and insulin-resistant states may require focusing on the effects on both total blood flow and microvascular flow, which could be the key to insulin's vascular action. Overall, the data from CEU measurement of microvascular volume (capillary recruitment) and capillary recruitment by 1-MX metabolism support the data of Chapter 5 where LDF measurements were used.

# CHAPTER 8

## Changes in Nutritive Blood Flow Patterns Induced by Insulin in Rat Muscle *In Vivo* of Colony, Lean and Obese Zucker Rats: A Study Using the Biochemical Marker, 1-Methylxanthine.

### 8.1 Introduction

In this Chapter the 1-MX method is used to assess responses to insulin in normal colony rats as well as lean and obese Zucker rats. The hypothesis is that the insulin response in the obese Zucker rats will be impaired when compared to lean Zuckers. Since the lean Zuckers are a mixture of homozygote leans and heterozygotes of lean and obese genes, a lower level of responsiveness relative to colony rats is conceiveable.

The genetically obese Zucker rat is regarded as a useful animal model of insulin resistance. Not unlike the insulin resistance in humans, the obese phenotype of the Zucker rat shows hyperinsulinemia (204), dyslipidemia (87) and hypertension (92). The obesity develops as a result of a recessive mutation in the gene for the leptin receptor (134). By four to five weeks of age obese rats weigh significantly more than their lean littermates (203). Insulin resistance then develops in muscle and liver (131;175) and may involve reduced insulin sensitivity as well as a blunted maximal responsiveness to insulin (44). There is clear evidence that the insulin resistance is intrinsic to the muscle fibres or myocytes. Thus it is not only apparent *in vivo* (45;131), but in the perfused hindlimb (87;160) and in individual muscles once they have been isolated and incubated (44). In addition, glycolysis, glucose oxidation and glycogen synthesis are all impaired in the muscle of obese Zucker rats (44). Explanations for the insulin resistance include alterations in the insulin signaling pathway in the obese. For example in skeletal muscle there is reduced expression of IRS1 and IRS2 (4), leading to decreased insulin stimulated

tyrosine phosphorylation and decreased PI3kinase activity associated with IRS1 (88). Insulin stimulated AKT1, AKT2 (88) and ERK2 (128) activity are reduced in obese rats, but there are no alterations in the levels of GLUT4 mRNA (195) or GLUT4 protein (64) in the obese Zucker rats.

Within the context of this thesis the obvious question that arises is whether there are haemodynamic alterations that may contribute to the insulin resistance of muscle that manifests *in vivo*. Some studies with isolated vessels suggest that this may be so. For example, the ability of insulin to attenuate vasoconstriction is impaired in obese Zucker rats (188;201). The focus in this Chapter is thus on comparing the relative responsiveness to insulin in terms of capillary recruitment in muscle as measured by the 1-MX method.

## 8.2 Methods

### 8.2.1 Animals

Male colony rats were bred at the University of Tasmania Animal House and were a hooded Wistar strain as used in earlier chapters. The Zucker lean (Fa/?) and obese (*fa/fa*) rats were male and 18 weeks old. They were purchased from Monash University, Melbourne, Australia. All rats were housed at a constant temperature of 21 ± 1°C in a 12h/12h light/dark cycle and allowed free access to water and a commercial diet as previously described (200). All procedures adopted and experiments undertaken were approved by the University of Tasmania Animal Ethics Committee.

### 8.2.2 Surgery

Procedures for the hyperinsulinaemic euglycaemic clamp or saline infusion of rats *in vivo* under anaesthesia are essentially as described in Chapter 2. In brief, colony hooded Wistar, Zucker lean and Zucker obese rats were treated similarly and underwent either of two protocols after a 60 min period of equilibration when BP and HR had stabilized

following surgery for cannulation, and positioning the hind leg flow probe. Protocol 1: Saline was infused over a 2h period in an amount equivalent to the volume of insulin and 30% glucose infused in Protocol 2. A bolus of allopurinol (10 μmol/kg) was injected at 55 min and then 1-MX was infused at 0.4 mg/min/kg over the final 60 min. A bolus of radioactive 2DG (50 μCi) was injected at 75 min. Arterial blood samples were taken ten minutes before the commencement of the saline infusion and at every ten minutes during the first hour and then every fifteen minutes in the second hour to monitor glucose levels. Arterial samples at 80, 85, 90, 105 and 120 min were also used to monitor radioactive 2DG. Protocol 2: Insulin was infused at 30 (hooded Wistars) or 20 mU/kg/min (Zuckers) in place of the saline as used in Protocol 1. Muscles were excised at the completion of the experiment and freeze clamped in liquid nitrogen to assess the [$^3$H]2-deoxyglucose-6-phosphate as described previously (200). The total blood volume withdrawn from the animals before the final arterial and venous samples did not exceed 1.5 ml and was easily compensated by the volume of fluid infused. Duplicate arterial (A) and venous (V) samples (300 μl) were taken at the end of the experiment (120 min) and placed on ice. These blood samples were immediately centrifuged and 100 μl of plasma mixed with 20 μl of 2M perchloric acid. The perchloric acid treated samples were then stored at -20°C until assayed for 1-MX. The rest of the plasma was used for glucose and insulin analysis.

### 8.2.3 Analytical methods

A glucose analyser (Yellow Springs Instruments, Model 2300 Stat Plus) was used to determine whole blood glucose (by the glucose oxidase method) during the insulin clamp. A blood sample of 25 μl was required for each determination. Insulin levels at the beginning and end of the experiment were determined from arterial plasma samples by ELISA assay (Mercodia, Sweden). Perchloric acid treated plasma samples were centrifuged for 10 min and the supernatant used to determine 1-MX, allopurinol and oxypurinol concentrations by reverse-phase HPLC as previously described (138;139). Xanthine oxidase activity was assessed from muscle homogenates as described previously (142).

### 8.2.4 2DG uptake assay

The frozen soleus, red gastrocnemius, white gastrocnemius, extensor digitorum longus, tibialis and plantaris muscles were ground under liquid nitrogen and homogenized using an Ultra Turrax™. Free and phosphorylated [$^3$H]2DG were separated by ion exchange chromatography using an anion exchange resin (AG1-X8) (81;91). Biodegradable Counting Scintillant-BCA, (Amersham, USA) was added to each radioactive sample and radioactivity determined using a scintillation counter (Beckman LS3801, USA). From this measurement and a knowledge of plasma glucose and the time course of plasma 2DG disappearance, R'g, which reflects glucose uptake into the muscle, was calculated as previously described by others (81;91). The combined data for the muscles are shown.

### 8.2.5 Data analysis

All data are expressed as means ± SE. Mean femoral blood flow was calculated from 5 second subsamples of the data, representing 500 flow measurements every 15 minutes. Vascular resistance in the hindleg was calculated as mean arterial blood pressure in millimetres of mercury divided by femoral blood flow in millilitres per minute and expressed as resistance units (RUs). Glucose uptake in the hindlimb was calculated from A-V glucose difference and multiplied by femoral blood flow and expressed as μmol/min. The 1-MX disappearance was calculated from A-V plasma 1-MX difference and multiplied by femoral blood flow (corrected for the volume accessible to 1-MX, 0.871, determined from plasma concentrations obtained after additions of standard 1-MX to whole rat blood) and expressed as nmoles/min.

### 8.2.6 Statistical analysis

In order to ascertain differences between treatment groups at the end of the experiment (120min), two way analysis of variance using the Student-Newman-Keuls method was performed. Significant differences ($P<0.05$) between insulin and saline treatment in each phenotype of rat, as well as differences between lean and obese rats undergoing the same

treatment were reported. An unpaired Student's t-test was used to determine whether there was a significant difference ($P<0.05$) between the glucose infusion rates at the conclusion of the experiments. All tests were performed using the SigmaStat™ statistical program (Jandel Software Corp.).

## 8.3 Results

### 8.3.1 Characteristics

At the time of study, obese Zucker rats (445 ± 5g) weighed significantly more than their lean littermates (322 ± 4 g; Table 8.1). Obese Zucker rats exhibited hyperinsulinemia and hyperglycemia, prior to either insulin or saline infusions, when compared with their lean littermates or colony rats (Table 8.1). Lean Zuckers did not differ from colony rats in any other respect even though they were slightly lighter (Table 8.1).

In order to make comparisons of insulin-mediated haemodynamic and metabolic changes data from colony rats were chosen where the dose of insulin infused had led to similar plateau insulin levels as the lean Zuckers. Thus as shown in Table 8.2 colony rats were infused with 30 mU/kg/min whereas both lean and obese Zuckers were infused with 20 mU/kg/min insulin. In colony and lean Zucker rats, plasma insulin levels were significantly higher as a result of insulin infusion compared with saline infusion. Colony rats with 30 mU/kg/min insulin were 9666 ± 660 whereas with saline they were 337 ± 31 pM. Lean Zuckers infused with 20 mU/kg/min had plasma insulin of 8630 ± 665 pM and infused with saline of 441 ± 70 pM. Similarly, in obese Zuckers, plasma insulin levels were 20190 ± 1281 pM and 5963 ± 815 pM following insulin and saline infusion, respectively. The higher basal insulin levels may reflect the fed state and the fact that the obese eat more than the lean. Clearly, an insulin infusion of 20mU.min$^{-1}$.kg$^{-1}$ resulted in significantly higher insulin levels in obese rats compared with the lean, and colony rats required a higher insulin infusion rate to attain similar plasma insulin levels as the lean Zuckers (Table 8.2).

**Table 8.1 Characteristics of colony hooded Wistar, lean and obese Zucker rats.** All values were measured at the commencement of saline or insulin infusion. Values are means ± SE for n = 14-17 rats in each group. #, Significantly different ($P < 0.05$) from lean Zucker rats; †, significantly different ($P < 0.05$) from colony rats.

| | Colony | Lean | Obese |
|---|---|---|---|
| Age (weeks) | 15 ± 3 | 18 ± 2 | 18 ± 2 |
| Body weight (g) | 245 ± 5 | 322 ± 4 | 445 ± 5 # |
| Plasma Insulin (pmol/l) | 183 ± 37 | 182 ± 21 | 4158 ± 491 # |
| Blood Glucose (mM) | 4.4 ± 0.1 | 4.8 ± 0.2 | 11.7 ± 0.6 # |
| Blood Pressure (mmHg) | 105 ± 3 | 107 ± 2 | 107 ± 1 |
| Heart Rate (Beats/min) | 351 ± 7 | 335 ± 9 | 329 ± 6 |
| Femoral Blood Flow (ml/min) | 0.76 ± 0.06 | 0.69 ± 0.05 | 0.69 ± 0.05 |

**Table 8.2 Comparison of colony, Zucker lean and obese rats in terms of their response to insulin under clamp conditions**

| | Colony hooded Wistar n = 6-8 | Lean Zucker n = 6-8 | Obese Zucker n = 6-8 |
|---|---|---|---|
| Insulin infusion for clamp (mU/kg/min) | 30 | 20 | 20 |
| Plasma insulin post saline control (pM) | 337 ± 31 | 441 ± 70 | 5963 ± 815# |
| Plasma insulin at end of clamp (pM) | 9666 ± 660* | 8630 ± 665 | 20190 ± 1281# |
| **Haemodynamics** | | | |
| Change in FBF -saline (ml/min) | 0.18 ± 0.02 | 0.12 ± 0.02 | 0.07 ± 0.04 |
| Change in FBF -insulin | 0.90 ± 0.21* | 0.63 ± 0.16* | 0.13 ± 0.03# |
| Change in VR -saline (RU) | -24 ± 6 | -11 ± 7 | -6 ± 9 |
| Change in VR -insulin | -62 ± 10* | -65 ± 12* | -18 ± 13# |
| 1-MX metabolism1 -saline (nmol/min) | 4.8 ± 0.4 | 7.6 ± 0.6 | 4.8 ± 0.4# |
| 1-MX metabolism –insulin | 7.7 ± 0.7* | 9.3 ± 0.7* | 3.6 ± 0.6# |
| **Metabolism** | | | |
| GIR plateau (mg/kg/min) | 25.5 ± 1.2* | 22.1 ± 0.8* | 8.0 ± 0.4*# |
| HGU –saline (μmol/min) | 0.16 ± 0.04 | 0.15 ± 0.05 | 0.13 ± 0.04 |
| HGU – insulin | 0.74 ± 0.08* | 1.12 ± 0.10* | 0.18 ± 0.05# |
| Combined lower leg muscles R'g –saline (μg/g/min) | 3.1 ± 0.3 | 5.0 ± 0.4 | 7.9 ± 1.1 |
| Combined lower leg muscles R'g –insulin | 16.3 ± 1.5 | 25.8 ± 2.7*† | 12.6 ± 2.6# |

Values apart from insulin infusion rates are means ± SE and were determined at the end of the experiment (120 min). Hind leg glucose uptake (HGU) was determined from arterio-venous difference and femoral blood flow at the end of the clamp. R'g represents values for 2-DG uptake by the combined lower leg muscles. All rats were fed. Values from the colony rats are from (202). *, Significantly different ($P < 0.05$) from corresponding saline treatment; #, significantly different ($P < 0.05$) from corresponding treatment in lean Zucker rat; †, lean Zucker significantly different ($P < 0.05$) from colony rat.

### 8.3.2 Haemodynamic effects

There was no significant difference in the basal mean arterial pressure or heart rate between colony, lean or obese rats (Table 8.1), nor did any difference develop as a result of a 2 hour insulin or saline infusion (data not shown). Similarly, basal femoral arterial blood flow also did not differ between the three groups (Table 8.1). However, whereas there was very little increase in femoral arterial blood flow with saline infusion, insulin significantly increased flow in the colony rats and lean Zuckers but not in the obese Zucker rats (Table 8.2). Accordingly, vascular resistance was decreased by insulin only in the colony rats and lean Zuckers (Table 8.2).

### 8.3.3 1-MX metabolism

The arterial plasma concentrations of oxypurinol were similar at approx. 6 μM in all three groups, colony, lean Zucker and obese Zucker (data not shown). Arterial 1-MX levels were slightly higher in both the lean and obese Zucker rat (approx. 30 μM) compared to the colony animals of approx. 23 μM (data not shown). Even so, it was clear that insulin increased 1-MX metabolism in both the colony and lean Zuckers but was without effect in the obese animals (Table 8.2).

### 8.3.4 Glucose metabolism

Basal blood glucose was significantly higher in the obese (11.7 ± 0.6 mM) than lean (4.8 ± 0.2 mM) or the colony rats (4.4 ± 0.1, Table 8.1). Glucose infusion rates were set to maintain these levels throughout the insulin clamp. As shown in Table 8.2, and because of the marked insulin resistance of the obese animals, glucose infusions were much less. Plateau values for glucose infusion of colony, lean and obese animals were 25.5 ± 1.2, 22.2 ± 1.1, and 7.7 ± 1.4 $mg.min^{-1}.kg^{-1}$, respectively. Glucose extraction across the hindleg was increased significantly by insulin in the colony and lean rats, but the small

increase induced by insulin in the obese rats was not significant (data not shown). Hindlimb glucose uptake, which is the product of glucose extraction and femoral blood flow, showed a similar trend (Table 8.2) with only the colony and lean Zuckers showing a stimulation due to insulin. Insulin resistance was also apparent in the obese rats when assessed by 2-deoxyglucose uptake into the combined muscles of the lower leg (Table 8.2). Thus, for insulin-mediated 2-deoxyglucose uptake in muscles of colony, lean and obese animals were $16.3 \pm 1.5$, $25.9 \pm 2.4$ and $12.6 \pm 2.6$ $\mu g.min^{-1}.g^{-1}$, respectively. Combined R'g for the lean Zucker was significantly higher than for the colony rat, even though all other related measures of glucose metabolism were similar (Table 8.2)

## 8.4 Discussion

In the present study capillary recruitment has been measured by determining arterio-venous extraction of 1-MX across the leg and femoral arterial blood flow. A number of findings emerged in addition to the clearly impaired response to insulin by the obese animals. First, it was evident that the stimulation of capillary recruitment in lean Zuckers was muted particularly when compared to the insulin-responsive colony rats (200) and may reflect partial insulin resistance of the genotype mix of the lean Zuckers which are either heterozygous (Fa/*fa*) or homozygous (Fa/Fa). A heterozygote effect is apparent for body weight, total body fat and insulin secretion (19). Second, in saline infused rats the hindlimb 1-MX disappearance was lower in obese rats compared with the lean. This may result from reduced muscle mass, lower capillary density (98), or decreased perfusion of existing capillaries in the basal state. The xanthine oxidase activity in muscle homogenates from obese Zucker rats tended to be reduced. This may be a reflection of a lower capillary density in the obese rats (98), although there is not consensus on this issue (176).

The fact that the basal hindleg glucose uptake and 2-deoxyglucose uptake were not elevated in the lean Zuckers in accordance with the higher 1-MX metabolism is not unexpected, since it is probably necessary to have insulin present to observe marked alterations in glucose uptake. Furthermore, it is likely that in the obese rats, the basal

glucose uptake is partly increased by mass action since the glucose levels were significantly higher than the lean group. This would offset any differences in glucose uptake due to the extent of perfusion, and result in similar levels in both groups.

The present study shows for the first time major impairments of insulin's haemodynamic effects in Zucker obese rats *in vivo*. The impairments manifested as markedly decreased responses to insulin in terms of hindlimb femoral arterial blood flow and capillary recruitment in obese animals when compared to age-matched leans. These findings add an important *in vivo* perspective to data already reported by others of impaired vascular responses to insulin in Zucker obese rat tissues *in vitro*. For example, Zemel *et al.*, (201) noted that isolated thoracic aortae from obese rats were more sensitive to phenylephrine-induced constriction, and moreover, the ability of insulin to attenuate this response was reduced. Similarly, Walker *et al.*, (187) found that norepinephrine induced vasoconstriction was attenuated by insulin in mesenteric arteries from lean rats, but not obese. In addition, endothelial function was abnormal in obese rats and the acetylcholine-induced dilation was reduced (187).

The impaired capillary recruitment in the obese Zuckers may contribute to the insulin resistance seen in these rats. Consistent with reports by others (131;175), the glucose infusion rate was reduced by 65% with no significant effect of insulin to increase either hindlimb or 2-deoxyglucose uptake in the obese rats, even at supra-physiological insulin levels. In addition, at more physiological levels (e.g. $3mU.min^{-1}.kg^{-1}$) there was no response to insulin with respect to either glucose uptake or haemodynamic measurements (data not shown).

The present findings also add to this laboratory's previous report where resting muscle oxygen uptake was impaired in the obese Zucker hindimb muscle (56) leading to the likelihood that impaired access for insulin and glucose extends to oxygen. Thus vascular changes involving regulation of flow distribution and/or dominance of non-nutritive flow may be contributory to both the obese phenotype and the insulin resistance. However, the mechanism responsible for the impaired response to insulin may relate more to impaired

insulin signaling in the vasculature than to dominance of non-nutritive flow. This view is supported by data from preliminary studies which show that contraction-mediated capillary recruitment (1-MX metabolism) is increased by 85% attaining similar levels to contraction in lean rats (192). Since insulin's activation of the PI 3-kinase, but not the MAP-kinase pathway is diminished in vascular tissues from obese Zuckers (85) and since NO has been implicated in insulin mediated increases in both total flow (152) (165) and capillary recruitment (179), defects in either NO production or the VSMC responsiveness to NO may underlie the diminished vascular insulin response *in vivo*, that is reported herein.

Failure to find a significant increase in hindleg or 2-deoxyglucose uptake in the obese rats in response to insulin, indicates that the insulin resistance is not solely due to the decreased muscle mass. Moreover, insulin resistance is apparent when muscles from obese rats are incubated, suggesting that there is an intrinsic defect in the tissue itself (44). Impairment of insulin's haemodynamic actions *in vivo* could contribute to the insulin resistance by reducing access for hormone and nutrient but would not be the sole cause of the insulin resistance in these animals.

The novel finding of impaired insulin-mediated haemodynamic effects in the obese Zucker would imply decreased access of insulin and glucose and therefore a diminished supply from plasma to interstitium. While this may not necessarily create a gradient at steady state, the time-dependent of delivery of glucose and/or insulin to the interstitium may be affected. It is of interest that Holmang *et al.*, (72) using microdialysis measurements in skeletal muscle found that the steady state interstitial and plasma insulin concentrations were similar in both lean and obese Zucker rats. They concluded that the insulin resistance of obese Zuckers is a result of a cellular defect, rather than a haemodynamic one. At this stage it is not known what effect changes in capillary recruitment as mediated by insulin have on steady state interstitial insulin levels, but it is highly likely that the time-dependent approach will be increased.

TNFα expression is elevated in adipose tissue of obese individuals and has been implicated as a cause of the associated insulin resistance (73). In support of this, treatment of obese Zucker rats with a soluble TNFα receptor-immunoglobulin G chimeric protein improved glucose infusion rate during hyperinsulinemic euglycemic clamp (74). Similarly, Cheung *et al.*, (27) showed that inhibition of TNFα activity through the adenovirus-5 mediated transfer of a TNF inhibitor gene, improved peripheral and hepatic insulin sensitivity in obese Zucker rats. Raised plasma levels of TNFα have been reported in obese Zuckers (89) and the blunted haemodynamic effects observed in these rats may be a consequence of this (200). However, elevated plasma free fatty acids may be more important (110) and responsible for the insulin resistance of the Zucker. Previous data from our laboratory supports this view and shows that acutely elevated free fatty acids in a non-obese strain markedly impair insulin-mediated capillary recruitment and muscle glucose uptake *in vivo* (38).

It is interesting that the colony and lean Zucker rats show very little difference. In fact the major difference was clearly in the handling of insulin. Thus an infusion of 30 mU/kg/min insulin was required to reach similar plasma insulin levels to lean Zucker animals which were receiving 20 mU/kg/min. All responses to insulin were remarkably similar in the colony and lean animals with the exception of a lower insulin-mediated R'g for the combined muscle of the lower leg.

To summarize, the 1-MX metabolism method was successfully used to show insulin-mediated capillary recruitment in insulin-responsive colony rats consistent with findings reported in earlier chapters using either LDF or CEU. In addition the method allowed the detection of a marked insulin ressitance in terms of capillary recruitment in the muscle of obese Zucker rats. The impairment in insulin-mediated capillary recruitment in the obese Zucker rats may contribute to the insulin resistance of muscle in these animals.

# CHAPTER 9

## General Discussion

### 9.1 Summary of thesis

The focus of this thesis has been the new technologies that have been developed to measure changes in microvascular perfusion in muscle. In particular the emphasis has been on the application of laser Doppler flowmetry for this purpose and comparisons have been made against the more-established methods of contrast enhanced ultrasound / microbubbles and the metabolism of 1-methyl xanthine. A principal goal in using the technique of laser Doppler flowmetry was to better understand the microvascular effects of insulin in muscle. But to do this, changes in microvascular perfusion needed to be measured in pump-perfused rat hindlimb muscle when shifts in the nutritive to non-nutritive flow ratio were altered by vasoconstrictors and total flow was maintained constant. Comparisons were then made *in vivo* with insulin action in normally responsive rats, in genetically obese insulin resistant Zucker rats, and in the muscle of healthy human subjects undergoing a hyperinsulinaemic euglycaemic clamp. Several important observations were made, particularly concerning LDF as a potential method for assessing changes in muscle microvascular perfusion.

### 9.2 Heterogeneity of nutritive and non-nutritive sites within muscle

First, the size of the LDF probe (in terms of fibre separation) was critical when this technique was used to assess microvascular perfusion. Thus in the first study of this thesis microprobes that could be impaled into the muscle tissue revealed a heterogeneity of sites when randomly placed. The sites differed dramatically in the signal generated when flow was altered by vasoconstrictor injection into the constant flow perfused rat hindlimb. Bolus injection of type A vasoconstrictor that is known to increase nutritive flow at the expense of non-nutritive flow revealed sites of three different character. The majority (approx. 60%) showed an increase in LDF signal coincident with the increases in oxygen uptake and pressure. In these experiments oxygen uptake was used as a surrogate

indicator of nutritive flow. Similarly, with the probe still positioned in this same site, a bolus injection of a type B vasoconstrictor produced a decrease in LDF signal, again in close temporal association with the expected decrease in oxygen uptake. The remaining sites were of quite different character, with approx. 20% responding such that the LDF signal moved in the opposite direction to that of the oxygen uptake; i.e. decreasing with type A vasoconstrictor and increasing with type B vasoconstrictor. Another 10% differed yet again and were probably a mixture of the two previously described sites where the LDF signal did not respond to either type of vascoconstrictor even though the pressure increased, possibly reflecting an increase in LDF signal superimposed upon a decrease. A considerably larger LDF probe that was approx. 4-fold the diameter of the impalable micro-probe detected only the majority response. Thus injection of a type A vasoconstrictor that increased oxygen uptake increased the signal and a type B vasoconstrictor that decreased the oxygen uptake, decreased the LDF signal. However, it is important to recall that a limitation of the larger probe is that it was only able to measure superficial regions and these may differ to some extent from those registered by the impaled probe.

Taken together these findings suggested that a heterogeneity of sites existed in muscle where the predominant type responded in concert with the change in nutritive flow. This might mean that these could be termed as nutritive and the smaller proportion sites as non-nutritive.

## 9.3 Capillary tortuosity

It is important to remember that these studies with randomly placed micro-probes and macro-probes were all conducted using the perfusesd rat hindlimb at constant total flow. A key question then arose as to the nature of the change in tissue perfusion that might explain the change in LDF signal when the vasoconstrictors were injected. A study using fabricated capillary systems led to the second main observation. Of the different models tested, and these included switching flow from capillaries of different diameter, sharing of flow by recruitment of previously unperfused capillaries, and redistributing flow from

short to long tortuous capillaries, only the latter could explain the hindlimb perfusion data. Thus for a nutritive site, the LDF probe which is randomly positioned, happens to be where there are a majority of long tortuous capillaries. A type A vasoconstrictor constricts access to the shorter non-nutritive capillaries which are largely outside the LDF field under measurement, and flow is redistributed into the longer more tortuous capillaries that cross the field of measurement several times. These longer more tortuous vessels would fulfill a role as nutritive by having a considerably greater available surface area for nutrient exchange. Similarly at this nutritive site a type B vasoconstrictor constricts access to the long tortuous capillaries and redirects flow to the shorter non-nutritive capillaries in the field of measurement and the LDF signal decreases. At the so-called non-nutritive or "NE negative" site, there must be a predominance of the shorter non-nutritive capillaries and so the signal decreases and increases, respectively when type A and B vasocontrictors are injected into the whole hindlimb upstream of the area under measurement. If the type A vasoconstrictor was acting simply to change the diameter of the vessels in the region of measurement, the signal would always increase. Clearly this scenario is inconsistent with the outcome from the type B vasoconstrictor, which led to a decrease in the LDF signal. Similarly, if flow were moving from one vessel of a manifold that fed several vessels of comparable diameter, the mean cell velocity would decrease and since LDF is very sensitive to velocity, the LDF signal would also decrease. Each of these suppositions was confirmed with the fabricated synthetic capillaries.

A concept involving regions of concentrated tortuous nutritive capillary networks separated from regions where these are relatively few fits reasonably well within the prespective of what is known of the muscle microvasculature Anatomical models of the muscle microvasculature depicted by Lindbom and Arfors and their colleagues (22) as well as those of Myrhage and Eriksson (114) show close co-existence of nutritive capillaries supplying the muscle cells with non-nutritive capillaries supplying neighboring connective tissue. For example, detailed drawings of the microvasculature of the rabbit tenuissimus muscle (22) show feed arteries that branch to supply transverse arterioles which in turn cross the muscle body (which in this muscle is flat) to firstly supply terminal arterioles and capillaries of the muscle then to end in vessels supplying

the connective tissue and attendant adipocytes (39). These latter capillaries are potentially nutritive for the fat cells and the connective tissue but can only be considered "non-nutritive" for the more metabolically active muscle cells. A number of studies using intravital microscopy has shown that relative flow in the two networks can be influenced by various physiologically relevant agents and conditions (22;103-105) that redistribute flow consistent within the two regions representing the nutritive and non-nutritive routes of muscle (35). Inspection of the illustration of the tenuissimus muscle [(22); Figure 9.1] suggest the region containing nutritive capillaries to be approximately 3000 μm wide and somewhat less for the non-nutritive (104).

If the difference between nutritive and non-nutritive capillaries was purely a result of the functional capacity of nutrient exchange to occur across the capillary wall (i.e. not a result of capillary architecture) then we would expect the LDF signal (especially from the larger probe) to be relatively unchanged as flow is switched from one route to another.

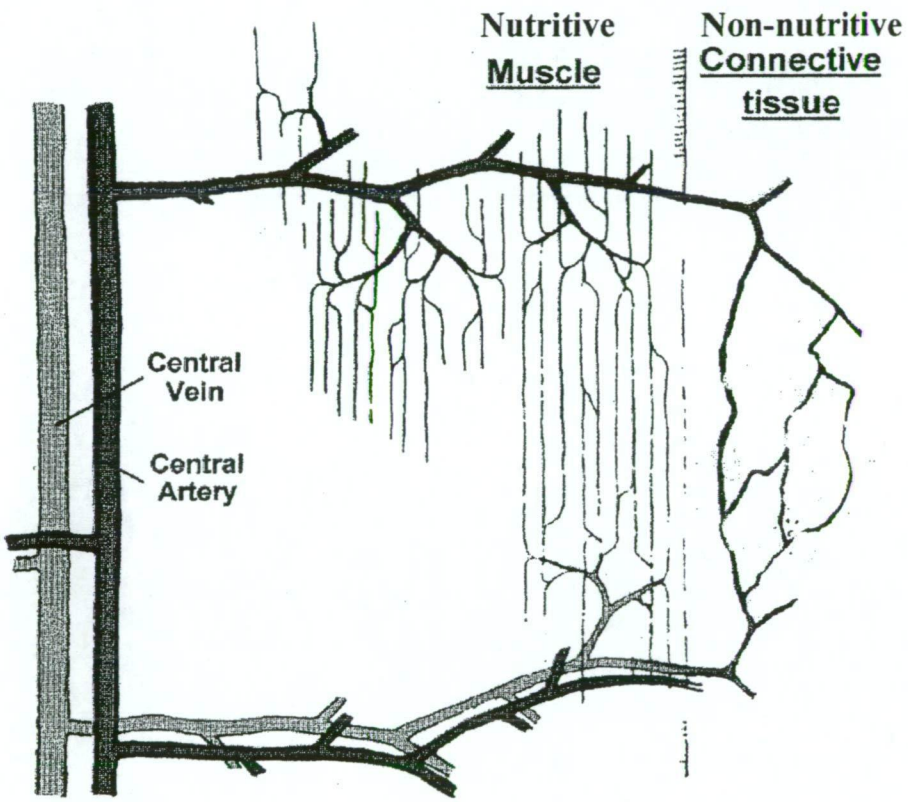


**Figure 9.1 Blood flow in the tenuissimus muscle of the rabbit.** This is drawn from intravital microscopy of this muscle during experiments where the distribution of flow in each route was altered by the application of various vasoactive substances to the superfusate (adapted from (22)).

Conceiveably the LDF micro-probe of 200 μm dia., as used in the present thesis might detect signal from one or other route, or even a mixture of the two depending on positioning. For muscles other than the tenuissimus that are cylindrical, the same vascular unit is observed (114), but now the transverse arteriole radiates out from the center of the muscle fibril and the connective tissue vessels are contained in the perimysium. Macro-probes are probably too large to detect a heterogeneity of structure and thus reflect changes in the predominant population of nutritive sites, even though the input from some non-nutritive sites within the field cannot be avoided, which would, depending on the extent of overlap, attenuate (since it is opposite) the signal from the nutritive site.

## 9.4 Insulin improves microvascular perfusion

The polymer tube model studies of this thesis thus provide a putative microvascular structure which allow at least some interpretation of the LDF signal. Thus in later chapters it was possible to assess the effect of insulin *in vivo* and to compare it with the effects of epinephrine, already known to increase limb blood flow without change in microvascular perfusion (138). It was also possible to conduct essentially identical experiments using the two other technologies of 1-MX metabolism and CEU/microbubbles and make comparisons. Application of LDF to *in vivo* studies led to the third major discovery that insulin under clamp conditions was able to increase LDF signal, detected either by surface scanning of the leg or by a stationay macroprobe positioned over the biceps femoris muscle. At the dose of insulin used (10mU/min/kg), the increase in LDF signal preceded the increase in limb blood flow by at least 10 min. In contrast, epinephrine which markedly increased limb blood flow had no effect on LDF signal. A flow-independent increase in LDF signal may thus be interpreted as reflecting an insulin-mediated increase or recruitment of nutritive flow into the long tortuous capillaries and a decrease in flow in the shorter non-nutritive capillaries. Epinephrine, although markedly increasing total blood flow did not increase capillary recruitment, the inference being that the increase in flow has been accommodated by the non-nutritive route.

## 9.5 The vasomotion response

The fourth major finding from this thesis was that physiological hyperinsulinaemia increased intramuscular microvascular reactive hyperaemia and vasomotion in healthy volunteers. To my knowledge this represented the first application of LDF technology to measuring muscle microvascular blood flow in humans *in vivo* during insulin clamp conditions. Whereas, the signal before and after insulin did not differ significantly (cf rats, (138)), there was a trend for an insulin-mediated increase. Perhaps more importantly, insulin significantly modified two aspects of vascular function. First, insulin increased the hyperaemic response to 3 min of ischaemia, and second, insulin increased the amplitude of vasomotion at low frequencies (Chapter 6). The finding that the hyperaemic response to ischaemia is increased following insulin treatment is similar to that already reported for skin (157) and suggests that insulin has acted to produce signal substances that enhance the relaxation of the terminal arterioles controlling entry to the nutritive capillary network in muscle. Vasodilation during reactive hyperaemia is thought to be determined at the level of the small arterioles. Thus the stimulatory effect of hyperinsulinaemia might be due to a decreased sensitivity to vasoconstrictor stimuli or an increased sensitivity to vasodilatory stimuli at the level of the small arterioles. At a molecular level, the mechanisms responsible for the increase in vascular perfusion after arterial occlusion are not fully understood. Previous studies have suggested that the hyperaemic response could be due to accumulation of metabolic vasodilators, such as nitric oxide, adenosine and prostaglandins, or to a myogenic or a neurogenic response (193). It seems unlikely that hyperinsulinaemia decreases sensitivity to vasoconstrictive effects, because, both in the isolated rat arteriole and in the human forearm, hyperinsulinaemia has been shown to increase vasoconstrictive effects by inducing endothelin-1 activity (25;58). In humans, insulin has been shown to stimulate vasodilatory effects by inducing endothelial nitric oxide (NO) production (166). A role for NO in the maximal hyperaemic response after arterial occlusion in muscle is supported by most (47;57;112), but not all studies (172) using venous occlusion plethysmography. The timing of the measurement may be

important for the determination of the relative contribution of NO, prostaglandin and other vasodilators in the post-ischemic hyperemia response. My view is that the findings are consistent with an insulin-mediated production of NO as has been proposed recently in rats where the insulin-mediated capillary recruitment in muscle *in vivo* was found to be blocked by a nitric oxide synthase inhibitor (179). Therefore, enhanced endothelial NO production might contribute to insulin-mediated changes in intramuscular reactive hyperaemia. Whether the production of NO by insulin can also account for the increase in low frequency vasomotion is not known and will be an important question to address in the future. In addition, the role of NO and other possible mechanisms in reactive hyperaemia in muscle vasculature, and insulin-mediated effects thereon, remain to be further investigated.

The LDF probe used in the human muscle studies (Chapter 6) was intermediate in size between the micro- and macro-probes used in Chapter 3. Of consequence, this probe (model 402; Perimed, Stockholm, Sweden, fibre separation = 0.15mm of overall diameter that fitted comfortably inside a 0.9 mm catheter) largely avoided the problem of the heterogeneity of sites with the very fine micro-probe. Again this would be interpreted as having predominantly measured changes in perfusion of the nutritive capillary network. A major aspect of the work embodied by this thesis was to assess the applicability of LDF for measuring changes in microvascular perfusion, specifically muscle nutritive flow. The data from the perfused rat hindlimb where total flow was maintained constant, showed a tight correlation between nutritive flow (deduced from oxygen uptake, a surrogate indicator) and LDF signal (Figure 3.3). However, *in vivo* during the hyperinsulinaemic euglycaemic clamp, flow was free to change and thus a conclusion that the LDF signal was increased as a consequence of capillary recruitment and independent of flow relied on the fact that the increase in bulk blood flow was slower to occur (e.g. see Figure 5.5). To resolve this there was considerable value in comparing all three methods. Table 9.1 shows that changes in LDF signal in response to insulin or epinephrine were comparable to those determined using either 1-MX metabolism or CEU/microbubbles. However, of the three methods only LDF is sensitive to changes in flow. Considering firstly the 1-MX method, when bulk flow increases the extraction

fraction across the vascular bed in question decreases proportionately. For the CEU technique, the measurement of microvascular volume (Chapter 7) is completely independent of mean cell velocity, and therefore bulk flow, providing bulk flow per se is unable to influence capillary recruitment. In contrast to each of the 1-MX and CEU methods, the LDF is quite sensitive to flow. This can be seen in the data of Chapter 3 when plotted as a 3-dimensional graph (Figure 9.2). Although LDF signal was increased

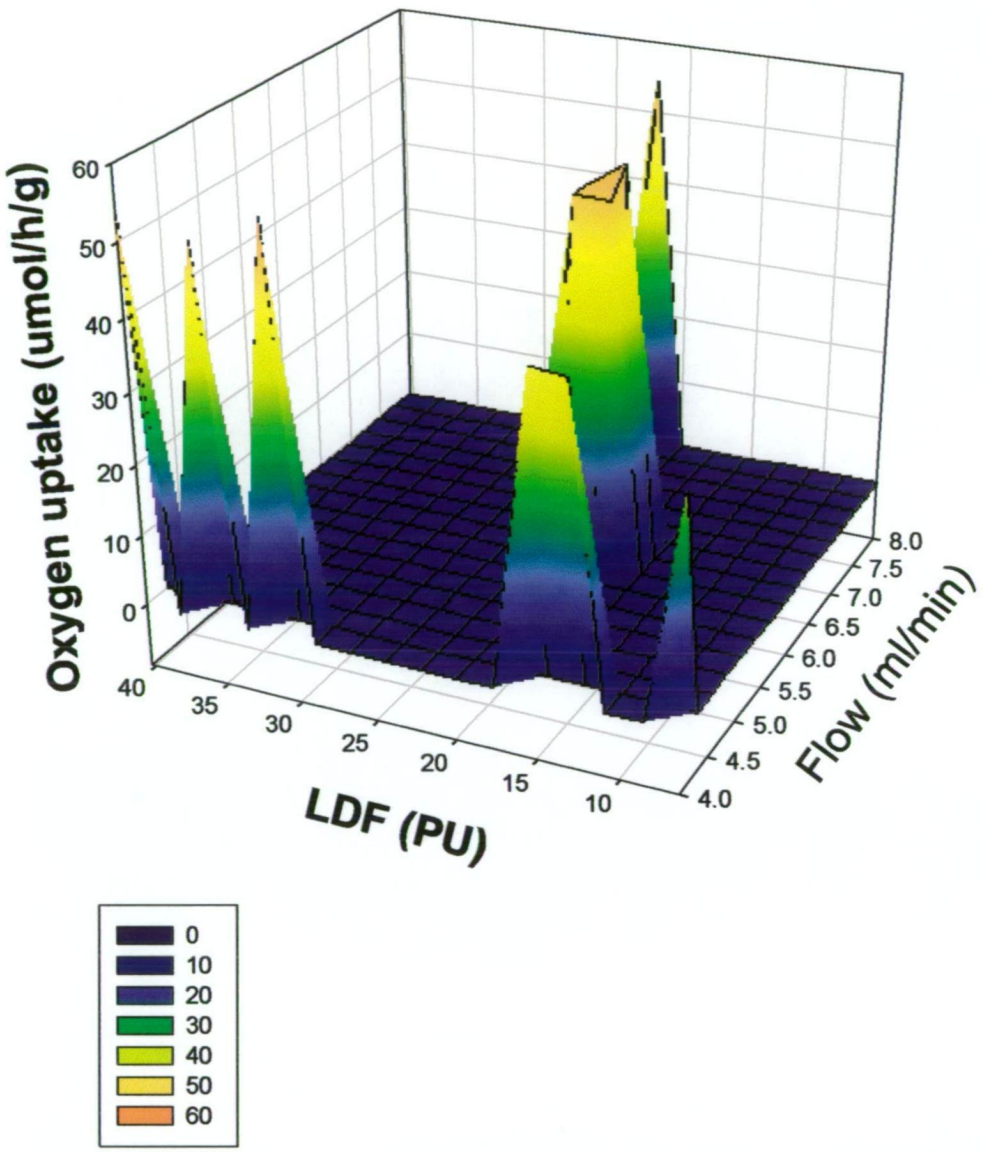


**Figure 9.2 3-D Plot of LDF and oxygen uptake as a function of pump-delivered flow.** Experiments were conducted using the isolated perfused rat hindlimb. When flow was held constant at 4ml/min LDF and oxygen uptake were each increased by norepinephrine, angiotensin II, or vasopressin (peaks to the left). When serotonin was added and again the flow kept constant at 4ml/min, LDF and oxygen uptake each decreased (singlepeak to the right). If no vasoconstrictors were added but flow was increased from 4 through 6 to 8ml/min the LDF signal and oxygen uptake also increased (peaks moving up the plane).

by type A vasoconstrictors that increased nutritive flow (oxygen uptake), an increase in bulk flow can independently increase both LDF and oxygen uptake. This places a considerable caveat on the general applicability of LDF as a technique for assessing changes in muscle nutritive flow, when bulk flow cannot be controlled.

## 9.6 Implications

From the experience gained in using all three techniques of 1-MX metabolism, LDF and CEU/microbubbles, I sought to explore whether a well-established model of insulin resistance, the genetically obese Zucker rat had impaired capillary recruitment in response to insulin. 1-MX metabolism was the method used to measure changes in capillary recruitment. The findings showed there was indeed a marked impairment when compared to the insulin responsive lean Zucker controls. This now adds to a number of other insulin resistant models which we have tested and all of which showed markedly impaired insulin-mediated capillary recruitment in association with impaired insulin-mediated muscle glucose uptake. These include insulin resistance from acutely administered TNFα (200), acutely administered Intralipid with heparin (38) and the acutely administered serotonergic agonist, α-methyl serotonin (139). With regard to the obese Zucker rat it is interesting to note that our group has recently noted that capillary recruitment due to muscle contraction is relatively normal as is contraction-mediated muscle glucose uptake (189). This implies that the failure of insulin to recruit capillary flow is most likely a problem of impaired insulin signalling between the receptor and NO production. Clearly this warrants close examination in the future.

## 9.7 Conclusion

In summary, the technique of LDF proved to be useful in further understanding the complexities of microvascular blood flow in muscle and its relationship to metabolism. Providing total flow to the muscle remained constant, changes in nutritive flow as manipulated by vasoconstrictors could be readily detected and there was a positive correlation between LDF signal and oxygen uptake. However, the fact that flow could

independently influence the LDF signal severly lessens the applicability to assessing capillary recruitment when total flow is also changing. A particular advantage of LDF was that it could be used to continuously record changes, where 1-MX metabolism technique is an end point approach and CEU can only be applied intermittently. In addition, LDF has provided for the first time evidence that insulin acts to enhance low frequency vasomotion in human muscle *in vivo*. Measurement of LDF signal from models of the microvascular networks has led to some testable concepts for the future.

## REFERENCE LIST


1. Abramson, D. I., N. Schkloven, M. N. Margolis, and I. A. Mirsky. Influence of massive doses of insulin on peripheral blood flow in man. *Am.J.Physiol* 128: 124-132, 1939.

2. Akbari, C. M., R. Saouaf, D. F. Barnhill, P. A. Newman, F. W. LoGerfo, and A. Veves. Endothelium-dependent vasodilatation is impaired in both microcirculation and macrocirculation during acute hyperglycemia. *J.Vasc.Surg.* 28: 687-694, 1998.

3. Allwood, M. J., H. Hensel, and J. Papenberg. Muscle and skin blood flow in the human forearm during insulin hypoglycaemia. *J.Physiol (Lond)* 147: 269-273, 1959.

4. Anai, M., M. Funaki, T. Ogihara, J. Terasaki, K. Inukai, H. Katagiri, Y. Fukushima, Y. Yazaki, M. Kikuchi, Y. Oka, and T. Asano. Altered expression levels and impaired steps in the pathway to phosphatidylinositol 3-kinase activation via insulin receptor substrates 1 and 2 in Zucker fatty rats. *Diabetes* 47: 13-23, 1998.

5. Anderson, E. A., R. P. Hoffman, T. W. Balon, C. A. Sinkey, and A. L. Mark. Hyperinsulinemia produces both sympathetic neural activation and vasodilation in normal humans. *J.Clin.Invest.* 87: 2246-2252, 1991.

6. Andrews, J., I. Klimes, B. Vasquez, M. Nagulesparan, and G. M. Reaven. Can mixed venous blood be used to measure insulin action during the hyperinsulinemic clamp? *Horm.Metab Res.* 16 Suppl 1:164-6.: 164-166, 1984.

7. Antonios, T. F., F. E. Rattray, D. R. Singer, N. D. Markandu, P. S. Mortimer, and G. A. MacGregor. Maximization of skin capillaries during intravital video-microscopy in essential hypertension: comparison between venous congestion, reactive hyperaemia and core heat load tests. *Clin.Sci.(Lond)* 97: 523-528, 1999.

8. Barlow, T. E., A. L. Haigh, and D. N. Walder. A search for arteriovenous anastomoses in skeletal muscle. *Proc.Physiol.Soc.* 80P-81P, 1958.

9. Barlow, T. E., A. L. Haigh, and D. N. Walder. Evidence for two vascular pathways in skeletal muscle. *Clin.Sci.* 20: 367-385, 1961.

10. Baron, A. D. Hemodynamic actions of insulin. *Am.J.Physiol.* 267: E187-E202, 1994.

11. Baron, A. D., G. Brechtel-Hook, A. Johnson, and D. Hardin. Skeletal muscle blood flow. A possible link between insulin resistance and blood pressure. *Hypertension* 21: 129-135, 1993.

12. Baron, A. D. and M. G. Clark. Role of blood flow in the regulation of muscle glucose uptake. *Annu.Rev.Nutr.* 17: 487-499, 1997.

13. Baron, A. D., M. Laakso, G. Brechtel, and S. V. Edelman. Mechanism of insulin resistance in insulin-dependent diabetes mellitus: a major role for reduced skeletal muscle blood flow. *J.Clin.Endocrinol.Metab.* 73: 637-643, 1991.

14. Baron, A. D., M. Laakso, G. Brechtel, B. Hoit, C. Watt, and S. V. Edelman. Reduced postprandial skeletal muscle blood flow contributes to glucose intolerance in human obesity. *J.Clin.Endocrinol.Metab.* 70: 1525-1533, 1990.

15. Baron, A. D., H. Steinberg, G. Brechtel, and A. Johnson. Skeletal muscle blood flow independently modulates insulin-mediated glucose uptake. *Am.J.Physiol.* 266: E248-E253, 1994.

16. Baron, A. D., M. Tarshoby, G. Hook, E. N. Lazaridis, J. Cronin, A. Johnson, and H. O. Steinberg. Interaction between insulin sensitivity and muscle perfusion on glucose uptake in human skeletal muscle: evidence for capillary recruitment. *Diabetes* 49: 768-774, 2000.

17. Bergman, R. N. New concepts in extracellular signaling for insulin action: the single gateway hypothesis. *Recent Prog.Horm.Res.* 52:359-85; discussion 385-7.: 359-385, 1997.

18. Bernardi, L., M. Rossi, P. Fratino, G. Finardi, E. Mevio, and C. Orlandi. Relationship between phasic changes in human skin blood flow and autonomic tone. *Microvasc.Res.* 37: 16-27, 1989.

19. Blonz, E. R., J. S. Stern, and D. L. Curry. Dynamics of pancreatic insulin release in young Zucker rats: a heterozygote effect. *Am J Physiol* 248: E188-E193, 1985.

20. Bonadonna, R. C., M. P. Saccomani, S. Del Prato, E. Bonora, R. A. Defronzo, and C. Cobelli. Role of tissue-specific blood flow and tissue recruitment in insulin-mediated glucose uptake of human skeletal muscle. *Circulation* 98: 234-241, 1998.

21. Bonen, A., M. G. Clark, and E. J. Henriksen. Experimental approaches in muscle metabolism: hindlimb perfusion and isolated muscle incubations. *Am.J.Physiol.* 266: E1-16, 1994.

22. Borgstrom, P., L. Lindbom, K. E. Arfors, and M. Intaglietta. Beta-adrenergic control of resistance in individual vessels in rabbit tenuissimus muscle. *Am.J.Physiol.* 254: H631-H635, 1988.

23. Caballero, A. E., S. Arora, R. Saouaf, S. C. Lim, P. Smakowski, J. Y. Park, G. L. King, F. W. LoGerfo, E. S. Horton, and A. Veves. Microvascular and macrovascular reactivity is reduced in subjects at risk for type 2 diabetes. *Diabetes* 48: 1856-1862, 1999.

24. Capaldo, B., G. Lembo, R. Napoli, V. Rendina, G. Albano, L. Sacca, and B. Trimarco. Skeletal muscle is a primary site of insulin resistance in essential hypertension. *Metabolism* 40: 1320-1322, 1991.

25. Cardillo, C., S. S. Nambi, C. M. Kilcoyne, W. K. Choucair, A. Katz, M. J. Quon, and J. A. Panza. Insulin stimulates both endothelin and nitric oxide activity in the human forearm. *Circulation* 100: 820-825, 1999.

26. Chaplin, D. J. and S. A. Hill. Temporal heterogeneity in microregional erythrocyte flux in experimental solid tumours. *Br.J.Cancer* 71: 1210-1213, 1995.

27. Cheung, A. T., D. Ree, J. K. Kolls, J. Fuselier, D. H. Coy, and M. Bryer-Ash. An in vivo model for elucidation of the mechanism of tumor necrosis factor-alpha (TNF-alpha)-induced insulin resistance: evidence for differential regulation of insulin signaling by TNF-alpha. *Endocrinology* 139: 4928-4935, 1998.

28. Clark, A. D. H., E. J. Barrett, S. Rattigan, M. G. Wallis, and M. G. Clark. Insulin stimulates laser Doppler signal by rat muscle in vivo consistent with nutritive flow recuitment. *Clin.Sci.* 100: 283-290, 2001.

29. Clark, A. D. H., J. M. Youd, S. Rattigan, E. J. Barrett, and M. G. Clark. Heterogeneity of laser Doppler flowmetry signal in perfused rat muscle indicative of nutritive and non-nutritive flow. *Am.J.Physiol* 280: H1324-H1333, 2001.

30. Clark, M. G., A. D. H. Clark, and S. Rattigan. Failure of laser Doppler signal to correlate with total flow in muscle: Is this a question of vessel architecture? *Microvasc.Res.* 60: 294-301, 2000.

31. Clark, M. G., E. Q. Colquhoun, K. A. Dora, S. Rattigan, T. P. D. Eldershaw, J. L. Hall, A. Matthias, and J. M. Ye. Resting muscle: A source of thermogenesis controlled by vasomodulators. In Milton, A. S., ed. Temperature Regulation: Recent physiological and pharmacological advances. Basel, Birkhauser Verlag. 1994, 355-320.

32. Clark, M. G., E. Q. Colquhoun, S. Rattigan, K. A. Dora, T. P. Eldershaw, J. L. Hall, and J. Ye. Vascular and endocrine control of muscle metabolism. *Am.J.Physiol.* 268: E797-E812, 1995.

33. Clark, M. G., S. Rattigan, L. H. Clerk, M. A. Vincent, A. D. Clark, J. M. Youd, and J. M. Newman. Nutritive and non-nutritive blood flow: rest and exercise. *Acta Physiol.Scand.* 168: 519-530, 2000.

34. Clark, M. G., S. Rattigan, K. A. Dora, J. M. B. Newman, J. T. Steen, K. A. Miller, and M. A. Vincent. Vascular and metabolic regulation of muscle. In Kinney, J. M. and H. N. Tucker, eds. Physiology, Stress, and Malnutrition: Functional Correlates, Nutritional Intervention. New York, Lippincott-Raven. 1997, 325-346.

35. Clark, M. G., S. Rattigan, J. M. Newman, and T. P. Eldershaw. Vascular control of nutrient delivery by flow redistribution within muscle: implications for exercise and post-exercise muscle metabolism. *Int.J.Sports Med.* 19: 391-400, 1998.

36. Clark, M. G., M. G. Wallis, E. J. Barrett, M. A. Vincent, S. M. Richards, L. H. Clerk, and S. Rattigan. Blood flow and muscle metabolism: a focus on insulin action. *Am.J.Physiol* 284: E241-E258, 2003.

37. Cleland, S. J., J. R. Petrie, S. Ueda, H. L. Elliott, and J. M. Connell. Insulin-mediated vasodilation and glucose uptake are functionally linked in humans. *Hypertension* 33: 554-558, 1999.

38. Clerk, L. H., S. Rattigan, and M. G. Clark. Lipid infusion impairs physiologic insulin-mediated capillary recruitment and muscle glucose uptake in vivo. *Diabetes* 51: 1138-1145, 2002.

39. Clerk, L. H., M. E. Smith, S. Rattigan, and M. G. Clark. Increased chylomicron triglyceride hydrolysis by connective tissue flow in perfused rat hindlimb. Implications for lipid storage. *J.Lipid Res.* 41: 329-335, 2000.

40. Coggins, M., J. Lindner, S. Rattigan, L. Jahn, E. Fasy, S. Kaul, and E. Barrett. Physiologic hyperinsulinemia enhances human skeletal muscle perfusion by capillary recruitment. *Diabetes* 50: 2682-2690, 2001.

41. Colquhoun, E. Q., M. Hettiarachchi, J. M. Ye, S. Rattigan, and M. G. Clark. Inhibition by vasodilators of noradrenaline and vasoconstrictor-mediated, but not skeletal muscle contraction-induced oxygen uptake in the perfused rat hindlimb; implications for non-shivering thermogenesis in muscle tissue. *Gen.Pharmacol.* 21: 141-148, 1990.

42. Colquhoun, E. Q., M. Hettiarachchi, J. M. Ye, E. A. Richter, A. J. Hniat, S. Rattigan, and M. G. Clark. Vasopressin and angiotensin II stimulate oxygen uptake in the perfused rat hindlimb. *Life Sci.* 43: 1747-1754, 1988.

43. Creager, M. A., C. S. Liang, and J. D. Coffman. Beta adrenergic-mediated vasodilator response to insulin in the human forearm. *J.Pharmacol.Exp.Ther.* 235: 709-714, 1985.

44. Crettaz, M., M. Prentki, D. Zaninetti, and B. Jeanrenaud. Insulin resistance in soleus muscle from obese Zucker rats. *Biochem.J.* 186: 525-534, 1980.

45. Crist, G. H., B. Xu, K. F. LaNoue, and C. H. Lang. Tissue-specific effects of in vivo adenosine receptor blockade on glucose uptake in Zucker rats. *FASEB J* 12: 1301-1308, 1998.

46. Cummins, H. Z., N. Knable, and Y. Yeh. Observation of diffusion braodening of Rayleigh scattered light. *Phys.Rev.Lett.* 12: 150-153, 1964.

47. Dakak, N., S. Husain, D. Mulcahy, N. P. Andrews, J. A. Panza, M. Waclawiw, W. Schenke, and A. A. Quyyumi. Contribution of nitric oxide to reactive hyperemia: impact of endothelial dysfunction. *Hypertension* 32: 9-15, 1998.

48. Davis, M. J. and P. J. Sikes. Myogenic responses of isolated arterioles: test for a rate-sensitive mechanism. *Am.J.Physiol.* 259: H1890-H1900, 1990.

49. Dawson, D., M. A. Vincent, E. J. Barrett, S. Kaul, A. Clark, H. Leong-Poi, and J. R. Lindner. Vascular recruitment in skeletal muscle during exercise and hyperinsulinemia assessed by contrast ultrasound. *Am.J.Physiol Endocrinol.Metab* 282: E714-E720, 2002.

50. Defronzo, R. A., E. Ferrannini, R. Hendler, P. Felig, and J. Wahren. Regulation of splanchnic and peripheral glucose uptake by insulin and hyperglycemia in man. *Diabetes* 32: 35-45, 1983.

51. Defronzo, R. A., E. Jacot, E. Jequier, E. Maeder, J. Wahren, and J. P. Felber. The effect of insulin on the disposal of intravenous glucose. Results from indirect calorimetry and hepatic and femoral venous catheterization. *Diabetes* 30: 1000-1007, 1981.

52. Dela, F., J. J. Larssen, K. J. Mikines, and H. Galbo. Normal effect of insulin to stimulate leg blood flow in NIDDM. *Diabetes* 44: 221-226, 1995.

53. Dora, K. A., S. Rattigan, E. Q. Colquhoun, and M. G. Clark. Aerobic muscle contraction impaired by serotonin-mediated vasoconstriction. *J.Appl.Physiol.* 77: 277-284, 1994.

54. Dora, K. A., S. M. Richards, S. Rattigan, E. Q. Colquhoun, and M. G. Clark. Serotonin and norepinephrine vasoconstriction in rat hindlimb have different oxygen requirements. *Am.J.Physiol.* 262: H698-H703, 1992.

55. Dosekun, F. O., J. Grayson, and D. Mendel. The measurement of metabolic and vascular responses in liver and muscle with observations on their responses to insulin and glucose. *J.Physiol (Lond)* 150: 581-606, 1960.

56. Eldershaw, T. P., S. Rattigan, K. A. Dora, E. Q. Colquhoun, M. G. Clark, M. A. Cawthorne, and R. E. Buckingham. Potential defect in the vascular control of nonshivering thermogenesis in the obese Zucker rat hind limb. *Can.J.Physiol.Pharmacol.* 72: 1567-1573, 1994.

57. Engelke, K. A., J. R. Halliwill, D. N. Proctor, N. M. Dietz, and M. J. Joyner. Contribution of nitric oxide and prostaglandins to reactive hyperemia in the human forearm. *J.Appl.Physiol.* 81: 1807-1814, 1996.

58. Eringa, E. C., C. D. Stehouwer, T. Merlijn, N. Westerhof, and P. Sipkema. Physiological concentrations of insulin induce endothelin-mediated vasoconstriction during inhibition of NOS or PI3-kinase in skeletal muscle arterioles. *Cardiovasc.Res.* 56: 464-471, 2002.

59. Ernstene, A. C. and M. D. Altschule. The effect of insulin hypoglycemia on the circulation. *J.Clin.Invest* 10: 521-528, 1931.

60. Ferrannini, E. and A. Mari. How to measure insulin sensitivity. *J.Hypertens.* 16: 895-906, 1998.

61. Ferrannini, E., S. Taddei, D. Santoro, A. Natali, C. Boni, D. Del Chiaro, and G. Buzzigoli. Independent stimulation of glucose metabolism and Na+-K+ exchange by insulin in the human forearm. *Am.J.Physiol* 255: E953-E958, 1988.

62. Fisher, B. M., G. Gillen, H. J. Dargie, G. C. Inglis, and B. M. Frier. The effects of insulin-induced hypoglycemia on cardiovascular function in normal man: studies using radionuclide ventriculography. *Diabetologia* 30: 841-845, 1987.

63. French, E. B. and R. Kilpatrick. The role of adrenaline in hypoglycaemic reactions in man. *Clin.Sci.* 14: 639-651, 1955.

64. Friedman, J. E., W. M. Sherman, M. J. Reed, C. W. Elton, and G. L. Dohm. Exercise training increases glucose transporter protein GLUT-4 in skeletal muscle of obese Zucker (fa/fa) rats. *FEBS Lett.* 268: 13-16, 1990.

65. Gelfand, R. A. and E. J. Barrett. Effects of physiologic hyperinsulinemia on skeletal muscle protein synthesis and breakdown in man. *J.Clin.Invest* 80: 1-6, 1987.

66. Ginsburg, J. and A. Paton. Effects of insulin after adrenalectomy. *Lancet* 271: 491-494, 1956.

67. Grant, R. T. and H. P. Wright. Anatomical basis for non-nutritive circulation in skeletal muscle exemplified by blood vessels of rat biceps femoris tendon. *J.Anat.* 106: 125-133, 1970.

68. Gustafsson, U., L. Torssell, F. Sjoberg, and A. Sollevi. Effect of systemic adenosine infusion on capillary flow and oxygen pressure distributions in skeletal muscle of the rabbit. *Int.J.Microcirc.Clin.Exp.* 13: 1-12, 1993.

69. Hammersen, F. The terminal vascular bed in skeletal muscle with special regard to the problem of shunts. In Crone, C. and N. A. Lassen, eds. Capillary Permeability. The Transfer of Molecules and Ions Between Capillary Blood and Tissue". Munksgaard Copenhagen. 1970, 351-371.

70. Hellsten, Y., U. Frandsen, N. Orthenblad, B. Sjodin, and E. A. Richter. Xanthine oxidase in human skeletal muscle following eccentric exercise: a role in inflammation. *J.Physiol.(Lond.)* 498: 239-248, 1997.

71. Hoffmann, U., I. Uckay, M. Fischer, S. Wen, U. K. Franzeck, and A. Bollinger. Simultaneous assessment of muscle and skin blood fluxes with the laser- Doppler technique. *Int.J.Microcirc.Clin.Exp.* 15: 53-59, 1995.

72. Holmang, A., K. Mimura, P. Bjorntorp, and P. Lonnroth. Interstitial muscle insulin and glucose levels in normal and insulin- resistant Zucker rats. *Diabetes* 46: 1799-1804, 1997.

73. Hotamisligil, G. S., P. Arner, J. F. Caro, R. L. Atkinson, and B. M. Spiegelman. Increased adipose tissue expression of tumor necrosis factor-alpha in human obesity and insulin resistance. *J.Clin.Invest.* 95: 2409-2415, 1995.

74. Hotamisligil, G. S., N. S. Shargill, and B. M. Spiegelman. Adipose expression of tumor necrosis factor-alpha: Direct role in obesity- linked insulin resistance. *Science* 259: 87-91, 1993.

75. Hudlicka, O. Basic mechanisms regulating muscle blood flow. Muscle blood flow: Its relation to muscle metabolism and function. Amersterdam, Swets & Zeitlinger. 1973, 29-54.

76. Hyman, C., S. Rosell, A. Rosén, R. R. Sonnenschein, and B. Uvnås. Effects of alterations of total muscular blood flow on local tissue clearance of radio-iodide in the cat. *Acta Physiol.Scand.* 46: 358-366, 1959.

77. Jaap, A. J., A. C. Shore, and J. E. Tooke. Relationship of insulin resistance to microvascular dysfunction in subjects with fasting hyperglycaemia. *Diabetologia* 40: 238-243, 1997.

78. Jackson, R. A., J. B. Hamling, P. M. Blix, B. M. Sim, M. I. Hawa, J. B. Jaspan, J. Belin, and J. D. Nabarro. The influence of graded hyperglycemia with and without physiological hyperinsulinemia on forearm glucose uptake and other metabolic responses in man. *J.Clin.Endocrinol.Metab* 63: 594-604, 1986.

79. Jackson, R. A., R. D. Roshania, M. I. Hawa, B. M. Sim, and L. DiSilvio. Impact of glucose ingestion on hepatic and peripheral glucose metabolism in man: an analysis based on simultaneous use of the forearm and double isotope techniques. *J.Clin.Endocrinol.Metab* 63: 541-549, 1986.

80. James, D. E., K. M. Burleigh, L. H. Storlien, S. P. Bennett, and E. W. Kraegen. Heterogeneity of insulin action in muscle: influence of blood flow. *Am.J.Physiol.* 251: E422-E430, 1986.

81. James, D. E., A. B. Jenkins, and E. W. Kraegen. Heterogeneity of insulin action in individual muscles in vivo: euglycemic clamp studies in rats. *Am.J.Physiol.* 248: E567-E574, 1985.

82. Jansson, P. A., J. P. Fowelin, H. P. von Schenck, U. P. Smith, and P. N. Lonnroth. Measurement by microdialysis of the insulin concentration in subcutaneous interstitial fluid. Importance of the endothelial barrier for insulin. *Diabetes* 42: 1469-1473, 1993.

83. Jarasch, E. D., G. Bruder, and H. W. Heid. Significance of xanthine oxidase in capillary endothelial cells. *Acta Physiol.Scand.* Suppl.548: 39-46, 1986.

84. Jayaweera, A. R., N. Edwards, W. P. Glasheen, F. S. Villanueva, R. D. Abbott, and S. Kaul. In vivo myocardial kinetics of air-filled albumin microbubbles during myocardial contrast echocardiography. Comparison with radiolabeled red blood cells. *Circ.Res.* 74: 1157-1165, 1994.

85. Jiang, Z. Y., Y. W. Lin, A. Clemont, E. P. Feener, K. D. Hein, M. Igarashi, T. Yamauchi, M. F. White, and G. L. King. Characterization of selective resistance to insulin signaling in the vasculature of obese zucker (fa/fa) rats. *J.Clin.Invest.* 104: 447-457, 1999.

86. Kastrup, J., J. Bulow, and N. A. Lassen. Vasomotion in human skin before and after local heating recorded with laser Doppler flowmetry. A method for induction of vasomotion. *Int.J.Microcirc.Clin.Exp.* 8: 205-215, 1989.

87. Kemmer, F. W., M. Berger, L. Herberg, F. A. Gries, A. Wirdeier, and K. Becker. Glucose metabolism in perfused skeletal muscle. Demonstration of insulin resistance in the obese Zucker rat. *Biochem.J.* 178: 733-741, 1979.

88. Kim, Y. B., O. D. Peroni, T. F. Franke, and B. B. Kahn. Divergent regulation of Akt1 and Akt2 isoforms in insulin target tissues of obese Zucker rats. *Diabetes* 49: 847-856, 2000.

89. Kimura, M., S. Tanaka, Y. Yamada, Y. Kiuchi, T. Yamakawa, and H. Sekihara. Dehydroepiandrosterone decreases serum tumor necrosis factor-alpha and restores insulin sensitivity: independent effect from secondary weight reduction in genetically obese Zucker fatty rats. *Endocrinology* 139: 3249-3253, 1998.

90. Kohzuki, H., S. Sakata, H. Misawa, and M. Takaki. $O_2$ delivery and the venous $PO_2$-$O_2$ uptake relationship in pump-perfused canine muscle. *Exp.Physiol.* 87: 53-61, 2002.

91. Kraegen, E. W., D. E. James, A. B. Jenkins, and D. J. Chisholm. Dose-response curves for in vivo insulin sensitivity in individual tissues in rats. *Am.J.Physiol.* 248: E353-E362, 1985.

92. Kurtz, T. W., R. C. Morris, and H. A. Pershadsingh. The Zucker fatty rat as a genetic model of obesity and hypertension. *Hypertension* 13: 896-901, 1989.

93. Kuznetsova, L. V., N. Tomasek, G. H. Sigurdsson, A. Banic, D. Erni, and A. M. Wheatley. Dissociation between volume blood flow and laser-Doppler signal from

rat muscle during changes in vascular tone. *Am.J.Physiol.* 274: H1248-H1254, 1998.

94. Kvandal, P., A. Stefanovska, M. Veber, K. H. Desiree, and K. K. Arvid. Regulation of human cutaneous circulation evaluated by laser Doppler flowmetry, iontophoresis, and spectral analysis: importance of nitric oxide and prostaglandines. *Microvasc.Res.* 65: 160-171, 2003.

95. Kvernebo, K., L. E. Staxrud, and E. G. Salerud. Assessment of human muscle blood perfusion with single-fiber laser Doppler flowmetry. *Microvasc.Res.* 39: 376-385, 1990.

96. Laakso, M., S. V. Edelman, G. Brechtel, and A. D. Baron. Decreased effect of insulin to stimulate skeletal muscle blood flow in obese man. *J.Clin.Invest.* 85: 1844-1852, 1990.

97. Laine, H., H. Yki-Jarvinen, O. Kirvela, T. Tolvanen, M. Raitakari, O. Solin, M. Haaparanta, J. Knuuti, and P. Nuutila. Insulin resistance of glucose uptake in skeletal muscle cannot be ameliorated by enhancing endothelium-dependent blood flow in obesity. *J.Clin.Invest.* 101: 1156-1162, 1998.

98. Lash, J. M., W. M. Sherman, and R. L. Hamlin. Capillary basement membrane thickness and capillary density in sedentary and trained obese Zucker rats. *Diabetes* 38: 854-860, 1989.

99. Leahy, M. J., F. F. de Mul, G. E. Nilsson, and R. Maniewski. Principles and practice of the laser-Doppler perfusion technique. *Technol.Health Care* 7: 143-162, 1999.

100. Ley, K., J. U. Meyer, M. Intaglietta, and K. E. Arfors. Shunting of leukocytes in rabbit tenuissimus muscle. *Am.J.Physiol.* 256: H85-H93, 1989.

101. Leyva, F., M. Rauchhaus, S. D. Anker, A. J. Proudler, I. F. Godsland, P. Stiefel, A. J. Coats, P. A. Poole-Wilson, and J. C. Stevenson. Non-invasive assessment of

vascular function. Paradoxical vascular response to intravenous glucose in coronary heart disease. *Eur.Heart J.* 21: 39-44, 2000.

102. Liang, C. S., J. U. Doherty, R. Faillace, K. Maekawa, S. Arnold, H. Gavras, and W. B. Hood. Insulin infusion in conscious dogs. *J.Clin.Invest.* 69: 1321-1336, 1982.

103. Lindbom, L. Distribution patterns of blood flow in the rabbit tenuissimus muscle in response to brief ischemia and muscle contraction. *Microvasc.Res.* 31: 143-156, 1986.

104. Lindbom, L. and K. E. Arfors. Non-homogeneous blood flow distribution in the rabbit tenuissimus muscle Differential control of total blood flow and capillary perfusion. *Acta Physiol.Scand.* 122: 225-233, 1984.

105. Lindbom, L. and K. E. Arfors. Mechanism and site of control for variation in the number of perfused capillaries in skeletal muscle. *Int.J.Microcirc.Clin.Exp.* 4: 19-30, 1985.

106. Linden, M. Can blood flow in separate small tubes be quantitatively assessed by high-resolution laser Doppler imaging. *Med.Biol.Eng.Comput.* 35: 575-580, 1997.

107. Linden, M., H. Golster, S. Bertuglia, A. Colantuoni, F. Sjoberg, and G. Nilsson. Evaluation of enhanced high-resolution laser Doppler imaging in an in vitro tube model with the aim of assessing blood flow in separate microvessels. *Microvasc.Res.* 56: 261-270, 1998.

108. Linden, M., A. Sirsjo, L. Lindbom, G. Nilsson, and A. Gidlof. Laser-Doppler perfusion imaging of microvascular blood flow in rabbit tenuissimus muscle. *Am.J.Physiol.* 269: H1496-H1500, 1995.

109. Lindner, J. R., F. S. Villanueva, J. M. Dent, K. Wei, J. Sklenar, and S. Kaul. Assessment of resting perfusion with myocardial contrast echocardiography: theoretical and practical considerations. *Am.Heart J.* 139: 231-240, 2000.

110. Liu, R. H., M. Mizuta, T. Kurose, and S. Matsukura. Early events involved in the development of insulin resistance in Zucker fatty rat. *Int.J.Obes.Relat.Metab.Disord.* 26: 318-326, 2002.

111. Maiman, T. H. Stimulated optical radiation in ruby. *Nature* 187: 493-494, 1960.

112. Meredith, I. T., K. E. Currie, T. J. Anderson, M. A. Roddy, P. Ganz, and M. A. Creager. Postischemic vasodilation in human forearm is dependent on endothelium-derived nitric oxide. *Am.J.Physiol* 270: H1435-H1440, 1996.

113. Minassian, C., N. Daniele, J. C. Bordet, C. Zitoun, and G. Mithieux. Liver glucose-6 phosphatase activity is inhibited by refeeding in rats. *J.Nutr.* 125: 2727-2732, 1995.

114. Myrhage, R. and E. Eriksson. Vascular arrangements in hindlimb muscles of the cat. *J.Anat.* 131: 1-17, 1980.

115. Natali, A., R. Bonadonna, D. Santoro, A. Q. Galvan, S. Baldi, S. Frascerra, C. Palombo, S. Ghione, and E. Ferrannini. Insulin resistance and vasodilation in essential hypertension. Studies with adenosine. *J.Clin.Invest.* 94: 1570-1576, 1994.

116. Natali, A., G. Buzzigoli, S. Taddei, D. Santoro, M. Cerri, R. Pedrinelli, and E. Ferrannini. Effects of insulin on hemodynamics and metabolism in human forearm. *Diabetes* 39: 490-500, 1990.

117. Natali, A., G. A. Quinones, N. Pecori, G. Sanna, E. Toschi, and E. Ferrannini. Vasodilation with sodium nitroprusside does not improve insulin action in essential hypertension. *Hypertension* 31: 632-636, 1998.

118. Nauck, M. A., R. W. Blietz, and C. Qualmann. Comparison of hyperinsulinaemic clamp experiments using venous, 'arterialized' venous or capillary euglycaemia. *Clin.Physiol* 16: 589-602, 1996.

119. Neviere, R., D. Mathieu, J. L. Chagnon, N. Lebleu, J. P. Millien, and F. Wattel. Skeletal muscle microvascular blood flow and oxygen transport in patients with severe sepsis. *Am.J.Respir.Crit.Care Med.* 153: 191-195, 1996.

120. Newman, J. M. and M. G. Clark. Stimulation and inhibition of resting muscle thermogenesis by vasoconstrictors in perfused rat hind limb. *Can.J.Physiol.Pharmacol.* 76: 867-872, 1998.

121. Newman, J. M., K. A. Dora, S. Rattigan, S. J. Edwards, E. Q. Colquhoun, and M. G. Clark. Norepinephrine and serotonin vasoconstriction in rat hindlimb control different vascular flow routes. *Am.J.Physiol.* 270: E689-E699, 1996.

122. Newman, J. M., J. T. Steen, and M. G. Clark. Vessels supplying septa and tendons as functional shunts in perfused rat hindlimb. *Microvasc.Res.* 54: 49-57, 1997.

123. Nilsson, G. E., T. Tenland, and P. A. Oberg. Evaluation of a laser Doppler flowmeter for measurement of tissue blood flow. *IEEE Trans.Biomed.Eng.* 27: 597-604, 1980.

124. Nuutila, P., M. Raitakari, H. Laine, O. Kirvela, T. Takala, T. Utriainen, S. Makimattila, O. P. Pitkanen, U. Ruotsalainen, H. Iida, J. Knuuti, and H. Yki-Jarvinen. Role of blood flow in regulating insulin-stimulated glucose uptake in humans. Studies using bradykinin, [15O]water, and [18F]fluoro-deoxy- glucose and positron emission tomography. *J.Clin.Invest.* 97: 1741-1747, 1996.

125. Obeid, A. N., N. J. Barnett, G. Dougherty, and G. Ward. A critical review of laser Doppler flowmetry. *J.Med.Eng.Technol.* 14: 178-181, 1990.

126. Oberg, P. A. Laser-Doppler flowmetry. *Crit.Rev.Biomed.Eng.* 18: 125-163, 1990.

127. Oberg, P. A., T. Tenland, and G. E. Nilsson. Laser-Doppler flowmetry--a non-invasive and continuous method for blood flow evaluation in microvascular studies. *Acta Med.Scand Suppl.* 687:17-24: 17-24, 1984.

128. Osman, A. A., J. Hancock, D. G. Hunt, J. L. Ivy, and L. J. Mandarino. Exercise training increases ERK2 activity in skeletal muscle of obese Zucker rats. *J Appl.Physiol* 90: 454-460, 2001.

129. Pappenheimer, J. R. Vasoconstrictor nerves and oxygen consumption in the isolated perfused hindlimb muscles of the dog. *J.Physiol.(Lond.)* 99: 182-200, 1941.

130. Pelberg, R. A., K. Wei, N. Kamiyama, J. Sklenar, J. Bin, and S. Kaul. Potential advantage of flash echocardiography for digital subtraction of B-mode images acquired during myocardial contrast echocardiography. *J.Am.Soc.Echocardiogr.* 12: 85-93, 1999.

131. Penicaud, L., P. Ferre, J. Terretaz, M. F. Kinebanyan, A. Leturque, E. Dore, J. Girard, B. Jeanrenaud, and L. Picon. Development of obesity in Zucker rats. Early insulin resistance in muscles but normal sensitivity in white adipose tissue. *Diabetes* 36: 626-631, 1987.

132. Pereda, S. A., J. W. Eckstein, and F. M. Abboud. Cardiovascular responses to insulin in the absence of hypoglycemia. *Am.J.Physiol* 202: 249-252, 1962.

133. Petrie, J. R., S. Ueda, A. D. Morris, H. L. Elliott, and J. M. Connell. Potential confounding effect of hand-warming on the measurement of insulin sensitivity. *Clin.Sci.(Lond)* 91: 65-71, 1996.

134. Phillips, M. S., Q. Liu, H. A. Hammond, V. Dugan, P. J. Hey, C. J. Caskey, and J. F. Hess. Leptin receptor missense mutation in the fatty Zucker rat. *Nat.Genet.* 13: 18-19, 1996.

135. Pitre, M., A. Nadeau, and H. Bachelard. Insulin sensitivity and hemodynamic responses to insulin in Wistar-Kyoto and spontaneously hypertensive rats. *Am.J.Physiol* 271: E658-E668, 1996.

136. Raitakari, M., M. J. Knuuti, U. Ruotsalainen, H. Laine, P. Makela, M. Teras, H. Sipila, T. Niskanen, and O. T. Raitakari. Insulin increases blood volume in human

skeletal muscle: studies using [15O]CO and positron emission tomography. *Am.J.Physiol.* 269: E1000-E1005, 1995.

137. Rattigan, S., G. J. Appleby, K. A. Miller, J. T. Steen, K. A. Dora, E. Q. Colquhoun, and M. G. Clark. Serotonin inhibition of 1-methylxanthine metabolism parallels its vasoconstrictor activity and inhibition of oxygen uptake in perfused rat hindlimb. *Acta Physiol.Scand.* 161: 161-169, 1997.

138. Rattigan, S., M. G. Clark, and E. J. Barrett. Hemodynamic actions of insulin in rat skeletal muscle: evidence for capillary recruitment. *Diabetes* 46: 1381-1388, 1997.

139. Rattigan, S., M. G. Clark, and E. J. Barrett. Acute vasoconstriction-induced insulin resistance in rat muscle in vivo. *Diabetes* 48: 564-569, 1999.

140. Rattigan, S., K. A. Dora, E. Q. Colquhoun, and M. G. Clark. Serotonin-mediated acute insulin resistance in the perfused rat hindlimb but not in incubated muscle: a role for the vascular system. *Life Sci.* 53: 1545-1555, 1993.

141. Rattigan, S., K. A. Dora, A. C. Y. Tong, and M. G. Clark. Perfused skeletal muscle contraction and metabolism improved by angiotensin II-mediated vasoconstriction. *Am.J.Physiol.* 271: E96-103, 1996.

142. Rattigan, S., M. G. Wallis, J. M. Youd, and M. G. Clark. Exercise training improves insulin-mediated capillary recruitment in association with glucose uptake in rat hind limb. *Diabetes* 50: 2659-2665, 2001.

143. Renaudin, C., E. Michoud, J. R. Rapin, M. Lagarde, and N. Wiernsperger. Hyperglycaemia modifies the reaction of microvessels to insulin in rat skeletal muscle. *Diabetologia* 41: 26-33, 1998.

144. Renkin, E. M. Effects of blood flow on diffusion kinetics in isolated, perfused hindlegs of cats: A double circulation hypothesis. *Am.J.Physiol.* 183: 125-136, 1955.

145. Renkin, E. M. Control of microcirculation and blood-tissue exchange. In Renkin, E. M., C. C. Michel, and S. R. Geiger, eds. Handbook of Physiology - The Cardiovascular System IV. American Physiological Society Bethesda. 1984, 627-687.

146. Richter, E. A., K. J. Mikines, H. Galbo, and B. Kiens. Effect of exercise on insulin action in human skeletal muscle. *J.Appl.Physiol.* 66: 876-885, 1989.

147. Rippe, B., A. Kamiya, and B. Folkow. Simultaneous measurements of capillary diffusion and filtration exchange during shifts in filtration-absorption and at graded alterations in the capillary permeability surface area product (PS). *Acta Physiol.Scand.* 104: 318-336, 1978.

148. Rowe, J. W., J. B. Young, K. L. Minaker, A. L. Stevens, J. Pallotta, and L. Landsberg. Effect of insulin and glucose infusions on sympathetic nervous system activity in normal man. *Diabetes* 30: 219-225, 1981.

149. Ruderman, N. B., C. R. Houghton, and R. Hems. Evaluation of the isolated perfused rat hindquarter for the study of muscle metabolism. *Biochem.J.* 124: 639-651, 1971.

150. Sarabi, M., L. Lind, J. Millgard, A. Hanni, A. Hagg, C. Berne, and H. Lithell. Local vasodilatation with metacholine, but not with nitroprusside, increases forearm glucose uptake. *Physiol Res.* 48: 291-295, 1999.

151. Schechner, J. S. and I. M. Braverman. Synchronous vasomotion in the human cutaneous microvasculature provides evidence for central modulation. *Microvasc.Res.* 44: 27-32, 1992.

152. Scherrer, U., D. Randin, P. Vollenweider, L. Vollenweider, and P. Nicod. Nitric oxide release accounts for insulin's vascular effects in humans. *J.Clin.Invest.* 94: 2511-2515, 1994.

153. Scherrer, U., P. Vollenweider, D. Randin, E. Jequier, P. Nicod, and L. Tappy. Suppression of insulin-induced sympathetic activation and vasodilation by dexamethasone in humans. *Circulation* 88: 388-394, 1993.

154. Scott, E. M., J. P. Greenwood, G. Vacca, J. B. Stoker, S. G. Gilbey, and D. A. Mary. Carbohydrate ingestion, with transient endogenous insulinaemia, produces both sympathetic activation and vasodilatation in normal humans. *Clin.Sci.(Lond)* 102: 523-529, 2002.

155. Serne, E. H., R. O. Gans, J. C. ter Maaten, G. J. Tangelder, A. J. Donker, and C. D. Stehouwer. Impaired skin capillary recruitment in essential hypertension is caused by both functional and structural capillary rarefaction. *Hypertension* 38: 238-242, 2001.

156. Serne, E. H., R. O. Gans, J. C. ter Maaten, P. M. ter Wee, A. J. Donker, and C. D. Stehouwer. Capillary recruitment is impaired in essential hypertension and relates to insulin's metabolic and vascular actions. *Cardiovasc.Res.* 49: 161-168, 2001.

157. Serne, E. H., R. G. IJzerman, R. O. Gans, R. Nijveldt, G. De Vries, R. Evertz, A. J. Donker, and C. D. Stehouwer. Direct evidence for insulin-induced capillary recruitment in skin of healthy subjects during physiological hyperinsulinemia. *Diabetes* 51: 1515-1522, 2002.

158. Serne, E. H., C. D. Stehouwer, J. C. ter Maaten, P. M. ter Wee, J. A. Rauwerda, A. J. Donker, and R. O. Gans. Microvascular Function Relates to Insulin Sensitivity and Blood Pressure in Normal Subjects. *Circulation* 99: 896-902, 1999.

159. Shamim-Uzzaman, Q. A., D. Pfenninger, C. Kehrer, A. Chakrabarti, N. Kacirotti, M. Rubenfire, R. Brook, and S. Rajagopalan. Altered cutaneous microvascular responses to reactive hyperaemia in coronary artery disease: a comparative study with conduit vessel responses. *Clin.Sci.(Lond)* 103: 267-273, 2002.

160. Sherman, W. M., A. L. Katz, C. L. Cutler, and R. T. Withers. Glucose transport: locus of muscle insulin resistance in obese Zucker rats. *Am.J.Physiol.Endocrinol.Metab.* 19: E374-E382, 1988.

161. Smits, G. J., R. J. Roman, and J. H. Lombard. Evaluation of laser-Doppler flowmetry as a measure of tissue blood flow. *J.Appl.Physiol.* 61: 666-672, 1986.

162. Sonnenschein, R. R. and L. Hirvonen. Effects of vasoactive drugs on blood flow and work performance in skeletal muscle. *Biochem.Pharmacol.* 8: 166, 1961.

163. Spraul, M., E. Ravussin, and A. D. Baron. Lack of relationship between muscle sympathetic nerve activity and skeletal muscle vasodilation in response to insulin infusion. *Diabetologia* 39: 91-96, 1996.

164. Stefanovska, A., M. Bracic, and H. D. Kvernmo. Wavelet analysis of oscillations in the peripheral blood circulation measured by laser Doppler technique. *IEEE Trans.Biomed.Eng* 46: 1230-1239, 1999.

165. Steinberg, H. O., G. Brechtel, A. Johnson, N. Fineberg, and A. D. Baron. Insulin-mediated skeletal muscle vasodilation is nitric oxide dependent. A novel action of insulin to increase nitric oxide release. *J.Clin.Invest.* 94: 1172-1179, 1994.

166. Steinberg, H. O., G. Brechtel, A. Johnson, K. Sunblad, and A. D. Baron. Insulin mediated vasodilation is a determinant of in vivo insulin mediated glucose uptake. *Diabetes* 44 Suppl: 56A, 1995.

167. Steinberg, H. O., H. Chaker, R. Leaming, A. Johnson, G. Brechtel, and A. D. Baron. Obesity/insulin resistance is associated with endothelial dysfunction. Implications for the syndrome of insulin resistance. *J.Clin.Invest.* 97: 2601-2610, 1996.

168. Steinberg, H. O., G. Paradisi, G. Hook, K. Crowder, J. Cronin, and A. D. Baron. Free fatty acid elevation impairs insulin-mediated vasodilation and nitric oxide production. *Diabetes* 49: 1231-1238, 2000.

169. Stern, M. D. In vivo evaluation of microcirculation by coherent light scattering. *Nature* 254: 56-58, 1975.

170. Tack, C. J., J. W. Lenders, D. S. Goldstein, J. A. Lutterman, P. Smits, and T. Thien. Haemodynamic actions of insulin. *Curr.Opin.Nephrol.Hypertens.* 7: 99-106, 1998.

171. Taddei, S., A. Virdis, P. Mattei, A. Natali, E. Ferrannini, and A. Salvetti. Effect of insulin on acetylcholine-induced vasodilation in normotensive subjects and patients with essential hypertension. *Circulation* 92: 2911-2918, 1995.

172. Tagawa, T., T. Imaizumi, T. Endo, M. Shiramoto, Y. Harasawa, and A. Takeshita. Role of nitric oxide in reactive hyperemia in human forearm vessels. *Circulation* 90: 2285-2290, 1994.

173. Takemiya, T. and J. Maeda. The functional characteristics of tendon blood circulation in the rabbit hindlimbs. *Jpn.J.Physiol.* 38: 361-374, 1988.

174. Tappy, L., D. Randin, P. Vollenweider, L. Vollenweider, N. Paquot, U. Scherrer, P. Schneiter, P. Nicod, and E. Jequier. Mechanisms of dexamethasone-induced insulin resistance in healthy humans. *J.Clin.Endocrinol.Metab.* 79: 1063-1069, 1994.

175. Terrettaz, J. and B. Jeanrenaud. In vivo hepatic and peripheral insulin resistance in genetically obese (fa/fa) rats. *Endocrinology* 112: 1346-1351, 1983.

176. Torgan, C. E., J. T. Brozinick, Jr., G. M. Kastello, and J. L. Ivy. Muscle morphological and biochemical adaptations to training in obese Zucker rats. *J Appl.Physiol* 67: 1807-1813, 1989.

177. Tseng, C. C., T. J. Kieffer, L. A. Jarboe, T. B. Usdin, and M. M. Wolfe. Postprandial stimulation of insulin release by glucose-dependent insulinotropic polypeptide (GIP). Effect of a specific glucose-dependent insulinotropic polypeptide receptor antagonist in the rat. *J.Clin.Invest* 98: 2440-2445, 1996.

178. Tyml, K. Red cell perfusion in skeletal muscle at rest and after mild and severe contractions. *Am.J.Physiol.* 252: H485-H493, 1987.

179. Vincent, M. A., E. J. Barrett, J. R. Lindner, M. G. Clark, and S. Rattigan. Inhibiting NOS blocks microvascular recruitment and blunts glucose uptake in response to insulin. *Am.J.Physiol* 285: E123-E129, 2003.

180. Vincent, M. A., D. Dawson, A. D. Clark, J. R. Lindner, S. Rattigan, M. G. Clark, and E. J. Barrett. Skeletal muscle microvascular recruitment by physiological hyperinsulinemia precedes increases in total blood flow. *Diabetes* 51: 42-48, 2002.

181. Vincent, M. A., S. Rattigan, and M. G. Clark. Microsphere infusion reverses vasoconstrictor-mediated change in hindlimb oxygen uptake and energy status. *Acta Physiol.Scand.* 164: 61-69, 1998.

182. Vollenweider, L., L. Tappy, R. Owlya, E. Jequier, P. Nicod, and U. Scherrer. Insulin-induced sympathetic activation and vasodilation in skeletal muscle. Effects of insulin resistance in lean subjects. *Diabetes* 44: 641-645, 1995.

183. Vollenweider, P., L. Tappy, D. Randin, P. Schneiter, E. Jequier, P. Nicod, and U. Scherrer. Differential effects of hyperinsulinemia and carbohydrate metabolism on sympathetic nerve activity and muscle blood flow in humans. *J.Clin.Invest.* 92: 147-154, 1993.

184. Vuilleumier, P., D. Decosterd, M. Maillard, M. Burnier, and D. Hayoz. Postischemic forearm skin reactive hyperemia is related to cardovascular risk factors in a healthy female population. *J.Hypertens.* 20: 1753-1757, 2002.

185. Wahab, P. J., A. W. Rijnsburger, M. Oolbekkink, and R. J. Heine. Venous versus arterialised venous blood for assessment of blood glucose levels during glucose clamping: comparison in healthy men. *Horm.Metab Res.* 24: 576-579, 1992.

186. Walder, D. N. The local clearance of radioactive sodium from muscle in normal subjects and those with peripheral vascular disease. *Clin.Sci.* 12: 153-167, 1953.

187. Walker, A. B., J. Dores, R. E. Buckingham, M. W. Savage, and G. Williams. Impaired insulin-induced attenuation of noradrenaline-mediated vasoconstriction in insulin-resistant obese Zucker rats. *Clin.Sci.* 93: 235-241, 1997.

188. Walker, A. B., M. W. Savage, J. Dores, and G. Williams. Insulin-induced attenuation of noradrenaline-mediated vasoconstriction in resistance arteries from Wistar rats is nitric oxide dependent. *Clin.Sci.* 92: 147-152, 1997.

189. Wallis, M. G., C. M. Wheatley, S. Rattigan, E. J. Barrett, A. D. H. Clark, and M. G. Clark. Insulin-mediated hemodynamic changes are impaired in muscle of Zucker obese rats. *Diabetes* 51: 3492-3498, 2002.

190. Wei, K., A. R. Jayaweera, S. Firoozan, A. Linka, D. M. Skyba, and S. Kaul. Quantification of myocardial blood flow with ultrasound-induced destruction of microbubbles administered as a constant venous infusion. *Circulation* 97: 473-483, 1998.

191. Wei, K., A. R. Jayaweera, S. Firoozan, A. Linka, D. M. Skyba, and S. Kaul. Quantification of myocardial blood flow with ultrasound-induced destruction of microbubbles administered as a constant venous infusion. *Circulation* 97: 473-483, 1998.

192. Wheatley, C. M., Rattigan, S., Richards, S. M., Barrett, E. J., and Clark, M. G. Skeletal muscle contraction stimulates capillary recruitment and glucose uptake in insulin-resistant obese Zucker rats. *Am. J. Physiol.* 2004: in press.

193. Wong, B. J., B. W. Wilkins, L. A. Holowatz, and C. T. Minson. Nitric oxide synthase inhibition does not alter the reactive hyperemic response in the cutaneous circulation. *J.Appl.Physiol* 95: 504-510, 2003.

194. Wynants, J., B. Petrov, J. Nijhof, and H. Van Belle. Optimization of a high-performance liquid chromatographic method for the determination of nucleosides and their catabolies. Application to cat and rabbit heart perfusates. *J.Chromatogr.* 386: 297-308, 1987.

195. Yamamoto, T., H. Fukumoto, G. Koh, H. Yano, K. Yasuda, K. Masuda, H. Ikeda, H. Imura, and Y. Seino. Liver and muscle-fat type glucose transporter gene expression in obese and diabetic rats. *Biochem.Biophys.Res.Commun.* 175: 995-1002, 1991.

196. Yang, Y. J., I. D. Hope, M. Ader, and R. N. Bergman. Insulin transport across capillaries is rate limiting for insulin action in dogs. *J.Clin.Invest.* 84: 1620-1628, 1989.

197. Yki-Jarvinen, H. and T. Utriainen. Insulin-induced vasodilatation: physiology or pharmacology? *Diabetologia* 41: 369-379, 1998.

198. Yki-Jarvinen, H., A. A. Young, C. Lamkin, and J. E. Foley. Kinetics of glucose disposal in whole body and across the forearm in man. *J.Clin.Invest* 79: 1713-1719, 1987.

199. Youd, J. M., J. M. Newman, M. G. Clark, G. J. Appleby, S. Rattigan, A. C. Tong, and M. A. Vincent. Increased metabolism of infused 1-methylxanthine by working muscle. *Acta Physiol.Scand.* 166: 301-308, 1999.

200. Youd, J. M., S. Rattigan, and M. G. Clark. Acute impairment of insulin-mediated capillary recruitment and glucose uptake in rat skeletal muscle in vivo by TNFa. *Diabetes* 49: 1904-1909, 2000.

201. Zemel, M. B., S. Reddy, and J. R. Sowers. Insulin attenuation of vasoconstrictor responses to phenylephrine in Zucker lean and obese rats. *Am.J.Hypertens.* 4: 537-539, 1991.

202. Zhang, L., M. A. Vincent, S. M. Richards, L. H. Clerk, S. Rattigan, M. G. Clark, and E. J. Barrett. Insulin sensitivity of muscle capillary recruitment in vivo. *Diabetes* 53: 447-453, 2004.

203. Zucker, L. M. Hereditary obesity in the rat associated with hyperlipemia. *Ann.N.Y.Acad.Sci.* 131: 447-458, 1965.

204. Zucker, L. M. and H. N. Antoniades. Insulin and obesity in the Zucker genetically obese rat "fatty". *Endocrinology* 90: 1320-1330, 1972.